Accessibility and Manipulation of Brain Signals for Neuroprosthetic Applications
by
Timothy C. Marzullo

A dissertation submitted in partial fulfillment
of the requirements for the degree of
Doctor of Philosophy
(Neuroscience)
in The University of Michigan
2008

Doctoral Committee:

       Professor Daryl R. Kipke, Chair
       Professor Stephen A. Maren
       Professor John C. Middlebrooks
       Associate Professor J. Wayne Aldridge
       Associate Professor Gina R. Poe

To Grandpa Marzullo, Master Craftsman
(1924-2006)

Table of Contents

List of Figures

Chapter I: Introduction

Chapter II. Suitability of the Cingulate Cortex for Neural Control

Chapter III. Spikes, Local Field Potentials, and Electrocorticogram Correlations in the
Motor Cortex of Rats

Chapter IV. A Sensorimotor Closed-loop Neural Interface Case Study

Chapter V. Conclusion

Abstract

Accessibility and Manipulation of Brain Signals for Neuroprosthetic Applications

by

Timothy C. Marzullo

Chair: Daryl R. Kipke, Ph.D.

The field of Neural Engineering spawned in response to the perpetual problem of neurology: injured central nervous system neurons do not regenerate or repair, and stem cell/molecular genetic solutions, while the ideal intervention, are far away from clinical utilization.

A current solution is to substitute computers and electrodes for neurons, as either transducers (cochlear implants, retinal implants, and visual cortex ECoG implants for sensory replacement), regulators (deep brain stimulations for Parkinson's disease), and output signal readers (motor cortex neuroprosthetics).

I have focused on improving the technology of motor neuroprosthetics, and in this dissertation I investigated three sub-systems of this relatively new technology in a rat model.

In my first experiment, I demonstrated that the cingulate cortex, part of the prefrontal cortex, can be used as an additional control signal for a motor neuroprosthetic device in the event that upper motor neurons of the motor cortex are degenerated by neurodegenerative diseases.

In my second experiment, I examined whether electrocorticograms (ECoGs) and local field potentials (LFPs) are independent from the spiking activity of motor neurons and could be thus used as additional control channels. I showed these signals are not necessarily independent, specifically, the spikes phase-lock to the field potentials at defined frequencies, and careful algorithms will have to be developed to combine spikes, LFPs, and ECoGs as different control channels for a neuroprosthetic device.

In my third experiment, I investigated the use of feedback in a neuroprosthetic model. I combined intracortical microstimulation (ICMS) of the visual cortex with simultaneous motor cortex ensemble recordings in real time to demonstrate the feasibility of a closed-loop neuroprosthesis. I showed that though sensory cortex ICMS can be combined with motor cortex recording in real-time in a viable preparation, increased technological development in simultaneous decoding with brain stimulation needs to occur before feasible clinical implementation can become a reality.

By reading and manipulating brain signals via microelectrodes, a basic level of neural control and neural replacement can be achieved. Until the day that physicians have access to technology that allows spinal cords to regrow and limbs to regenerate, current technology allows us to achieve some measure of success by replacing neurons with electrodes.

Chapter I

Introduction

It is an unfortunate tenet of neuroscience that severed spinal cords do not repair, leaving a patient affected with such trauma with varying degrees of paralysis. The brain is still alive, movement intentions can still be willed by a paralyzed patient, but the movement intention signals cannot bypass the site of spinal cord injury (Hochberg et al., 2006). Thus, there is an effort in the neural engineering field to access the movement command signals directly from the brain, extract and decode them, and then use the signals to control a neuroprosthetic device such as a computer cursor (Hochberg et al., 2006), an artificial limb (Velliste et al., 2008), or a functional electrical stimulation system of musculature (Weber et al., 2007). The work in this dissertation presents experiments investigating three systems of neuroprosthetic design for limb control: 1) alternative cortical areas beyond motor cortex, 2) the co-variation of field potentials and spikes as an information channel, and 3) the use of sensory cortex feedback as an additional information source about the state of a neural controller. What follows in this chapter is an overview of the technological development of decoding intention signals from the brain, followed by an introduction and experimental justification of the experiments making up this dissertation.

In the 1960's, awake, behaving chronic microelectrode recording technology and analog electronics advanced such that experiments utilizing real-time manipulation of brain signals became possible. In the first experiments, single neurons of the striatum in rats (Olds, 1965) and the motor cortex of monkeys (Fetz, 1969) were isolated with extracellular unit recording techniques (using microwires), and the subjects were trained to increase the discharge rate of respective units in order to receive a reward. In these preparations, the behavior was not clamped; the animals could use any strategy with which to increase the discharge rate of the units. In the Olds study (see Figure 1), to
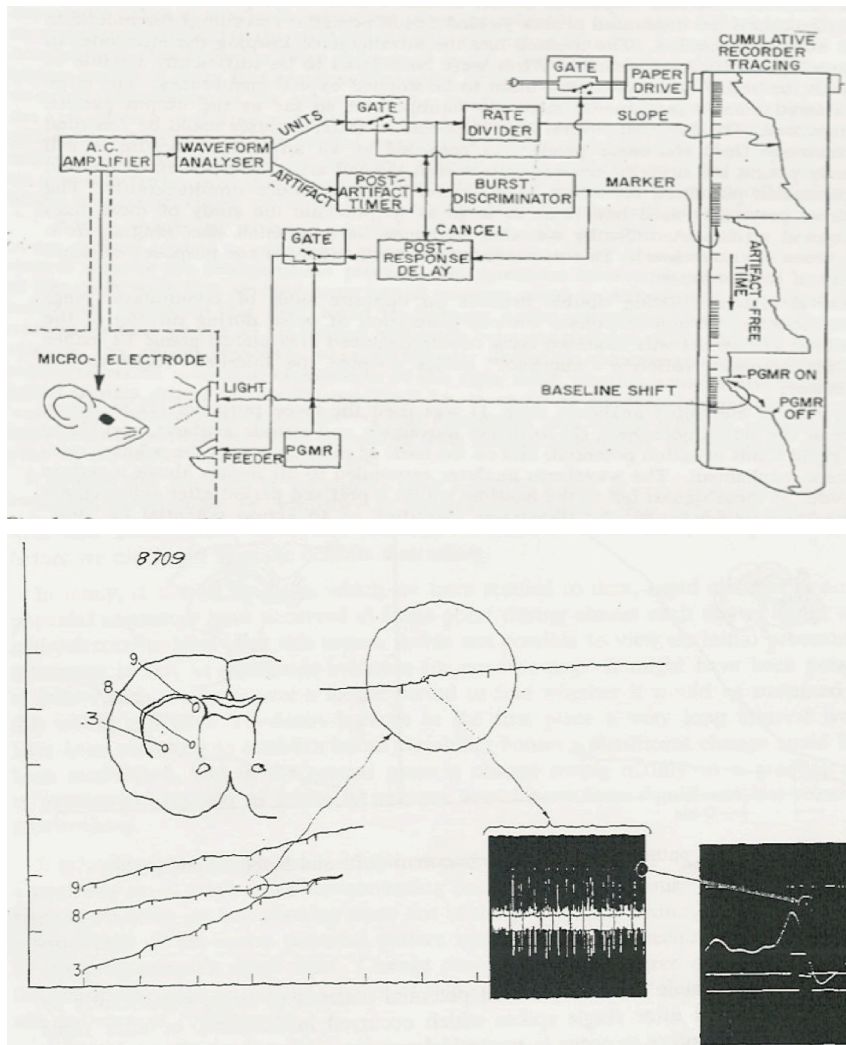
Figure 1.1: Data from Original Olds Work. Top: Experiment and hardware Design. Bottom: Sample of three electrode recordings in the rat. Y-axis shows firing rate (actual values not available in manuscript). X-axis shows time on the order of minutes. Notice rats were able to increase firing rates of the selected units in the caudate and internal capsule (Olds 1965).

investigate the mechanisms of reinforcement learning in the brain, the rats received feedback of single units in the striatum, hippocampus, and reticular activating system. Isolated units were held continuously for 2-4 days, and during periods when the rats were awake, every 10 minutes a light would turn on in the cage, and the rat then had two minutes to increase the unit discharge rate to trigger the food magazine. Unfortunately, beyond a few examples of operant conditioning in the striatum, the data describing the ultimate number of units trained, learning rate, and percentage trainable units with regards to brain area were not included in the manuscript. James Olds noted "repeated
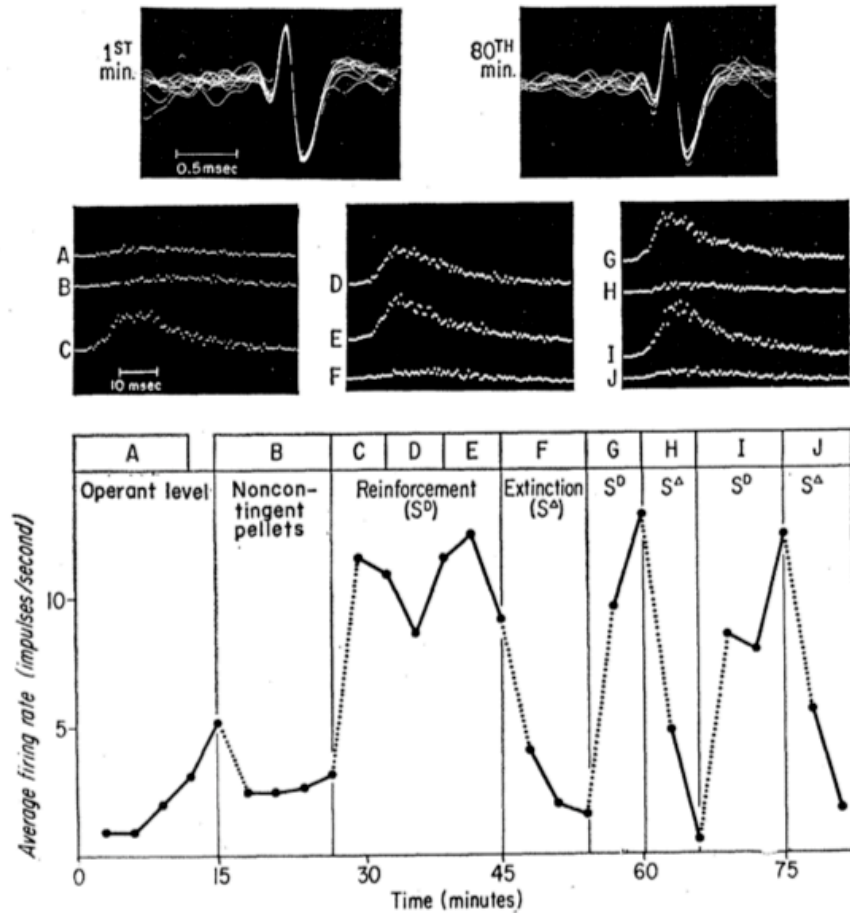
Figure 1.2: Data from Original Fetz work. A single unit was isolated (top) from the monkey motor cortex for 80 minutes. Middle section of figure shows interspike interval histograms from the epochs shown in bottom graph. S^D and S^A show periods of reinforcement and extinction. Notice when increasing firing rates are rewarded, the monkey is rapidly able to modulate and maintain high firing rates that are absent in extinction conditions (Fetz 1969).

failures with probes in the forebrain and midbrain areas," but concluded it was most likely due to difficulty in recording units for long duration in the said brain regions.

In Fetz's seminal work (Fetz, 1969), he implanted the motor cortex of rhesus monkeys with microwires, isolated one or two single units per day, and gave the monkeys auditory feedback of the discharge rate (simply the output of the spiking audio monitor) of the single units. The monkeys were then rewarded with food pellets for increasing the discharge rate of the single units. Quite remarkably, the monkeys were able to learn the task within 30 minutes after a single unit was isolated (see Figure 2). Fetz noted the monkeys would move their arms during the reinforcement process; most likely this motor behavior was the consequence of the increasing neural discharge rate. The monkeys were

able to do the task even in the absence of the auditory feedback, and the monkeys were also able to do the task when somatosensory cortex units were used instead of the motor cortex.

In 1971, Fetz published a more comprehensive paper in which he simultaneously operantly conditioned specific muscle patterns and motor cortex recordings (Fetz and Finocchio, 1971). In one experiment, the investigators would operantly condition the forearm muscle's electromyogram (EMG) amplitude while monitoring motor cortex firing rates; in another experiment, the investigators would operantly condition the motor cortex neurons while monitoring the forearm muscle's EMG. In both experiments, they found that muscle contractions and increasing motor cortex discharge rate were correlated. However, when they introduced the contingency of simultaneous suppression of muscle activity concurrent with increased neural discharge rate, the monkey was able to suppress the EMG activity while still increasing the motor discharge. The corollary, where increases in muscle EMG activity were rewarded with simultaneous suppression of motor unit activity, were much more difficult for the monkeys, though with extensive training the monkeys could slightly suppress motor unit discharge.

In 1977 E.M. Schmidt and his colleagues at the National Institutes of Health performed similar experiments on the operant conditioning of motor cortex neurons (Schmidt et al., 1977). In these experiments, single units of the motor cortex were again isolated, but the frequency discharge rate of the neurons was divided into 8 frequency bands (for example, if a neuron's lowest firing rate was 2 Hz, the highest firing rate was 40 Hz, then the 2 Hz-40 Hz firing rate range would be divided into 8 equal size segments). Each of these 8 frequency bands was then assigned its own light in a bank of 8 lights. A green target light would appear at one light, and the monkey would have to modulate its discharge rate, indicated by a red annulus surrounding the corresponding light on the bank, until the red annulus matched up to the green target for a minimum of 450 ms. After this initial target acquisition, a new green target light would appear at a separate location, and the monkey would again have to move the red annulus to the new target. Of the 28 neurons in the motor cortex examined over a period of 99 days, 79% (or 22 neurons) could be trained. Again, the investigators noticed refined muscle movements during this task. Indeed, in a later work Schmidt remarked (Schmidt et al., 1978):
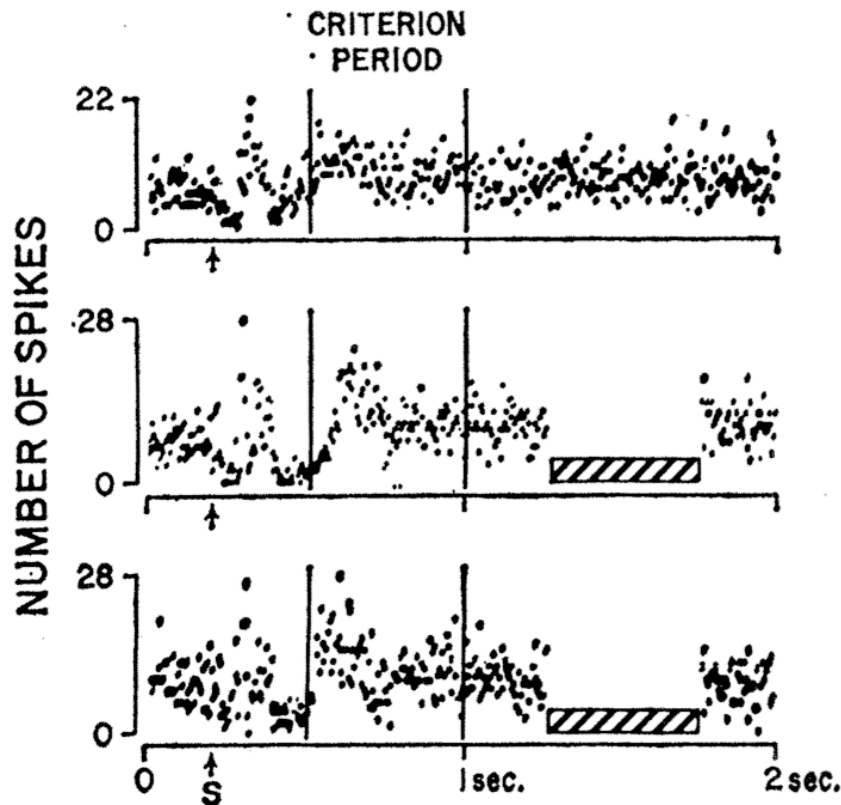
Figure 1.3: Operant Conditioning of Visual Cortex responses in immobilized cats with medial forebrain bundle stimulation as reward. Arrow indicates time of stimulus delivery (light flash), and animal was rewarded for increasing the firing rates of the visual cortex evoked responses. Top shows unconditioned responses, and middle and bottom rows show conditioned responses. Notice increase in firing rate during the criterion period in the second and third rows (Shinkman et. al 1974).

"Throughout this paper, reference will be made to "conditioning" of individual neurons. However, what appears to be conditioned in these experiments is a movement, and the neuron under study is correlated with that movement."

Such operant conditioning techniques can also be done in preparations where movement is constricted by paralytic compounds. In 1974, Shinkman and his colleagues operantly conditioned neurons in the visual cortex of cats immobilized by gallamine triethiodide (Flaxedil, an acetylcholine muscle receptor antagonist) with electrical brain stimulation of the lateral hypothalamus as reward (Shinkman et al., 1974). Of 40 cells tested, 21 were found to be operantly conditionable (see Figure 3). Given recent papers showing visual cortex responses can be modulated by reward and attention effects (Fries et al., 2001, Shuler and Bear, 2006), the results are perhaps not surprising.

Other than Shinkman's visual cortex results, the majority of operant conditioning research seems to show that the subjects were not solely modulating their units; the animals were modulating their motor behavior. Work in the late 70's, in which the dorsal columns were severed in similar monkey motor cortex operant conditioning preparations (Wyler and Burchiel, 1978), drastically reduced the animals ability to do the task, and when the ventral roots were cut at the C_{5-7} level (Wyler et al., 1979), the monkeys were unable to do the task completely. The investigators in these studies concluded that the operant conditioning of motor units in previous work was most likely due to afferent feedback from the proprioceptive mechanoreceptors in the muscles feeding back up to the pyramidal cells of the motor cortex. The most compelling argument for this is that the monkey would sometimes move its flaccid arm with its good arm to drive the task, arguing effectively for the use of the proprioceptive feedback driving the motor cortex neurons.

Following this survey of the early literature, it is apparent that animals can be trained to modulate the activity of neurons of the neocortex, but the modulation may be the effect of afferent feedback of the limbs or attentional effects. However, these experiments did lay the groundwork for the hypothesis that perhaps operant conditioning techniques could be used to control a neuroprosthetic device (Schmidt, 1980). Knowledge of the fundamental neural coding of movement in the motor cortex had to advance before further development could occur.

Neural coding knowledge of the voluntary control of movement considerably advanced in the 1980's with Georgopoulos and Schwartz's work investigating population coding in the motor cortex (Georgopoulos et al., 1986, Georgopoulos et al., 1989). By serially recording motor cortex units over time in a monkey performing an eight-direction task, it was possible to reconstruct the trajectory of the monkey's arm using a cosine tuning function from the population of the total recorded ensemble (see Figure 4). Furthermore, in subsequent work in which the monkey had to move its arm in an opposite direction to that of a target, the population vectors of the motor cortex rotated from the direction of the actual target to the direction of the monkey's arm, providing compelling evidence that the responses of the motor cortex are adaptive at fast time courses (within 200-300 ms). Additional work by Schwartz's group and others has found that the motor
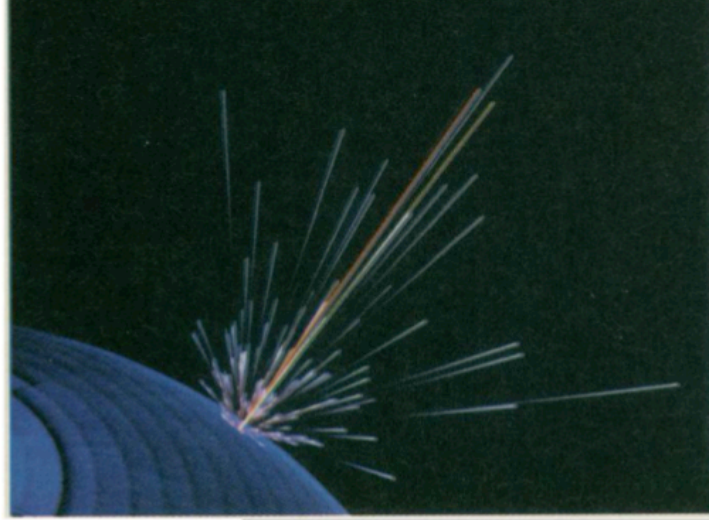
Figure 1.4: Population encoding of direction. White lines represent serially recorded single units' population vector contribution of a movement during a monkey reaching in one direction (yellow). Orange line depicts summed population vector of motor cortex firing rates, showing that the ensemble of the motor cortex faithfully encodes the movement direction (Georgopoulos et. al 1986).

cortex encodes acceleration (Georgopoulos et al., 1982), muscle force (Evarts, 1968), joint angles (Graziano et al., 2004), and higher-order functions as diverse as motor planning (Donoghue et al., 1998) and imagined movements (Hochberg et al., 2006).

Such increased, though still incomplete, understanding of the neural coding of movement made it possible to reconstruct limb trajectory in real-time, given improvements in multielectrode design. There has been a concurrent effort by electrical systems engineers to design and build advanced high-density multi-electrode arrays (Anderson et al., 1989, Guillory and Normann, 1999, Williams et al., 1999, Nicolelis et al., 2003). These efforts in improving microelectrode technology enabled the further developments in neuroprosthetics that occurred in the late 1990's and early 2000's.

The first demonstration of real-time limb trajectory reconstruction occurred in 1999 with the work by Chapin's group achieving real-time ensemble decoding of paw trajectory in rats. Rats were chronically implanted with microwire arrays in the motor cortex, and the rats were then trained to step onto a lever in order to drive the movement of a water-delivering lever arm that swung towards the rat's mouth. Once the rats learned this task, the multi-channel recording was decoded in real-time with a linear filter such
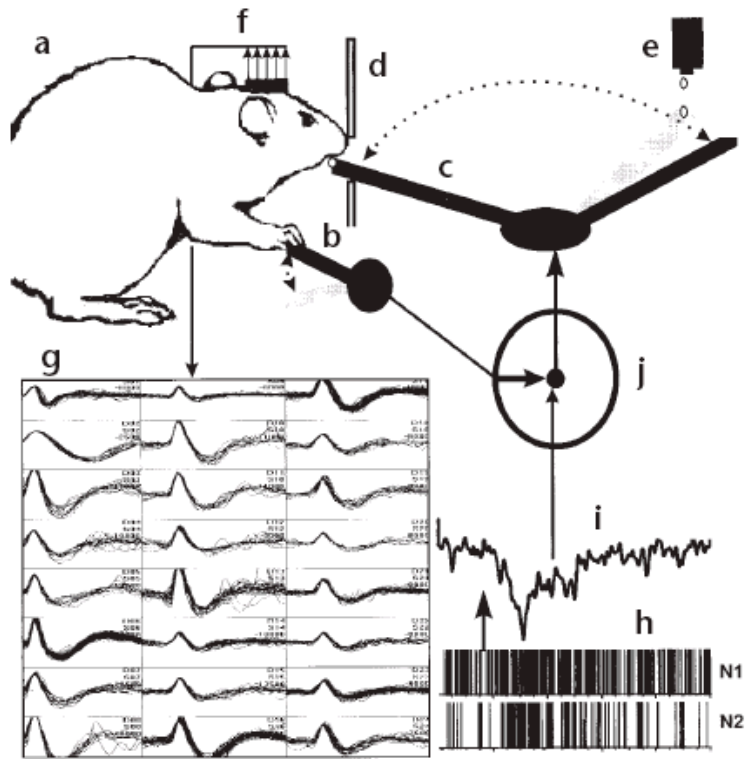
Figure 1.5: First control of a lever arm by cortical activity. Top shows behavioral apparatus whereby rat was trained to hit a lever to drive a water arm towards its mouth as ensemble activity of the paw area of motor cortex are simultaneously recorded and decoded. After algorithm calibration, the water arm was driven by the motor cortex ensemble activity alone (Chapin et. al 1999).

that the neural activity alone controlled the lever arm (Chapin et al., 1999). Four of the six rats were able to do the task, and often the rats would stop hitting the lever altogether and still be able to drive the water arm with their neural activity (see Figure 5).

The first indication that such technology could also be used in human patients occurred in the late 1990's with the work by neurosurgeon Phil Kennedy implanting quadriplegics with two-channel electrodes in the motor cortex. These patients were "locked-in," that is, unable to interact with their external world due to complete loss of limb control. Upon implantation of the electrodes, patients were able to slowly control a cursor to spell out responses to questions by modulating the activity of their motor cortex (Kennedy and Bakay, 1998, Kennedy et al., 2000).
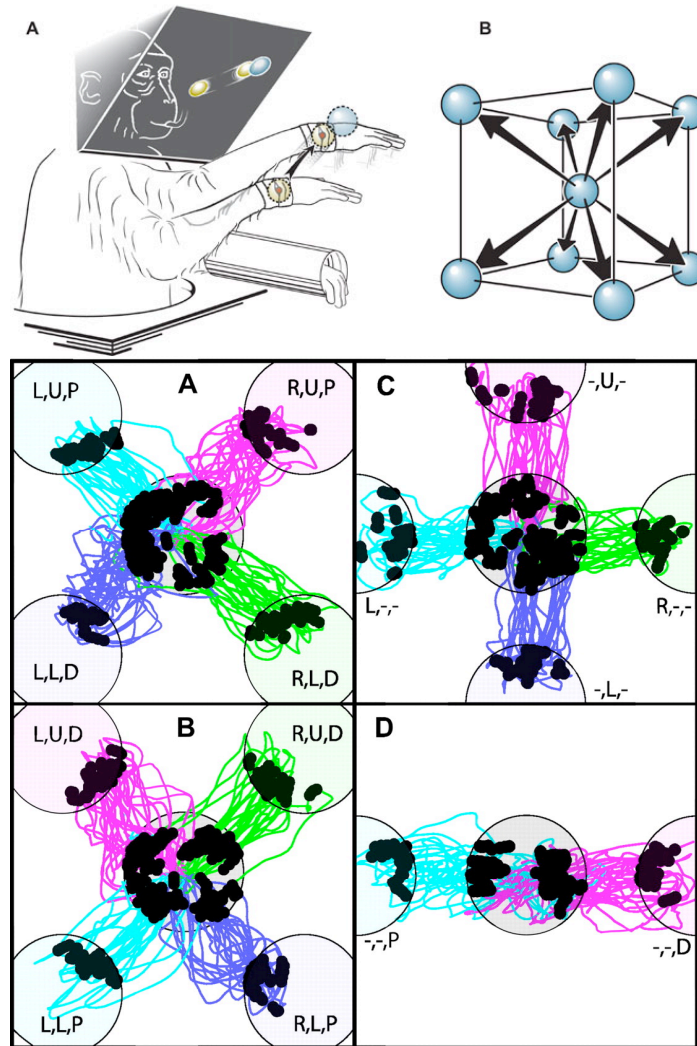
Figure 1.6: First 3D reconstruction of limb trajectory in real time via a virtual reality display. Top: Monkeys were trained to make limb movements to eight directions. Bottom: After population vector ensemble algorithm was calibrated, the cursor was controlled by the motor cortex activity. A, B: Trajectory of neural cursor to the eight targets during individual trials. C, D: Trajectory of neural cursor when novel targets were presented (Taylor et. al 2002).

Following these initial reports, neuroscientists and engineers of the past decade have improved the technology of limb and cursor control. The first 2D cursor control experiments (Serruya et al., 2002) initially decoded limb trajectory using approximately 30 neurons as a monkey moved a manipulandum across a two-dimensional surface to drive a cursor to a target on a computer screen. Once the coefficients were set for the decoding algorithm (set of linear filters regressing neural firing rate to hand trajectory), the monkey's neural activity then drove the cursor to the target. Of note is that the animal was immediately able to do the task under neural control, though the animal was still

9

making movements.

The first 3D cursor control (Taylor et al., 2002) was accomplished using a similar preparation as the (Serruya et al., 2002) work, but the monkey was moving its hands in one of eight directions in a three-dimensional center out task using a virtual reality display to move a cursor (see Figure 6). Again, once the monkeys learned the task and the algorithm coefficients were set (using an ensemble population vector algorithm), control of the 3D cursor was then driven by the motor cortex ensemble.

In the preceding experiments, cursor control was slow; time to target was often 1-2 seconds. A concurrent thread in neuroprosthetics research is improving the speed of the decoding. Work by (Santhanam et al., 2006) achieved decoding of target acquisition approaching 100-300 ms. Specifically, the monkey was implanted in a motor planning area of the dorsal premotor zone of the neocortex, and the monkey was trained to hold its finger in the center of a computer screen. A target would appear in the periphery of the screen, and after a delay period the monkey would then move its finger to the target. Since the premotor cortex is involved in movement planning, the neural activity would encode the endpoint of the target during the delay period before the monkey would actually begin to move its finger. In the neuroprosthetic mode of the task, the monkey's motor planning towards target would be decoded in real-time, and the monkey was rewarding for "planning" to move towards the target without actually moving its finger from the center of the screen. As the dorsal motor cortex was encoding endpoint location, and not trajectory, acquisition to target was much faster than traditional trajectory encoding neuroprosthetic experiments. The monkeys could rapidly attain targets within 100-300 ms of presentation.

Such sequence of developments culminated in 2006 with a report by J.P. Donoghue's group on two dimensional cursor control using cortical modulation in human quadriplegics (Hochberg et al., 2006). Patients were implanted with a 100 channel "Utah" array in the motor cortex, and the patients were asked to imagine various muscle flexions and extensions of the shoulder, arm, and hand. The investigators found, similar to previous work (Schnitzler et al., 1997), that the human motor cortex encodes imagined movements (see Figure 7). The motor cortex firing patterns were then fed into a control algorithm (the same linear filter as in the (Serruya et al., 2002) work discussed above),
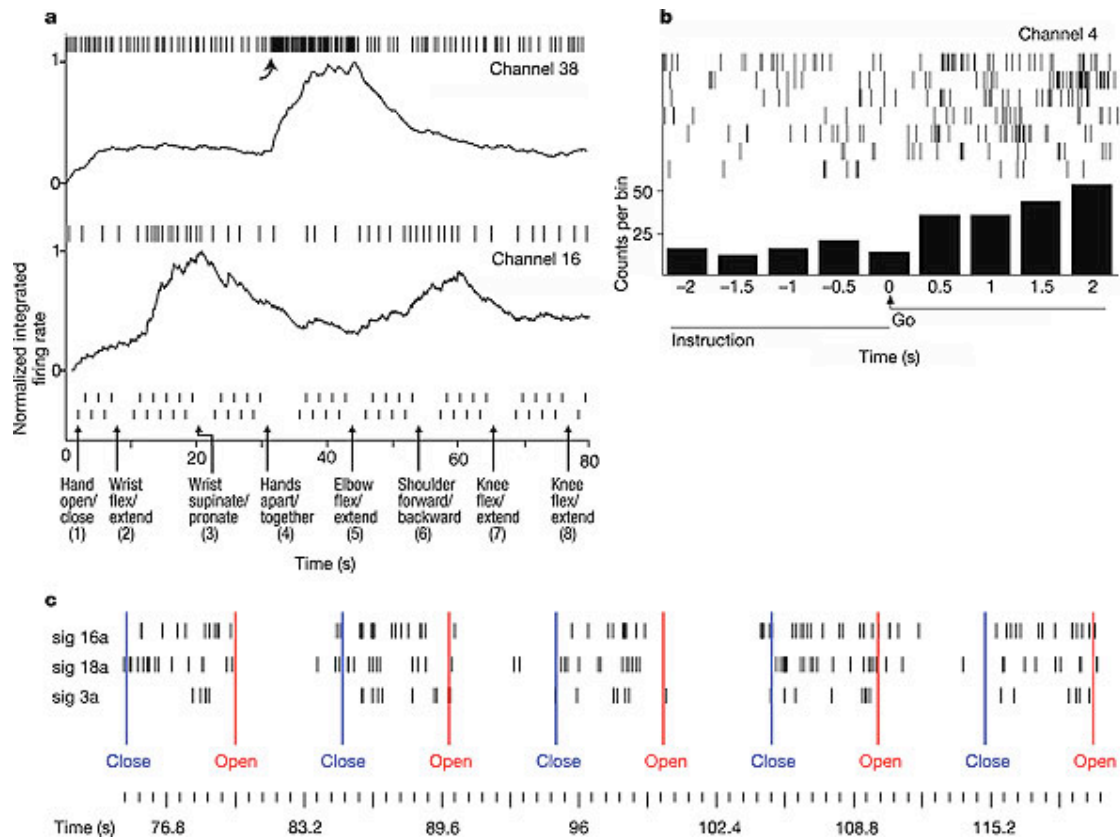
Figure 1.7: Decoding of Motor Cortex ensemble activity in a paralyzed human. A: Two neurons which modulated activity upon certain imagined movements. B: Rasters show increased neural discharge of another neuron that also increased firing during an imagined movement. C: Rasters show three neurons which are modulating when the patient imagined opening and closing his hand (Hochburg et. al 2006).

and the subject was able to control a computer cursor and various other devices. However, within 6 months the signal quality from the electrode arrays began to deteriorate, and the implants were ultimately removed.

Recently, Andrew Schwartz's group has successfully demonstrated a monkey controlling a robot arm to feed itself (Velliste et al., 2008). Monkeys were implanted bilaterally in the shoulder/elbow region of the motor cortex, the monkeys' arms were lightly restrained, and the monkeys would watch the robotic arm being controlled by technicians. The motor cortex would modulate with regards to the observed movement of the robotic arm, and these modulations would then be used to calibrate the cortical control algorithm, using the population vector described above (Taylor et al., 2002). Through slow shaping procedures, two monkeys learned to neurally control the arm with four degrees of freedom (x-axis plane, y-axis plane, z-axis plane, and the gripper) to grab
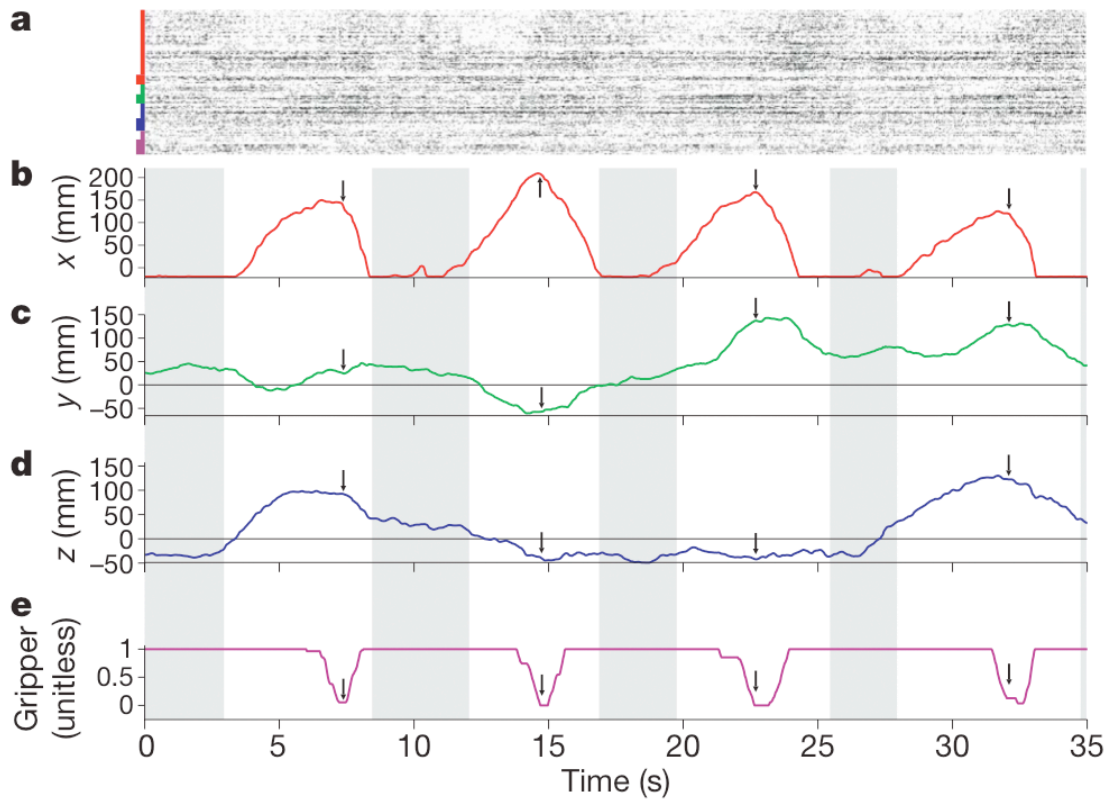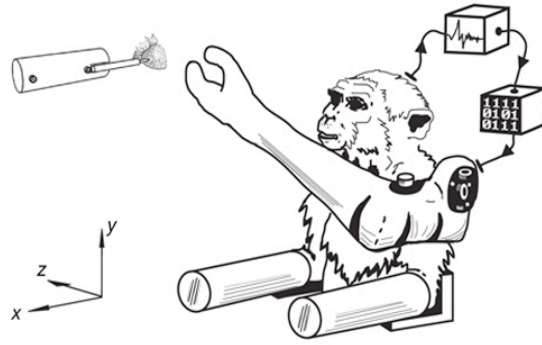
Figure 1.8: Use of the motor cortex ensemble activity to control a robotic arm. Top: Behavioral schematic. Bottom: a: Rasters of individual neurons during robotic arm control task. Colors of bars to left of rasters indicate what degree of freedom the respective neurons were controlling b: x-axis, c: y-axis, d: z-axis, e: gripper control pieces of food to feed itself. The only feedback the monkey had to control the arm was its visual observation of the moving arm (See Figure 8).

The above research summarizes the iterative developments in the new technology of neuroprosthetic devices. However, as with the development of any new technology, many scientific questions and engineering issues exist regarding the long-term manipulation of cortical signals for neuroprosthetics. Specifically, current unsolved

problems include: What is the optimal neocortical location for limb control? Can local field potentials be used as an additional information source? Would delivering feedback to the sensory cortex improve operator performance of a neuroprosthetic device? What is the optimal number of channels for controlling a neuroprosthetic device? How can the longevity of electrodes be improved? What is the best control algorithm?

This dissertation, using a rat model, focuses on three of the questions above regarding neuroprosthetic design, which are discussed below.

1) Alternative brain areas for control.

Many of the studies in the early 2000's focused on the motor cortex as the source of voluntary control signals for neuroprosthetics. If someone is injured by a traumatic spinal cord injury, the motor cortex is still alive and capable of generating movement command signals, as the work discussed above by (Kennedy et al., 2000) (Hochberg et al., 2006) has indeed shown. However, there are cases of paralysis that are not due to spinal cord injury. According to the Foundation for Spinal Cord Injury Prevention, Care & Cure (FSCIPCC), there are 225,000 to 296,000 paralyzed persons in the United States and a subsection of this population is paralyzed by upper motor neuron degenerative diseases, specifically: Amyotrophic Lateral Sclerosis (ALS) (which degenerates both upper and lower motor neurons) and Primary Lateral Sclerosis (PLS) (which affects only upper motor neurons.) According to the ALS Association and the Spastic Paraplegia Foundation (SPF), there are currently 30,000 cases of ALS and 2000 cases of PLS in the U.S. Thus, though the motor cortex may be the ideal candidate cortical site for a neuroprosthetic output signal due to its historically verified role in encoding voluntary movement (Fritsch and Hitzig, 1870, Fetz, 1969, Donoghue and Wise, 1982, Georgopoulos et al., 1988, Finger, 1994, Murthy and Fetz, 1996b, Donoghue et al., 1998), the motor cortex may not be ideal in a small target group of patients with upper motor neuron degeneration diseases.

In this subpopulation, prefrontal areas of the cortex may still be capable of generating a motor command signal to control a neuroprosthetic device. We examined the feasibility of alternative prefrontal areas for neuroprosthetic signals. The rat prefrontal cortex is not as extensive in functional localization as in primates, and only four
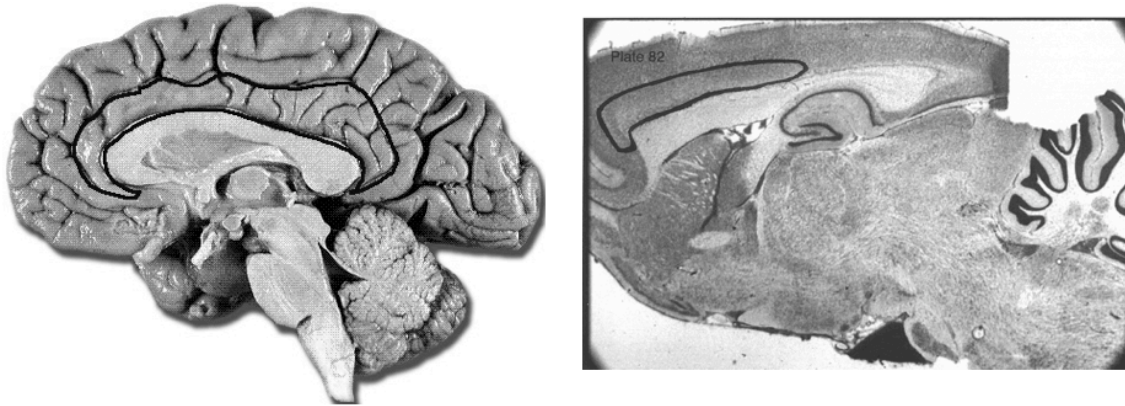
Figure 1.9: Location of the cingulate cortex (circled in black) in the human (left) and rat (right). Images from Paxinos and Watson (1998) and Brainstorm 2.0 neuroanatomy program.

candidate prefrontal brain areas of the rat were revealed in the literature (Uylings et al., 2003): the orbitalfrontal corticies, a "frontal association area," the cingulate cortex, and the infralimbic/prelimbic areas. These brain regions serve a number of different functions. The orbital corticies are used in odor discrimination and also receive spatial information from the hippocampus (Gallagher et al., 1999, Lipton et al., 1999). The prefrontal corticies (infralimbic and prelimbic) function in learning and memory, particularly extinction (Kurzina, 1990, Birrell and Brown, 2000, Dias and Honey, 2002, Milad and Quirk, 2002), and the function/existence of the frontal association area in rats is debated and not well characterized (Donoghue and Wise, 1982, Passingham et al., 1988).

The cingulate cortex is a compelling prospective candidate for an alternative command signal as it is involved in a wide diversity of behavior (see Figure 9 for comparative anatomy in rats and humans). In rats, the cingulate cortex is involved in behavioral inhibition (i.e. when rats have to hold a behavioral action, such as a nosepoke, for a certain delay period in order to be rewarded, the rats will make more errors with cingulate lesions (Muir et al., 1996)), stimulus-reward associations (Takenouchi et al., 1999, Cardinal et al., 2003), reward-based motor planning (Walton et al., 2003), trace-conditioning (Han et al., 2003), and attention in complex discrimination tasks (Bussey et al., 1997). In monkey electrophysiology studies, the cingulate cortex is involved in reward-based motor planning and reward expectancy (Shima and Tanji, 1998, Shidara

and Richmond, 2002, Hadland et al., 2003). In humans, the cingulate cortex has been correlated with many behavioral states, including loneliness (Eisenberger and Lieberman, 2004), religious experiences (Beauregard and Paquette, 2006), political persuasion (Amodio et al., 2007), error detection (Devinsky et al., 1995), pain perception (Harris et al., 2007), the placebo effect (Wager et al., 2004), and optimism (Sharot et al., 2007). Thus, though cingulate cortex function is diverse, its role in motor planning may make it a compelling alternative site for a control signal for a neuroprosthesis.

Given the diversity of the functions of the cingulate cortex, we investigated whether such a brain area can come under subject control for use in directing a neuroprosthetic device. Since clinical neuroprosthetics do not have access to known movement parameters corresponding to neural response properties, either due to paralysis or neurodegeneration, we adopted the approach of similar work in our group (Gage et al., 2005) by training the cingulate cortex without *a priori* knowledge of the neural response properties. A series of rats were implanted in the cingulate cortex, and the rats were trained to modulate the single unit cingulate cortex neural discharge to response to tone stimuli.

2) The Co-Variation of Spikes with the LFP and ECoG

The fundamental problem of chronically recording extracellular spikes is that the electrode needs to be 100-200 μm from the cell body to isolate the unit with sufficient signal-to-noise ratio (SNR) (Humphrey and Schmidt, 1990, Buzsaki, 2004). Such close proximity of the electrode to the biopotential source yields the problem that the area of brain tissue most likely to have a chronic foreign body response, and hence scar and kill the tissue surrounding the implant, contains the neurons of interest (Szarowski et al., 2003). Thus, there has been increasing interest in the community of recording from, and attempting to understand and decode, local field potentials and potentially using the signals to drive a neuroprosthetic controller (see Figure 10 for a representation of field potentials).

The physiological source of the field potentials (grouping LFPs, ECoGs, and EEGs in one broad class) is more difficult to identify than the physiological source of spikes. The primary source for many interpretations of the field potential are studies by
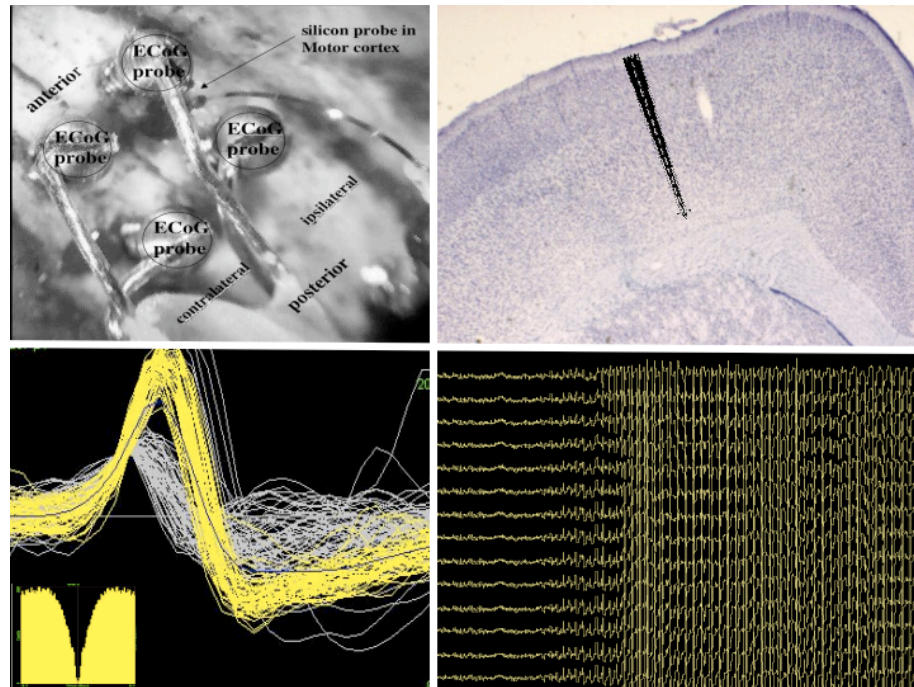
Figure 1.10: Demonstration of Neural Recordings. Top left shows a surgical image of a rat implanted with the "Michigan" silicon probe in the motor cortex. Top right shows overlay of single shank 16 site probe sampling all layers of motor cortex. Bottom left shows single unit (in yellow) isolated from an electrode site. Bottom right shows 16 LFPs simultaneously during a period of rat spindle oscillations.

(Freeman and Nicholson, 1975, Nicholson and Freeman, 1975, Mitzdorf, 1985); these reports examined field potentials using current source density analysis, pharmacological manipulations, and modeling studies. The conclusion of these studies was that the magnitude of the field potentials due to coherent excitatory post-synaptic potentials (EPSPs) is 2-3x higher than the contribution of coherent action potentials (APs), which in turn is orders of magnitude higher than the inhibitory post synaptic potentials (IPSPs). Mitzdorf and his colleagues concluded, however, that field potentials are more related to post-synaptic excitatory potentials than action potentials because 1) APs seldom occur simultaneously and last less than 2 ms, while synaptic potentials last 10 ms and are regionally localized, 2) The high frequency conductance changes of action potentials cause membrane dipoles with source/sink pairs too close to observe with field potentials, and 3) Action potentials at the soma are tripoles, which decay as $1/r^3$, rather than dipoles, which decay as $1/r^2$. Thus, it has become a common acceptance in the neurophysiology community that local field potentials in the neocortex are due to EPSPs.

What, if anything, do field potentials mean in terms of mechanistic use by the brain? The physical cause of field potential oscillations is still under debate, but work in the visual system of cats and monkeys has found that power in the gamma frequencies (30-70 Hz) is modulated by attention (Gray and Singer, 1989, Bekisz and Wrobel, 1999, Fries et al., 2001, Womelsdorf et al., 2006, Fries et al., 2008); specifically, the gamma power increases in the local field potential when recording from a receptive field of a visual stimulus of which an animal is attending to (see figures 11-12). Work has also found increased 15-20 Hz coherence between electrodes sites in the inferior temporal cortex in monkeys during correct performance of trials performing a delayed-match-to-sample task (Tallon-Baudry et al., 2004), and other groups have indeed shown increased coherence in specific frequencies between brain areas during specific behavioral tasks (Bekisz and Wrobel, 1999, Liang et al., 2002). These findings have led to the hypothesis that coherence in the local field potentials between brain regions is a method of cortical communication (Fries, 2005). Some groups have also reported increased coherence between motor cortex and muscle groups at 40-70 Hz in reaction time tasks (Schoffelen et al., 2005).

As local field potentials are recordable for longer duration than traditional extracellular unit recording methods (Murthy and Fetz, 1996b, Destexhe et al., 1999), and local field potentials do indeed modulate in behavioral tasks, it has been hypothesized that local field potentials could also be used to control a neuroprosthetic device (Galvan et al., 2001, Schwartz et al., 2006). There are only two short "prototype" level reports of local field potential modulation in humans (Kennedy et al., 2004a, Kennedy et al., 2004b). Demonstrating multiple degree-of-freedom (dof) control using LFPs is still an active and open subject of research for neural engineers.

A simultaneous thread in the neuroprosthetic field is electroencephalogram and electrocorticogram-based research in humans, led by Jonathan Wolpaw at the Wadsworth Center in Albany, NY, and Niels Birbaumer at the University of Tübingen in Germany. In this continuously ongoing work, human patients (both mobile and paralyzed) are trained to modulate their scalp recorded field potential activity (electroencephalogram, or EEG) to control a cursor on a computer screen (Birbaumer et al., 1999, Wolpaw and McFarland, 2004). However, such self-control of one's EEG takes months of training due

to fact that the EEG has a low signal-to-noise ratio (the skull serves as both a low pass filter and a resistor to the brain-related related potentials, causing brain signals picked up by scalp electrodes to be severely attenuated (Nunez and Srinivasan, 2006)). Multiple groups are now examining the feasibility of brain surface field potential recordings (electrocorticograms, or ECoG), both epidural and subdural, as a source of a neuroprosthetic control signal. In recent experiments using epileptic patients implanted with ECoG mapping arrays and largely immobilized in their hospital room, ECoG-based cursor control can occur within a half an hour of training (Leuthardt et al., 2004, Schalk et al., 2007, Schalk et al., 2008).
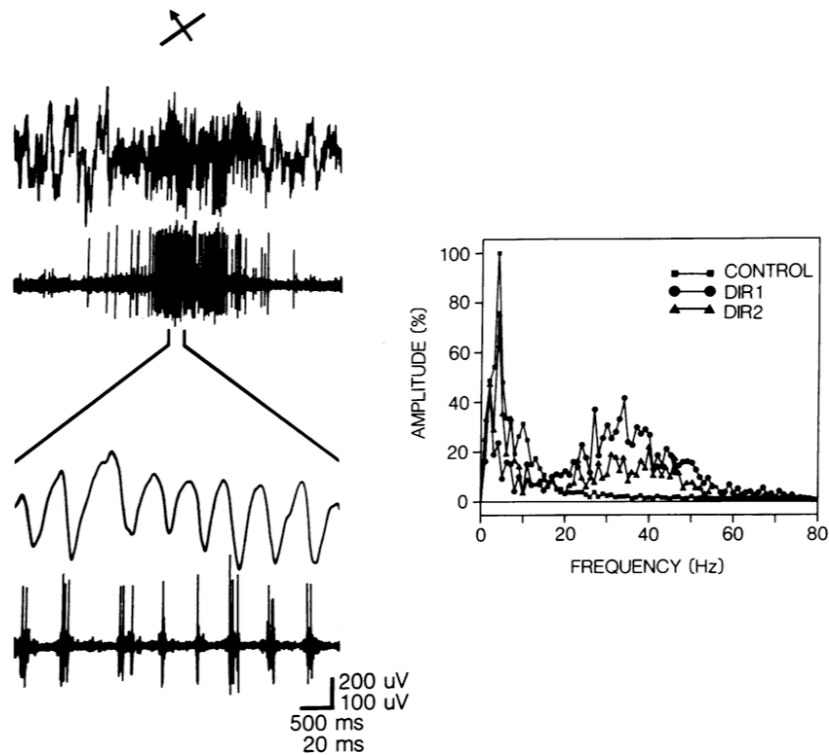
Figure 1.11: Increased Spiking with Gamma Synchrony in Visual Cortex of Cats. A moving bar was presented to the receptive field of a visual cortex unit in the awake cat. Notice increased high frequency components in the field potential (top) concurrent with increased spiking discharge in the neuron and the spikes fire in specific phases of the oscillations. Right: power spectral density of local field potential when visual cortex cells were presented the appropriate stimulus for the receptive fields. Notice decreased power in the <10 Hz frequencies and increased power in the 30-50 Hz frequencies (Gray and Singer 1989).
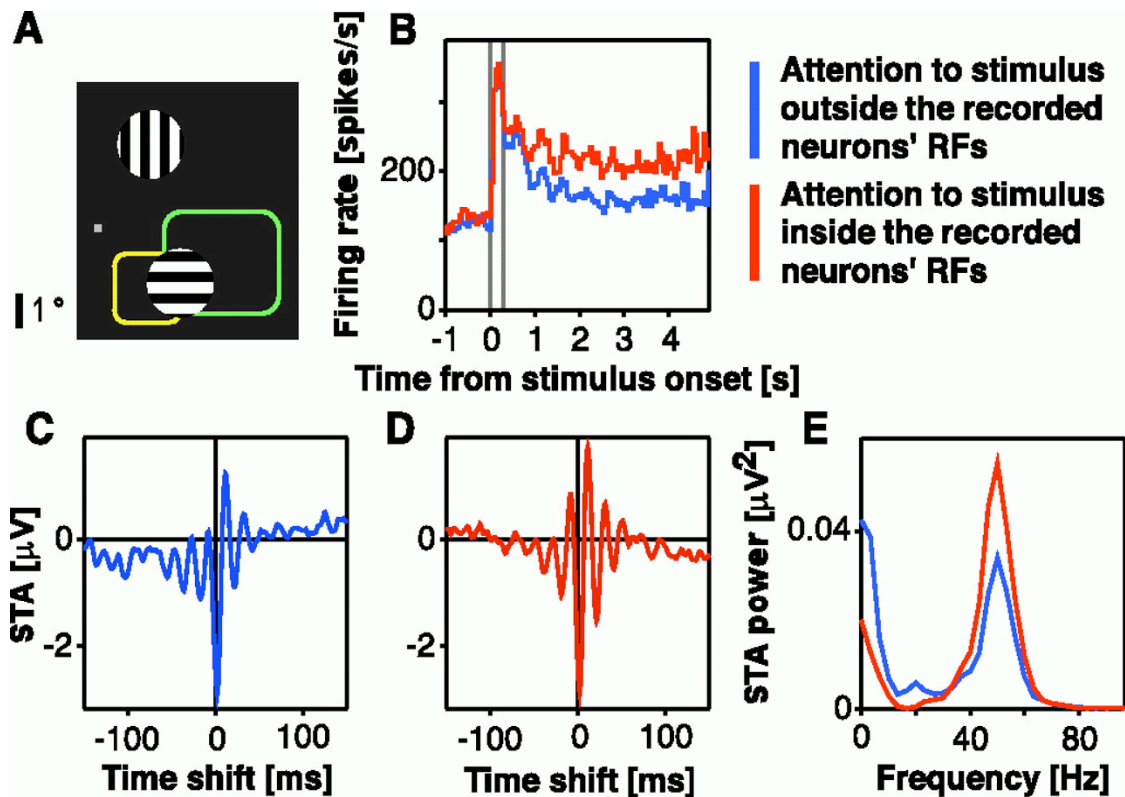
Figure 1.12: Increased spike and local field potential gamma band coherence as a function of attention. In this experiment, two neurons were isolated in monkey visual cortex, and the receptive fields were mapped. The monkey was required to attend to one of the stimuli during a delay period without moving its eyes. When a monkey was attending to a stimulus, there was increased coherence (represented by increased power in the spike triggered average (STA)) in the 40-70 Hz frequencies. B: Spiking response to stimulus when the monkey was attending versus not. C: Spike-triggered average of spike with LFP during delay period when the attention was outside the receptive field, and D: when the attended stimulus was inside the receptive field. E: the power spectrum of the respective spike-triggered averages (Fries et. al 2001).

ECoGs and LFPs may be more stable input signals than the spiking activity of single neurons, though spiking activity, when available, offers a finer resolution signal of the brain state activity (Schwartz 2008, unpublished observations). Therefore, combining the ECoGs, LFPs, and spiking activity may be the optimally stable, information-rich source for neuroprosthetic control signals. First the co-relationships between the field potentials and spikes need to be investigated. As the neocortex and hippocampus literature has indeed shown that spikes tend to fire in phase with certain frequency ranges of the field potential during specific behavioral epochs (Murthy and Fetz, 1996a, Fries et al., 2001, Womelsdorf et al., 2006, Kjelstrup et al., 2008) (see Figure 11), we
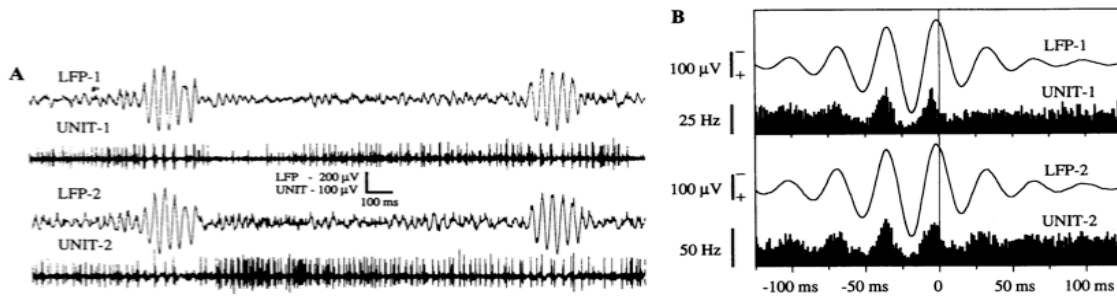
Figure 1.13: Correlations of spiking and local field potential activity in monkey motor cortex. A: Two spike/LFP pairs during periods when a monkey was exploring a puzzle box with its hands. Periods of spiking modulation and field potential oscillation are evident. B: Spike-triggered average of spikes with LFPs during periods of local field potential oscillation. Notice spikes are firing in phase with the 20 Hz oscillations of the motor cortex LFP (Murthy and Fetz 1996).

hypothesized that spikes of motor cortex neurons would also phase lock to specific frequencies of the field potential during different behavioral epochs.

The majority of neuroprosthetics target the motor cortex (for review, see (Schwartz, 2004); thus, we focused our attention on oscillations of the motor cortex during motor learning tasks. In monkeys, a "preparatory potential" of the 25-35 Hz beta rhythm occurs when monkeys are actively exploring or planning to move (Murthy and Fetz, 1996a, Murthy and Fetz, 1996b), and the single units isolated during these experiments indicated the spikes were phase-locking to the 25-35 Hz rhythm (See Figure 13). Other groups have found additional ~20 Hz potential modulation during the preparatory phase of movements in monkeys (Donoghue et al., 1998, Baker et al., 1999) and a quadriplegic human (Hochberg et al., 2006). In spite of this, it was recently found that <13 Hz frequency bands and 60-200 Hz frequency bands code for movement direction more accurately than 20-50 Hz in a center-out reaching task (Mehring et al., 2003, Mehring et al., 2004, Rickert et al., 2005). Moran and his colleagues additionally found high frequencies (50 – 200 Hz) in both ECoGs and LFPs encode movement direction in eight and four directions, respectively (Leuthardt et al., 2004, Heldman et al., 2006).

In order to investigate the dependence of spikes on field potentials, we sampled spikes, LFPs, and ECoGs simultaneously in a chronic preparation during multiple behavioral states: ketamine-induced anesthesia, a motor learning task, and a neuroprosthetic task. In the motor learning task, rats were trained to simultaneously place

both forepaws on levers on the cage floor while performing a simple nosepoke task and holding the position for 1-5 seconds. After the rats learned this task, the rats were then trained in "neuroprosthetic" mode whereby they had to modulate the spiking activity of cells in the motor cortex during the delay period in order to receive a food reward.

We hypothesized that as the spiking activity becomes more modulating and variant (from anesthetized → motor learning → neuroprosthetic mode), the synchronization of the spiking activity with the LFP and ECoG will progressively decrease in the low frequency range and increase in the high frequency range. Thus, perhaps the <15 Hz LFP activity will become independent of local spiking activity during the motor learning and neuroprosthetic tasks, where the spiking activity will become phase-locked to high frequency gamma LFP modulations.

3) Closing the Loop: Sensory Feedback with Simultaneous Motor Decoding.

Electrical stimulation of central nervous system tissue has been used extensively as a tool in neuroscience, most notably beginning in 1870 (Fritsch and Hitzig, 1870) with the discovery of the canine motor cortex. During the 1960's and onwards, electrical stimulation has been used in human patients as a tool for exploring perception (Penfield and Perot, 1963), for sensory replacement in the form of cochlear implants (for review, see (Moller, 2006)), and most recently as a treatment for Parkinson's disease by stimulating the subthalamic nucleus (Johnson et al., 2008).

Electrical stimulation is also being explored as a treatment for paralysis by stimulating musculature directly (for reviews, see (Morita et al., 2007, Popovic and Sinkjaer, 2007). Signals recorded from the sensory nerves of limbs are used as a feedback signal for the control of electrical stimulation of musculature (Popovic et al., 1993, Strange and Hoffer, 1999, Weber et al., 2007).

Microstimulation of neocortical tissue has also been used as an experimental tool to examine the neurophysiology of perception. Specifically, work in the somatosensory cortex of monkeys has shown that intracortical microstimulation (ICMS) patterns mimicking the natural neural patterns of vibration sensation of the fingertips results in identical performance in detection tasks (Romo et al., 2000). Work in rats has shown a distinct psychometric curve in response to current level of cortical microstimulation
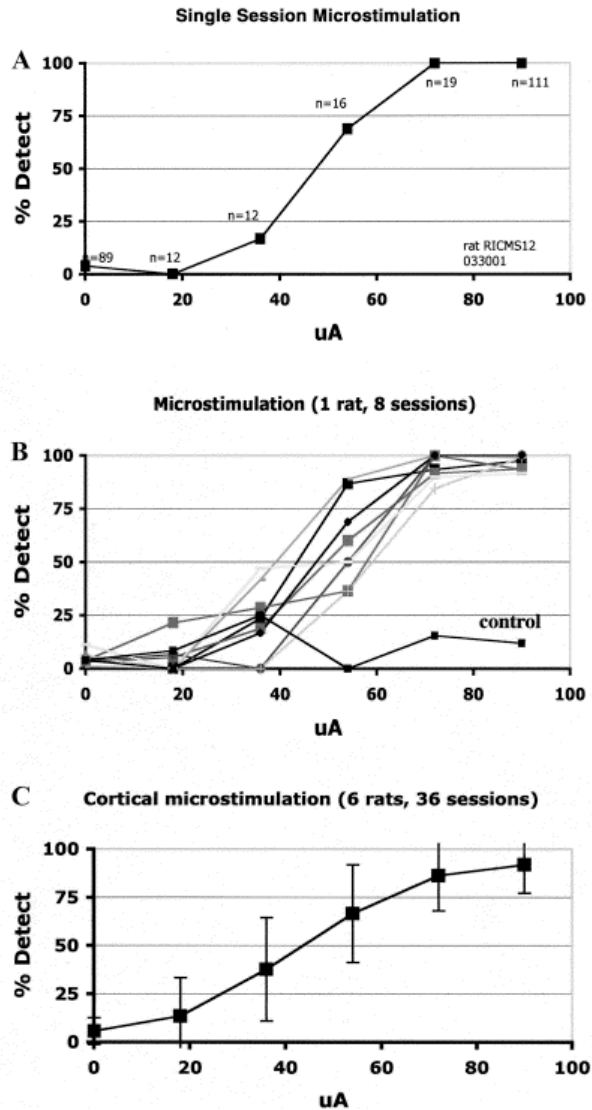
Figure 1.14: Detection of Microstimulation of Auditory Cortex. A: Psychometric function of 1 rat trained over multiple sessions to detect intracortical microstimulation (ICMS) of auditory cortex as a function of current amplitude. B: Pyschometric Curve of 1 rat over 8 sessions. Control shows when stimulator was turned off. C: Psychometric curves of 6 rats trained to detect cortical microstimulation of auditory cortex. All results compellingly show that rats can detect and respond to sensory cortex ICMS (Rousche et. al 2003).

(Rousche et al., 2003) (see Figure 14). Recent work has also shown that monkeys can be trained to detect and discriminate a variety of microstimulation codes in the somatosensory cortex: a rate based code (whereby the number of pulses between two different electrode channels is different), a detection code (whereby the monkeys responded to whether microstimulation was delivered or not), and a spatial code (whereby the monkey detected different sequences of electrodes being stimulated)

22

(Fitzsimmons et al., 2007). Typically, intracortical microstimulation is understood such that pulse rate affects the firing rate of neurons in the excited tissue and pulse amplitude affects the volume of stimulated excited tissue (i.e. higher amplitudes will excite a greater amount of tissue) (Merrill et al., 2005).

As the technology of neuroprosthetic devices improves, many groups foresee a need to implement the simultaneous use of haptic feedback via sensory cortex intracortical microstimulation (ICMS) to give a user more information on the "state" of a device controlled by his/her motor cortex ensemble recordings (Abbott, 2006, Fagg et al., 2007, Fitzsimmons et al., 2007, London et al., 2008). The majority of neuroprosthetic systems currently only offer feedback via a cursor on a screen, giving the user a visual correlate of the motor cortex ensemble activity (Serruya et al., 2002, Taylor et al., 2002, Carmena et al., 2003, Musallam et al., 2004, Lebedev et al., 2005, Hochberg et al., 2006, Santhanam et al., 2006). In the recent work by (Velliste et al., 2008), in which a monkey controlled a robotic arm to feed itself, the monkey had to watch the arm at all times in order to operate it. Though the monkey could still do the task, such visual feedback alone is crude. Many motor skills require more than visual feedback of the state of the limbs. Playing musical instruments, typing on a keyboard, and running all require force and haptic feedback.

Thus, in an ideal artificial neuroprosthetic limb, a user would be able to receive all of the feedback a natural human limb receives via the peripheral sensory nervous system of muscle force, joint dynamics, etc. Indeed, some groups are beginning to study ICMS of somatosensory cortex with the ultimate goal of combining it with motor cortex ensemble decoding (Fitzsimmons et al., 2007, London et al., 2008). To date, however, no groups have combined ICMS of sensory cortex simultaneously with motor cortex ensemble decoding.

In the final work of this dissertation, ICMS of sensory neocortex was used as a feedback signal in a subject simultaneously trained to modulate its motor cortex ensemble. Electrode arrays were implanted in both the motor and visual corticies of rats. Through a series of iterative development steps as algorithms and hardware were continually improved, rats were trained in motor ensemble modulation tasks where the "go" stimulus to initiate a trial consisted of direct current injection into the visual cortex.

The ensemble dynamics of the motor cortex firing rates were then linearly transformed into visual cortex ICMS signals delivered as real-time feedback to the rats.

<div align="center">*****</div>

This dissertation covers three components of contemporary neuroprosthetic systems design: alternative cortical areas (chapter 2), alternative cortical signals (chapter 3), and sensory cortex feedback (chapter 4). The following three chapters describe these three experiments in detail. At the time of this dissertation completion, chapter 2 has been published, chapter 3 is in preparation for manuscript submission, and chapter 4 has been submitted.

References:

ABBOTT, A. (2006) Neuroprosthetics: in search of the sixth sense. *Nature,* 442**,** 125-7.

AMODIO, D. M., JOST, J. T., MASTER, S. L. & YEE, C. M. (2007) Neurocognitive correlates of liberalism and conservatism. *Nat Neurosci,* 10**,** 1246-7.

ANDERSON, D. J., NAJAFI, K., TANGHE, S. J., EVANS, D. A., LEVY, K. L., HETKE, J. F., XUE, X. L., ZAPPIA, J. J. & WISE, K. D. (1989) Batch-fabricated thin-film electrodes for stimulation of the central auditory system. *IEEE Trans Biomed Eng,* 36**,** 693-704.

BAKER, S. N., KILNER, J. M., PINCHES, E. M. & LEMON, R. N. (1999) The role of synchrony and oscillations in the motor output. *Exp Brain Res,* 128**,** 109-17.

BEAUREGARD, M. & PAQUETTE, V. (2006) Neural correlates of a mystical experience in Carmelite nuns. *Neurosci Lett,* 405**,** 186-90.

BEKISZ, M. & WROBEL, A. (1999) Coupling of beta and gamma activity in corticothalamic system of cats attending to visual stimuli. *Neuroreport,* 10**,** 3589-94.

BIRBAUMER, N., GHANAYIM, N., HINTERBERGER, T., IVERSEN, I., KOTCHOUBEY, B., KUBLER, A., PERELMOUTER, J., TAUB, E. & FLOR, H. (1999) A spelling device for the paralysed. *Nature,* 398**,** 297-8.

BIRRELL, J. M. & BROWN, V. J. (2000) Medial frontal cortex mediates perceptual attentional set shifting in the rat. *J Neurosci,* 20**,** 4320-4.

BUSSEY, T. J., MUIR, J. L., EVERITT, B. J. & ROBBINS, T. W. (1997) Triple dissociation of anterior cingulate, posterior cingulate, and medial frontal cortices on visual discrimination tasks using a touchscreen testing procedure for the rat. *Behav Neurosci,* 111**,** 920-36.

BUZSAKI, G. (2004) Large-scale recording of neuronal ensembles. *Nat Neurosci,* 7**,** 446-51.

CARDINAL, R. N., PARKINSON, J. A., MARBINI, H. D., TONER, A. J., BUSSEY, T. J., ROBBINS, T. W. & EVERITT, B. J. (2003) Role of the anterior cingulate cortex in the control over behavior by Pavlovian conditioned stimuli in rats. *Behav Neurosci,* 117**,** 566-87.

CARMENA, J. M., LEBEDEV, M. A., CRIST, R. E., O'DOHERTY, J. E., SANTUCCI, D. M., DIMITROV, D., PATIL, P. G., HENRIQUEZ, C. S. & NICOLELIS, M. A. (2003) Learning to control a brain-machine interface for reaching and grasping by primates. *PLoS Biol,* 1**,** E42.

CHAPIN, J. K., MOXON, K. A., MARKOWITZ, R. S. & NICOLELIS, M. A. (1999) Real-time control of a robot arm using simultaneously recorded neurons in the motor cortex. *Nat Neurosci,* 2**,** 664-70.

DESTEXHE, A., CONTRERAS, D. & STERIADE, M. (1999) Spatiotemporal analysis of local field potentials and unit discharges in cat cerebral cortex during natural wake and sleep states. *J Neurosci,* 19**,** 4595-608.

DEVINSKY, O., MORRELL, M. J. & VOGT, B. A. (1995) Contributions of anterior cingulate cortex to behaviour. *Brain,* 118 (Pt 1)**,** 279-306.

DIAS, R. & HONEY, R. C. (2002) Involvement of the rat medial prefrontal cortex in novelty detection. *Behav Neurosci,* 116**,** 498-503.

DONOGHUE, J. P., SANES, J. N., HATSOPOULOS, N. G. & GAAL, G. (1998) Neural discharge and local field potential oscillations in primate motor cortex during voluntary movements. *J Neurophysiol,* 79**,** 159-73.

DONOGHUE, J. P. & WISE, S. P. (1982) The motor cortex of the rat: cytoarchitecture and microstimulation mapping. *J Comp Neurol,* 212**,** 76-88.

EISENBERGER, N. I. & LIEBERMAN, M. D. (2004) Why rejection hurts: a common neural alarm system for physical and social pain. *Trends Cogn Sci,* 8**,** 294-300.

EVARTS, E. V. (1968) Relation of pyramidal tract activity to force exerted during voluntary movement. *J Neurophysiol,* 31**,** 14-27.

FAGG, A. H., HATSOPOULOS, N. G., DE LAFUENTE, V., MOXON, K. A., NEMATI, S., REBESCO, J. M., ROMO, R., SOLLA, S. A., REIMER, J., TKACH, D., POHLMEYER, E. A. & MILLER, L. E. (2007) Biomimetic brain machine interfaces for the control of movement. *J Neurosci,* 27**,** 11842-6.

FETZ, E. E. (1969) Operant conditioning of cortical unit activity. *Science,* 163**,** 955-8.

FETZ, E. E. & FINOCCHIO, D. V. (1971) Operant conditioning of specific patterns of neural and muscular activity. *Science,* 174**,** 431-5.

FINGER, S. (1994) *Origins of neuroscience : a history of explorations into brain function,* New York, Oxford University Press.

FITZSIMMONS, N. A., DRAKE, W., HANSON, T. L., LEBEDEV, M. A. & NICOLELIS, M. A. (2007) Primate reaching cued by multichannel spatiotemporal cortical microstimulation. *J Neurosci,* 27**,** 5593-602.

FREEMAN, J. A. & NICHOLSON, C. (1975) Experimental optimization of current source-density technique for anuran cerebellum. *J Neurophysiol,* 38**,** 369-82.

FRIES, P. (2005) A mechanism for cognitive dynamics: neuronal communication through neuronal coherence. *Trends Cogn Sci,* 9**,** 474-80.

FRIES, P., REYNOLDS, J. H., RORIE, A. E. & DESIMONE, R. (2001) Modulation of oscillatory neuronal synchronization by selective visual attention. *Science,* 291**,** 1560-3.

FRIES, P., WOMELSDORF, T., OOSTENVELD, R. & DESIMONE, R. (2008) The effects of visual stimulation and selective visual attention on rhythmic neuronal synchronization in macaque area V4. *J Neurosci,* 28**,** 4823-35.

FRITSCH, G. & HITZIG, E. (1870) Uber die elektrische erregbarkeit des grosshirns. *Archiv fur Anatomie und Physiologie.*

GAGE, G. J., LUDWIG, K. A., OTTO, K. J., IONIDES, E. L. & KIPKE, D. R. (2005) Naive coadaptive cortical control. *J Neural Eng,* 2**,** 52-63.

GALLAGHER, M., MCMAHAN, R. W. & SCHOENBAUM, G. (1999) Orbitofrontal cortex and representation of incentive value in associative learning. *J Neurosci,* 19**,** 6610-4.

GALVAN, V. V., CHEN, J. & WEINBERGER, N. M. (2001) Long-term frequency tuning of local field potentials in the auditory cortex of the waking guinea pig. *J Assoc Res Otolaryngol,* 2**,** 199-215.

GEORGOPOULOS, A. P., KALASKA, J. F., CAMINITI, R. & MASSEY, J. T. (1982) On the relations between the direction of two-dimensional arm movements and cell discharge in primate motor cortex. *J Neurosci,* 2**,** 1527-37.

GEORGOPOULOS, A. P., KETTNER, R. E. & SCHWARTZ, A. B. (1988) Primate motor cortex and free arm movements to visual targets in three-dimensional

space. II. Coding of the direction of movement by a neuronal population. *J Neurosci,* 8, 2928-37.

GEORGOPOULOS, A. P., LURITO, J. T., PETRIDES, M., SCHWARTZ, A. B. & MASSEY, J. T. (1989) Mental rotation of the neuronal population vector. *Science,* 243, 234-6.

GEORGOPOULOS, A. P., SCHWARTZ, A. B. & KETTNER, R. E. (1986) Neuronal population coding of movement direction. *Science,* 233, 1416-9.

GRAY, C. M. & SINGER, W. (1989) Stimulus-specific neuronal oscillations in orientation columns of cat visual cortex. *Proc Natl Acad Sci U S A,* 86, 1698-702.

GRAZIANO, M. S., PATEL, K. T. & TAYLOR, C. S. (2004) Mapping from motor cortex to biceps and triceps altered by elbow angle. *J Neurophysiol,* 92, 395-407.

GUILLORY, K. S. & NORMANN, R. A. (1999) A 100-channel system for real time detection and storage of extracellular spike waveforms. *J Neurosci Methods,* 91, 21-9.

HADLAND, K. A., RUSHWORTH, M. F., GAFFAN, D. & PASSINGHAM, R. E. (2003) The anterior cingulate and reward-guided selection of actions. *J Neurophysiol,* 89, 1161-4.

HAN, C. J., O'TUATHAIGH, C. M., VAN TRIGT, L., QUINN, J. J., FANSELOW, M. S., MONGEAU, R., KOCH, C. & ANDERSON, D. J. (2003) Trace but not delay fear conditioning requires attention and the anterior cingulate cortex. *Proc Natl Acad Sci U S A,* 100, 13087-92.

HARRIS, R. E., CLAUW, D. J., SCOTT, D. J., MCLEAN, S. A., GRACELY, R. H. & ZUBIETA, J. K. (2007) Decreased central mu-opioid receptor availability in fibromyalgia. *J Neurosci,* 27, 10000-6.

HELDMAN, D. A., WANG, W., CHAN, S. S. & MORAN, D. W. (2006) Local field potential spectral tuning in motor cortex during reaching. *IEEE Trans Neural Syst Rehabil Eng,* 14, 180-3.

HOCHBERG, L. R., SERRUYA, M. D., FRIEHS, G. M., MUKAND, J. A., SALEH, M., CAPLAN, A. H., BRANNER, A., CHEN, D., PENN, R. D. & DONOGHUE, J. P. (2006) Neuronal ensemble control of prosthetic devices by a human with tetraplegia. *Nature,* 442, 164-71.

HUMPHREY, D. R. & SCHMIDT, E. M. (1990) Extracellular single-unit recording methods. IN BOULTON, A. A., BAKER, G. B. & VANDERWORLD, C. H. (Eds.) *Neurophysiological Techniques: Applications to Neural Systems.* Humana Press.

JOHNSON, M. D., MIOCINOVIC, S., MCINTYRE, C. C. & VITEK, J. L. (2008) Mechanisms and targets of deep brain stimulation in movement disorders. *Neurotherapeutics,* 5, 294-308.

KENNEDY, P., ANDREASEN, D., EHIRIM, P., KING, B., KIRBY, T., MAO, H. & MOORE, M. (2004a) Using human extra-cortical local field potentials to control a switch. *J Neural Eng,* 1, 72-7.

KENNEDY, P. R. & BAKAY, R. A. (1998) Restoration of neural output from a paralyzed patient by a direct brain connection. *Neuroreport,* 9, 1707-11.

KENNEDY, P. R., BAKAY, R. A., MOORE, M. M., ADAMS, K. & GOLDWAITHE, J. (2000) Direct control of a computer from the human central nervous system. *IEEE Trans Rehabil Eng,* 8, 198-202.

KENNEDY, P. R., KIRBY, M. T., MOORE, M. M., KING, B. & MALLORY, A. (2004b) Computer control using human intracortical local field potentials. *IEEE Trans Neural Syst Rehabil Eng,* 12**,** 339-44.

KJELSTRUP, K. B., SOLSTAD, T., BRUN, V. H., HAFTING, T., LEUTGEB, S., WITTER, M. P., MOSER, E. I. & MOSER, M. B. (2008) Finite scale of spatial representation in the hippocampus. *Science,* 321**,** 140-3.

KURZINA, N. P. (1990) Neuronal activity of medial wall of frontal cerebral cortex of rats at various stages of learning. *Neurosci Behav Physiol,* 20**,** 535-40.

LEBEDEV, M. A., CARMENA, J. M., O'DOHERTY, J. E., ZACKSENHOUSE, M., HENRIQUEZ, C. S., PRINCIPE, J. C. & NICOLELIS, M. A. (2005) Cortical ensemble adaptation to represent velocity of an artificial actuator controlled by a brain-machine interface. *J Neurosci,* 25**,** 4681-93.

LEUTHARDT, E. C., SCHALK, G., WOLPAW, J. R., OJEMANN, J. G. & MORAN, D. W. (2004) A brain-computer interface using electrocorticographic signals in humans. *J Neural Eng,* 1**,** 63-71.

LIANG, H., BRESSLER, S. L., DING, M., TRUCCOLO, W. A. & NAKAMURA, R. (2002) Synchronized activity in prefrontal cortex during anticipation of visuomotor processing. *Neuroreport,* 13**,** 2011-5.

LIPTON, P. A., ALVAREZ, P. & EICHENBAUM, H. (1999) Crossmodal associative memory representations in rodent orbitofrontal cortex. *Neuron,* 22**,** 349-59.

LONDON, B. M., JORDAN, L. R., JACKSON, C. R. & MILLER, L. E. (2008) Electrical stimulation of the proprioceptive cortex (area 3a) used to instruct a behaving monkey. *IEEE Trans Neural Syst Rehabil Eng,* 16**,** 32-6.

MEHRING, C., NAWROT, M. P., DE OLIVEIRA, S. C., VAADIA, E., SCHULZE-BONHAGE, A., AERTSEN, A. & BALL, T. (2004) Comparing information about arm movement direction in single channels of local and epicortical field potentials from monkey and human motor cortex. *J Physiol Paris,* 98**,** 498-506.

MEHRING, C., RICKERT, J., VAADIA, E., CARDOSA DE OLIVEIRA, S., AERTSEN, A. & ROTTER, S. (2003) Inference of hand movements from local field potentials in monkey motor cortex. *Nat Neurosci,* 6**,** 1253-4.

MERRILL, D. R., BIKSON, M. & JEFFERYS, J. G. (2005) Electrical stimulation of excitable tissue: design of efficacious and safe protocols. *J Neurosci Methods,* 141**,** 171-98.

MILAD, M. R. & QUIRK, G. J. (2002) Neurons in medial prefrontal cortex signal memory for fear extinction. *Nature,* 420**,** 70-4.

MITZDORF, U. (1985) Current source-density method and application in cat cerebral cortex: investigation of evoked potentials and EEG phenomena. *Physiol Rev,* 65**,** 37-100.

MOLLER, A. R. (2006) History of cochlear implants and auditory brainstem implants. *Adv Otorhinolaryngol,* 64**,** 1-10.

MORITA, I., KEITH, M. W. & KANNO, T. (2007) Reconstruction of upper limb motor function using functional electrical stimulation (FES). *Acta Neurochir Suppl,* 97**,** 403-7.

MUIR, J. L., EVERITT, B. J. & ROBBINS, T. W. (1996) The cerebral cortex of the rat and visual attentional function: dissociable effects of mediofrontal, cingulate,

anterior dorsolateral, and parietal cortex lesions on a five-choice serial reaction time task. *Cereb Cortex,* 6**,** 470-81.

MURTHY, V. N. & FETZ, E. E. (1996a) Oscillatory activity in sensorimotor cortex of awake monkeys: synchronization of local field potentials and relation to behavior. *J Neurophysiol,* 76**,** 3949-67.

MURTHY, V. N. & FETZ, E. E. (1996b) Synchronization of neurons during local field potential oscillations in sensorimotor cortex of awake monkeys. *J Neurophysiol,* 76**,** 3968-82.

MUSALLAM, S., CORNEIL, B. D., GREGER, B., SCHERBERGER, H. & ANDERSEN, R. A. (2004) Cognitive control signals for neural prosthetics. *Science,* 305**,** 258-62.

NICHOLSON, C. & FREEMAN, J. A. (1975) Theory of current source-density analysis and determination of conductivity tensor for anuran cerebellum. *J Neurophysiol,* 38**,** 356-68.

NICOLELIS, M. A., DIMITROV, D., CARMENA, J. M., CRIST, R., LEHEW, G., KRALIK, J. D. & WISE, S. P. (2003) Chronic, multisite, multielectrode recordings in macaque monkeys. *Proc Natl Acad Sci U S A,* 100**,** 11041-6.

NUNEZ, P. L. & SRINIVASAN, R. (2006) *Electric Fields of the Brain,* New York, New York, Oxford University Press.

OLDS, J. (1965) Operant conditioning of single unit responses. *Proc XXIII Int Congress Physiol Sci*. Tokyo.

PASSINGHAM, R. E., MYERS, C., RAWLINS, N., LIGHTFOOT, V. & FEARN, S. (1988) Premotor cortex in the rat. *Behav Neurosci,* 102**,** 101-9.

PENFIELD, W. & PEROT, P. (1963) The Brain's Record of Auditory and Visual Experience. A Final Summary and Discussion. *Brain,* 86**,** 595-696.

POPOVIC, D. B. & SINKJAER, T. (2007) Neuromodulation of lower limb monoparesis: functional electrical therapy of walking. *Acta Neurochir Suppl,* 97**,** 387-93.

POPOVIC, D. B., STEIN, R. B., JOVANOVIC, K. L., DAI, R., KOSTOV, A. & ARMSTRONG, W. W. (1993) Sensory nerve recording for closed-loop control to restore motor functions. *IEEE Trans Biomed Eng,* 40**,** 1024-31.

RICKERT, J., OLIVEIRA, S. C., VAADIA, E., AERTSEN, A., ROTTER, S. & MEHRING, C. (2005) Encoding of movement direction in different frequency ranges of motor cortical local field potentials. *J Neurosci,* 25**,** 8815-24.

ROMO, R., HERNANDEZ, A., ZAINOS, A., BRODY, C. D. & LEMUS, L. (2000) Sensing without touching: psychophysical performance based on cortical microstimulation. *Neuron,* 26**,** 273-8.

ROUSCHE, P. J., OTTO, K. J., REILLY, M. P. & KIPKE, D. R. (2003) Single electrode micro-stimulation of rat auditory cortex: an evaluation of behavioral performance. *Hear Res,* 179**,** 62-71.

SANTHANAM, G., RYU, S. I., YU, B. M., AFSHAR, A. & SHENOY, K. V. (2006) A high-performance brain-computer interface. *Nature,* 442**,** 195-8.

SCHALK, G., KUBANEK, J., MILLER, K. J., ANDERSON, N. R., LEUTHARDT, E. C., OJEMANN, J. G., LIMBRICK, D., MORAN, D., GERHARDT, L. A. & WOLPAW, J. R. (2007) Decoding two-dimensional movement trajectories using electrocorticographic signals in humans. *J Neural Eng,* 4**,** 264-75.

SCHALK, G., MILLER, K. J., ANDERSON, N. R., WILSON, J. A., SMYTH, M. D., OJEMANN, J. G., MORAN, D. W., WOLPAW, J. R. & LEUTHARDT, E. C. (2008) Two-dimensional movement control using electrocorticographic signals in humans. *J Neural Eng,* 5**,** 75-84.

SCHMIDT, E. M. (1980) Single neuron recording from motor cortex as a possible source of signals for control of external devices. *Ann Biomed Eng,* 8**,** 339-49.

SCHMIDT, E. M., BAK, M. J., MCINTOSH, J. S. & THOMAS, J. S. (1977) Operant conditioning of firing patterns in monkey cortical neurons. *Exp Neurol,* 54**,** 467-77.

SCHMIDT, E. M., MCINTOSH, J. S., DURELLI, L. & BAK, M. J. (1978) Fine control of operantly conditioned firing patterns of cortical neurons. *Exp Neurol,* 61**,** 349-69.

SCHNITZLER, A., SALENIUS, S., SALMELIN, R., JOUSMAKI, V. & HARI, R. (1997) Involvement of primary motor cortex in motor imagery: a neuromagnetic study. *Neuroimage,* 6**,** 201-8.

SCHOFFELEN, J. M., OOSTENVELD, R. & FRIES, P. (2005) Neuronal coherence as a mechanism of effective corticospinal interaction. *Science,* 308**,** 111-3.

SCHWARTZ, A. B. (2004) Cortical neural prosthetics. *Annu Rev Neurosci,* 27**,** 487-507.

SCHWARTZ, A. B., CUI, X. T., WEBER, D. J. & MORAN, D. W. (2006) Brain-controlled interfaces: movement restoration with neural prosthetics. *Neuron,* 52**,** 205-20.

SERRUYA, M. D., HATSOPOULOS, N. G., PANINSKI, L., FELLOWS, M. R. & DONOGHUE, J. P. (2002) Instant neural control of a movement signal. *Nature,* 416**,** 141-2.

SHAROT, T., RICCARDI, A. M., RAIO, C. M. & PHELPS, E. A. (2007) Neural mechanisms mediating optimism bias. *Nature,* 450**,** 102-5.

SHIDARA, M. & RICHMOND, B. J. (2002) Anterior cingulate: single neuronal signals related to degree of reward expectancy. *Science,* 296**,** 1709-11.

SHIMA, K. & TANJI, J. (1998) Role for cingulate motor area cells in voluntary movement selection based on reward. *Science,* 282**,** 1335-8.

SHINKMAN, P. G., BRUCE, C. J. & PFINGST, B. E. (1974) Operant conditioning of single-unit response patterns in visual cortex. *Science,* 184**,** 1194-6.

SHULER, M. G. & BEAR, M. F. (2006) Reward timing in the primary visual cortex. *Science,* 311**,** 1606-9.

STRANGE, K. D. & HOFFER, J. A. (1999) Restoration of use of paralyzed limb muscles using sensory nerve signals for state control of FES-assisted walking. *IEEE Trans Rehabil Eng,* 7**,** 289-300.

SZAROWSKI, D. H., ANDERSEN, M. D., RETTERER, S., SPENCE, A. J., ISAACSON, M., CRAIGHEAD, H. G., TURNER, J. N. & SHAIN, W. (2003) Brain responses to micro-machined silicon devices. *Brain Res,* 983**,** 23-35.

TAKENOUCHI, K., NISHIJO, H., UWANO, T., TAMURA, R., TAKIGAWA, M. & ONO, T. (1999) Emotional and behavioral correlates of the anterior cingulate cortex during associative learning in rats. *Neuroscience,* 93**,** 1271-87.

TALLON-BAUDRY, C., MANDON, S., FREIWALD, W. A. & KREITER, A. K. (2004) Oscillatory synchrony in the monkey temporal lobe correlates with performance in a visual short-term memory task. *Cereb Cortex,* 14**,** 713-20.

TAYLOR, D. M., TILLERY, S. I. & SCHWARTZ, A. B. (2002) Direct cortical control of 3D neuroprosthetic devices. *Science,* 296, 1829-32.

UYLINGS, H. B., GROENEWEGEN, H. J. & KOLB, B. (2003) Do rats have a prefrontal cortex? *Behav Brain Res,* 146, 3-17.

VELLISTE, M., PEREL, S., SPALDING, M. C., WHITFORD, A. S. & SCHWARTZ, A. B. (2008) Cortical control of a prosthetic arm for self-feeding. *Nature,* 453, 1098-101.

WAGER, T. D., RILLING, J. K., SMITH, E. E., SOKOLIK, A., CASEY, K. L., DAVIDSON, R. J., KOSSLYN, S. M., ROSE, R. M. & COHEN, J. D. (2004) Placebo-induced changes in FMRI in the anticipation and experience of pain. *Science,* 303, 1162-7.

WALTON, M. E., BANNERMAN, D. M., ALTERESCU, K. & RUSHWORTH, M. F. (2003) Functional specialization within medial frontal cortex of the anterior cingulate for evaluating effort-related decisions. *J Neurosci,* 23, 6475-9.

WEBER, D. J., STEIN, R. B., EVERAERT, D. G. & PROCHAZKA, A. (2007) Limb-state feedback from ensembles of simultaneously recorded dorsal root ganglion neurons. *J Neural Eng,* 4, S168-80.

WILLIAMS, J. C., RENNAKER, R. L. & KIPKE, D. R. (1999) Long-term neural recording characteristics of wire microelectrode arrays implanted in cerebral cortex. *Brain Res Brain Res Protoc,* 4, 303-13.

WOLPAW, J. R. & MCFARLAND, D. J. (2004) Control of a two-dimensional movement signal by a noninvasive brain-computer interface in humans. *Proc Natl Acad Sci U S A,* 101, 17849-54.

WOMELSDORF, T., FRIES, P., MITRA, P. P. & DESIMONE, R. (2006) Gamma-band synchronization in visual cortex predicts speed of change detection. *Nature,* 439, 733-6.

WYLER, A. R. & BURCHIEL, K. J. (1978) Operant control of pyramidal tract neurons: the role of spinal dorsal columns. *Brain Res,* 157, 257-65.

WYLER, A. R., BURCHIEL, K. J. & ROBBINS, C. A. (1979) Operant control of precentral neurons in monkeys: evidence against open loop control. *Brain Res,* 171, 29-39.

Chapter II

Suitability of the Cingulate Cortex for Neural Control

Abstract:

Recent neuroprosthetic work has focused on the motor cortex as a source of voluntary control signals. However, the motor cortex can be damaged in upper motor neuron degenerative diseases such as primary lateral sclerosis and amyotrophic lateral sclerosis. The possibility exists that prefrontal areas may also be used in neuroprosthetic devices. Here we report the use of the cingulate cortex in a neuroprosthetic model. Seven rats were able to significantly modulate spiking activity in the cingulate cortex in order to receive reward. Furthermore, experiments with single neurons provide evidence that the cingulate cortex neuronal modulation is highly flexible and thus useful for a neuroprosthetic device.

I. Introduction:

We are currently witnessing a renaissance in the technology of neuroprosthetic devices. Using invasive microelectrodes in humans, monkeys, and rats, many research groups have demonstrated two or three-dimensional control of cursors via manipulation of brain signals (for review, see (Schwartz, 2004)). As the motor cortex is involved in voluntary movement control, it has been the chief candidate for invasive neuroprosthetic devices (Fetz, 1969, Kennedy et al., 2000, Wessberg et al., 2000, Serruya et al., 2002, Taylor et al., 2002, Taylor et al., 2003, Vetter et al., 2003, Gage et al., 2005, Hochberg et al., 2006).

However, neurodegenerative diseases, particularly amyotrophic lateral sclerosis (ALS) and primary lateral sclerosis (PLS), can damage upper motor neurons (Morrison et al., 1998, Eisen and Weber, 2001), thus reducing the electrophysiological viability of the

primary motor cortex for clinical neuroprosthetic devices. Recent studies have examined the parietal cortex (Musallam et al., 2004) and premotor areas (Musallam et al., 2004, Lebedev et al., 2005, Santhanam et al., 2006) as candidate brain areas for neuroprosthetic devices. We examined whether the cingulate cortex, part of the prefrontal neocortex, could be an alternative useful site for a neuroprosthetic control signal.

The cingulate cortex is a compelling brain area for a neuroprosthetic device as it is involved in a wide diversity of behavior. In monkey electrophysiology studies, the cingulate cortex is involved in reward-based motor planning and reward expectancy (Shima and Tanji, 1998, Shidara and Richmond, 2002, Hadland et al., 2003). In rodents, the cingulate cortex is involved in behavioral inhibition (Muir et al., 1996), stimulus-reward associations (Takenouchi et al., 1999, Cardinal et al., 2003), reward-based motor planning (Walton et al., 2003), trace-conditioning (Han et al., 2003), and attention in complex discrimination tasks (Bussey et al., 1997). In humans, the cingulate cortex has been correlated with many behavioral states, including error detection, reward-based motor planning, and pain perception (Devinsky et al., 1995, Gehring and Willoughby, 2002, Williams et al., 2004).

Given the diversity of the functions of the cingulate cortex, we aimed to investigate whether such a brain area can come under subject control for use in directing a neuroprosthetic device. Since clinical neuroprosthetics do not have access to known movement parameters corresponding to neural response properties, either due to paralysis or neurodegeneration, we adopted the approach of similar work in our group (Gage et al., 2005) by training the cingulate cortex without *a priori* knowledge of the neural response properties.

Here we report self-modulation of neuronal responses of the cingulate cortex in awake, behaving subjects. Seven of seven rats were able to modulate cingulate cortex single and multi-neuron responses. By individually training single neurons and multi-neuron responses, we have determined, by assuming a binomial probability model with 95% confidence intervals, that 52-84% of cingulate cortex neurons can be trained for use in controlling a neuroprosthetic device. We also demonstrated the flexibility of the cingulate cortex neural responses by requiring different responses from single neurons. Finally, we analyzed the ensemble dynamics of cingulate cortex neurons simultaneously

recorded when only individual neurons or multi-neuron clusters were trained. We found that the cingulate cortex ensemble response does not necessarily follow the activity of trained neurons, suggesting multiple independent channels may be available for control of a neuroprosthetic device.

II. Methods:

A. Animal Surgeries

All animal procedures were approved by the University of Michigan University Committee on Use and Care of Animals and were in accordance with the National Institutes of Health guidelines.

Eight 300 gram, three months old Sprague Dawley rats were chronically implanted with silicon substrate multi-site microelectrode arrays in the cingulate cortex. Surgery was done as previously described (Vetter et al., 2004). Anesthesia was maintained through intraperitoneal injections of a mixture of 50 mg/ml ketamine, five mg/ml xylazine, and one mg/ml acepromazine at an injection volume of 0.125 ml/100 g body weight. Every subsequent hour of surgery, 0.1 ml ketamine (50 mg/ml) was delivered to the animal to maintain anesthesia. Each animal was secured to a standard stereotaxic frame, and three stainless steel bone screws were inserted into the skull. A stainless steel ground wire attached to the electrode connector was connected to one bone screw over the parietal cortex to provide a ground point and temporary mechanical support until the connector was permanently cemented to the skull using dental acrylic. A craniotomy (approximately three mm by two mm) was made over the target cortical area, and the dura mater was cut away to reveal the cortical surface. The electrode array was inserted by hand using #5 fine Teflon-coated forceps into the target cortical area. The surface of the brain was sealed with the biocompatible hydrogel ALGEL (Neural Intervention Technologies, Ann Arbor, MI), the electrode assembly was wrapped with GelFoam (Pfizer, Inc., New York), and the entire assembly was sealed with dental acrylic. The skin around the acrylic was tightened with sutures, anti-bacterial cream was applied, and the animal was then given two days to recover from the surgery.

Eight rats were implanted with one microelectrode array having four identical penetrating shanks separated by 200 μm. Each 3.8 mm shank contained four recording sites at the shank tips separated by 200 μm (catalog # 4x4_4mm200chron, Center for

Neural Communication Technology, University of Michigan, Ann Arbor). Each electrode site had a surface recording area of 1250 μm^2.

We chose our implantation coordinates to span a region of the cingulate cortex involved in reward-based motor planning (Walton et al., 2003, de Wit et al., 2006). The coordinates used for all cingulate cortex implantations spanned cingulate cortex subareas Cg1 and Cg2: 1.5-2.5 mm anterior to bregma, 0.3-0.7 mm lateral from bregma, and 1.6-2.5 mm deep from the surface of the brain (Paxinos and Watson, 1998). The seven rats ultimately used in the data presented here had unit activity that lasted at least three weeks. Three of the rats had a right hemisphere implant, and four rats had a left hemisphere implant. Operant conditioning training began immediately after surgical recovery; cingulate cortex implantation was only verified after training completion with histology.

B. Electrophysiology and Behavior System

Units were sorted via a Multichannel Neuron Acquisition System (Plexon, Inc., Dallas, TX) and spike times were relayed with nominal delays (1 ms) via TCP/IP to a dual 1.25 GHz Dell Dimension Computer (Dell, Inc., Austin, TX) that both analyzed the spike activity using in-house designed software (Mathworks, Inc., Natick, MA) and controlled the behavioral box (Coulborne Instruments, Inc., Allentown, PA). During each experimental session neural electrophysiological data from the 16 electrode channels sampled at 40 kHz were simultaneously amplified and bandpass filtered (450 – 5000 Hz). Manual spike sorting was conducted prior to each experimental session. The auditory stimuli were delivered via a speaker (Yamaha NS-10M Studio, Yamaha Corporation, Buena Park, CA) located 35 cm directly above the test box. The system delivered a near-flat frequency response between 500 Hz and 32 kHz. The system was calibrated to a position at the food delivery tray, although calibration measurements indicated that the test box approximated a free field.

C. Behavioral Training

All rats entering training were kept at 85% of their free-feeding weight. For each behavioral session, the rats were plugged into the headstage and commutator cables and placed into the behavioral box. Rats were typically trained six days a week, at 2-5 sessions per day.

Single units and multi-unit clusters were selected for training by the experimenter prior to each session. Each behavioral session consisted of 200 trials. Each trial began with a two second baseline period during which the average firing rate and standard deviation was calculated via a sliding window of 500 ms in 100 ms steps for the selected single neuron or multi-neuron cluster. After the baseline period, a 0.1-1 second one kHz tone was presented, and the rat was given 2-4 seconds to increase the 500 ms firing rate, sliding in 100 ms steps, beyond a threshold level. The threshold was calculated by:

$$\mu + \beta\sigma = R$$

where μ is the baseline mean firing rate, β is a user defined coefficient, σ is the baseline firing rate standard deviation, and R is the threshold for reward. If the rat successfully exceeded the threshold during the response window, the rat was reinforced with a 45 mg food pellet. A pseudorandom 8-12 second intertrial interval occurred before the beginning of the next trial.

In pilot experiments, we empirically found that operant rates of 30-40% were optimal for learning within 2-3 days. β was thus selected on a cell-by-cell basis to keep the operant rate at ~35%. For cells trained to increase firing rate, the distribution of β was 2.6 ± 1.1 (mean, standard deviation), meaning in a typical session the rat had to modulate its firing rate 2.6 standard deviations above the baseline firing rate to receive reward. For cells trained to decrease firing rate, the distribution of β was -2.0 ± 0.5 (mean, standard deviation), meaning in a typical session the rat had to modulate its firing rate 2.0 standard deviations below the baseline firing rate to receive reward. Thus, the mean chance reward rate for all trained cells was kept at $36.1\% \pm 7.7\%$ (mean, standard deviation). After each session, chance was recalculated, and occasionally β was changed from session to session to keep the operant rates at ~35%. Otherwise β did not change for a given cell.

Monte Carlo simulations were performed to verify if the animal was performing above chance (Manly, 1997). After each behavioral session, the neurophysiological data was randomized by shuffling the tone cue times while keeping the spike trains intact. The entire behavioral session data was run 200 times offline with the same training algorithm described above, but each Monte Carlo simulation run used a new set of randomized tone presentations. The distribution of the percent correct was then used to determine statistical significance. Two hundred runs of the Monte Carlo simulation were found

empirically to be high enough for a stabilized mean and variance (i.e., both no longer changed, to the first decimal place, with higher numbers of runs). If the animal performed at a percent correct rate that was greater than the 95% distribution of the Monte Carlo simulations ($p<0.05$), the session was considered a demonstration of learning. The mean of the Monte Carlo simulation for each session was also used as our metric of chance performance (operant rate) for a given session.

To determine if a recorded unit showed a significant inhibitory or excitatory response, confidence intervals were calculated for the peri-stimulus time histograms (PSTH's) using the NeuroExplorer software package (NeuroExplorer, Littleton, MA). The computations for these intervals assumed spike trains are the result of independent Poisson-point processes as described in the literature (Abeles, 1982). Unit responses that crossed the upper 95% confidence interval during the response window were labeled as excitatory responses while those that crossed the lower 95% confidence interval during the response window were labeled as inhibitory responses, similar to previous work in our group (Gage et al., 2005).

However, in line with expectation coding aspects of the cingulate cortex (Takenouchi et al., 1999), some cells later in the training process (see figures 2 and 4) appeared to have slight excitatory or inhibitory responses to the tone before training had begun for that cell. If the cells had excitatory responses prior to training, the cells were then trained to decrease their firing rates (negative ß). If the cells had inhibitory responses prior to training, they were, as usual, trained to increase their firing rates (positive ß). Some cells, as shown in figure 4C, had a brief transient response to the tone, though Monte Carlo simulations revealed that this was not sufficient for the rat to achieve reward above chance. Both the Monte Carlo simulations and the PSTH's had to show significant modulation ($p<0.05$) in response to the tone stimulus in order for the cell to be classified as trained.

To determine the distribution of neurons in the cingulate cortex that could be used for a control signal for a neuroprosthetic device, each single neuron or multi-neuron cluster was required to be stable for at least two-three days, or at least eight sessions of behavioral training, for it to be classified as "untrained" or "trained." Occasionally, a single neuron or multi-neuron cluster would not be statistically significant ($p > 0.05$) at
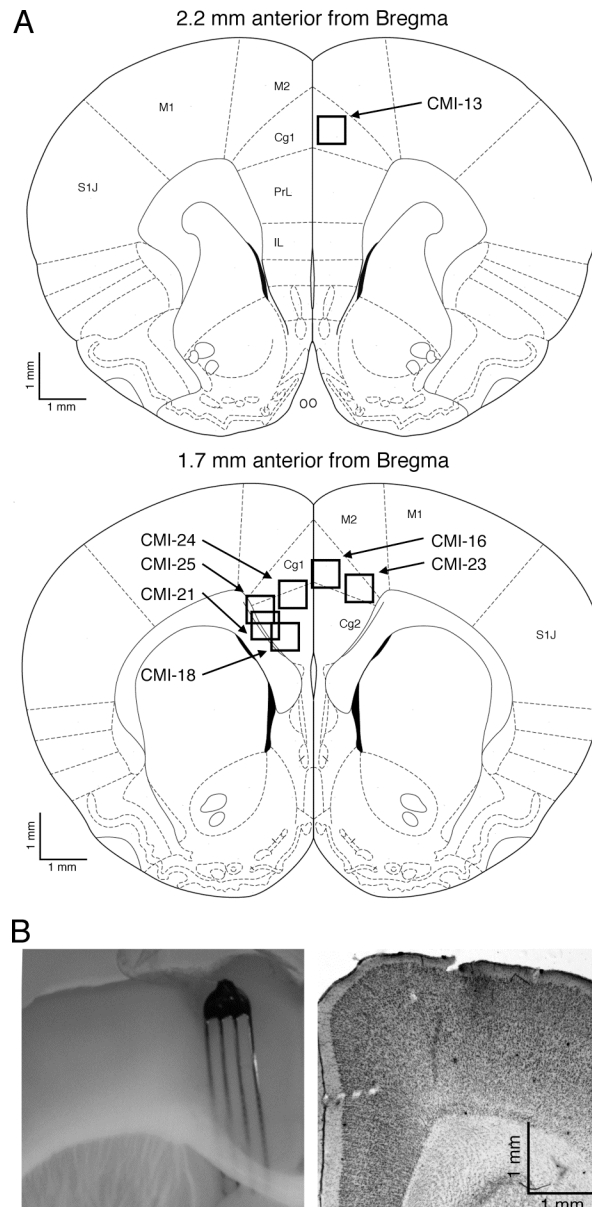
Figure 2.1 Legend: **Electrode Placement**

(**A**) Schematic depicting microelectrode array placements for the seven rats used for training. Cg1 = Cingulate Cortex Area 1; Cg2 = Cingulate Cortex Area 2; IL = Infralimbic Cortex. S1J = Primary Somatosensory Cortex, Jaw Region; M1 = Primary Motor Cortex; M2 = Secondary Motor Cortex; PrL = Prelimbic Cortex (Adapted with permission from Paxinos and Watson, 1998). CMI numbers designate individual rats. (**B**) Right: Photomicrograph of electrode track tips for CMI-13. Coronal slice is 40 μm thick. Of the four tracks for the four electrode shanks, two electrode shanks were in layer one. As layer one consists mostly of axons and dendrites, no cells were isolatable from those two electrode shanks. Left: Photomicrograph of intact electrode in brain slice of CMI-25. Coronal slice is 250 μm thick in order to visualize intact electrode. The electrode displaced slightly ventrally upon slicing, causing some tips to enter the corpus callosum. Thus, shank medial lateral position is accurate while depth is exaggerated.

two ms (Connors et al., 1982, Connors and Gutnick, 1990, Nadasdy et al., 1999, Harris et al., 2000).

If a single neuron was stable and demonstrated learning, the rule of reinforcement was changed. In this special case, ß was switched from a positive to a negative value, such that the firing rate had to decrease (rather than increase) in response to the tone in order for the subject to receive reinforcement. This was done to examine the flexibility of the single unit responses. Multi-unit clusters were not used in this manipulation, as we could not ensure that multi-unit clusters consisted of two or more neurons modulating differentially. Single neurons were tracked over days by examining the autocorrelogram for identical refractory periods and bursting characteristics and again additionally verifying the stability of the spike waveform through isolation in PCA space.

At the close of the study, to test whether feedback of auditory stimuli would affect the ability of the cingulate cortex to be trained for a neuroprosthetic device, two rats were trained with auditory feedback, similar to previous work in our group (Gage et al., 2005). Briefly, μ (from above equation, the baseline firing rate) was represented as a 1 kHz tone. R (the threshold for reward), was represented as a 5 kHz tone. The gradations of auditory feedback were then linearly transformed to represent the neural response firing rate of the rat such that if the rat's neural firing rate approached R on a given trial, the feedback, updating in 100 ms steps, would approach 5 kHz.

D. Histology

Upon completion of training, the rats were euthanized by intraperitoneal overdose of sodium pentobarbital. Following transcardial perfusion with 4% formaldehyde, the brain was removed, sectioned into coronal 40 μm slices, and stained with conventional cresyl violet Nissl stains. The sections were then analyzed using a Leica MZFLIII light microscope (Leica Microsystems, Inc., Germany) to determine probe placement. Rat CMI-25 was sliced in 250 μm sections, and left unstained, for intact probe visualization *in situ* (see Fig. 1).

III. Results

Of the eight rats implanted, seven had unit activity sufficient (lasting greater than three weeks) for the training experiments. See Figure 1A for electrode placement in the seven rats used for training.

Animal	Duration Units	Trained SUs of Total	Trained MUAs of Total
CMI-13	176 days (sacrificed)	1 of 4	3 of 7
CMI-16	85 days (sacrificed)	3 of 4	1 of 1
CMI-18	24 days (implant failure)	2 of 2	0 of 0
CMI-21	65 days (sacrificed)	1 of 1	2 of 4
CMI-23	165 days (implant failure)	3 of 3	1 of 2
CMI-24	56 days (sacrificed)	0 of 0	3 of 3
CMI-25	97 days (implant failure)	1 of 1	2 of 2
		Total=11 of 15 (73%)	Total=12 of 19 (63%)

Net=23 trained of 34 total (68%)

2.Table.1 Legend: **Subjects and Training Summary**

Performance and neural viability for the seven rats used in this study. SU: Single Unit (Single Neuron), MUA: Multi-Unit Activity (Multi-Neuron Cluster). Trained of total refers to number of successfully trained neurons or multi-neuron clusters out of the total selected for training. CMI-24 and CMI-25 were trained with auditory feedback representative of neural firing rate.
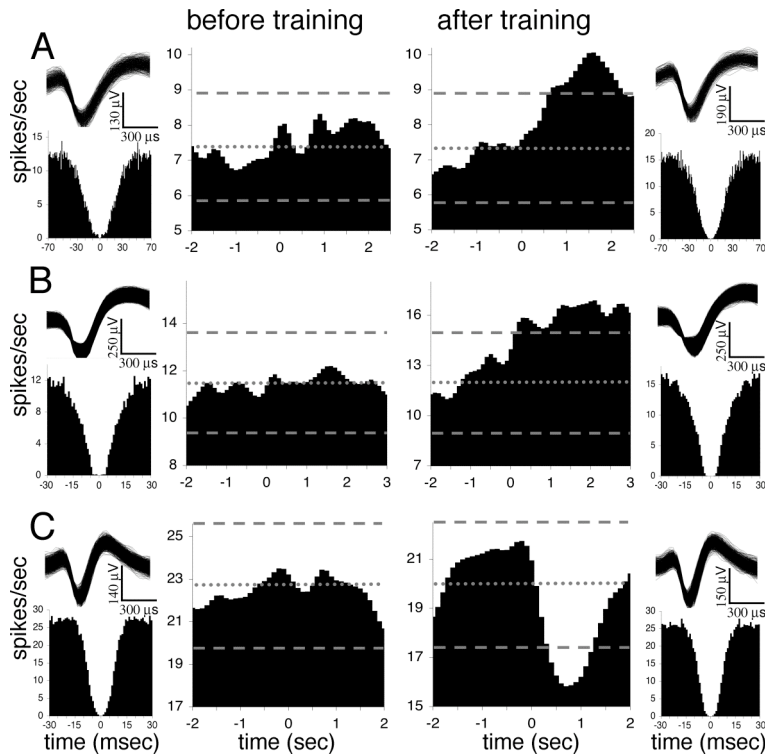
Figure 2.2 Legend: Single Neuron Modulation

Examples of three single neurons (**A-C**), from three rats (CMI-18, CMI-23, and CMI-13, respectively), that improved responses upon training. Waveforms and autocorrelograms for the behavioral session are shown adjacent to the peri-stimulus time histogram (PSTH). As in all subsequent figures, waveform samples are collapsed over each other at the threshold crossing point of the time discrimination window. PSTH layout is as follows: Zero indicates time tone was delivered to animal. PSTH's are plotted to represent the neuron minimum and maximum firing rate. Each PSTH represents the 200 trials of a single behavioral session. Dotted lines indicate neuron's mean firing rate. Dashed lines indicate neuron's 95% confidence intervals for mean firing rate. Confidence lines and means were calculated on raw data for the entire behavioral session (NeuroExplorer, Littleton, MA). The neurons in **A** and **B** were trained to increase firing rate after the tone, whereas the neuron in **C** was trained to decrease firing rate after the tone. PSTH's are Gaussian smoothed over five bin widths of 100 ms/bin.

Individual neurons and multi-neuron clusters were trained from the population of seven rats to test if the cingulate cortex could be useful for a neuroprosthetic device. Following surgical recovery, it took the seven rats an average of seven days to learn the task and begin modulating their cingulate cortex (mean sessions to first learning: 20). If a subject demonstrated learning for a single neuron or multi-neuron cluster, then another neuron or multi-neuron cluster was selected for training. Table 1 shows the statistics for the single neuron and multi-neuron cluster modulation. Out of 15 single neurons tested,
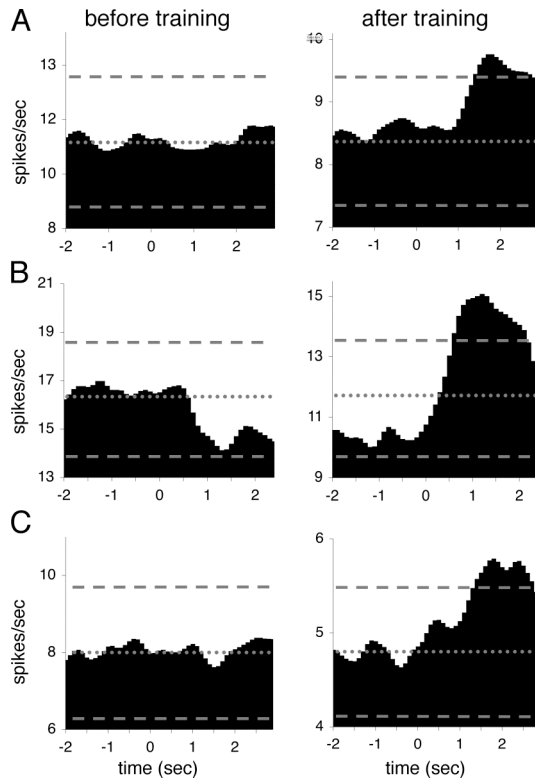
Figure 2.3 Legend: Multi-neuron Cluster Modulation

Examples of three multi-neuron clusters (**A-C**), from three rats (CMI-25, CMI-21 and CMI-24, respectively), that improved responses upon training. PSTH layout is the same as figure 2. All multi-neuron clusters were trained to increase firing rate after the tone. PSTH's are Gaussian smoothed over five bin widths of 100 ms/bin. The multi-neuron clusters in **A** and **C** were trained with auditory feedback delivered to the rats.

11 showed significant modulation with training. Out of 19 multi-neuron clusters tested, 12 showed significant modulation with training. Figures 2 and 3 show example single neuron and multi-neuron responses to the tone cue before and after training. The average learning time for all cells was 3 ± 1.3 days (8.2 ± 4.5 sessions, mean, standard deviation). The average learning time for single neurons was 3.5 ± 1.4 days (9.9 ± 4.6 sessions, mean, standard deviation), and the average learning time for multi-neurons clusters was 2.7 ± 1.1 days (7.1 ± 4.0 sessions, mean, standard deviation). We did not find any effect of learning time in early-trained cells vs. later-trained cells either within rats or across all rats.

Two rats, of the total seven, were trained with auditory feedback representative of the neural response firing rate. For the six total cells trained with auditory feedback, the mean learning time was 3.0 ± 1.5 days (7.0 ± 4.6 sessions, mean, standard deviation). For the 17 cells trained without auditory feedback, the mean learning time was 3.1 ± 1.2 days (8.8 ± 4.5 sessions, mean, standard deviation).

To test the flexibility of the cingulate cortex in response to varying algorithm rules, we performed a brief subsequent experiment examining single neuron responses. Once a subject was trained to increase a neuron's firing rate in response to the tone to receive food reward, the subject was trained to decrease the neuron's firing rate after the
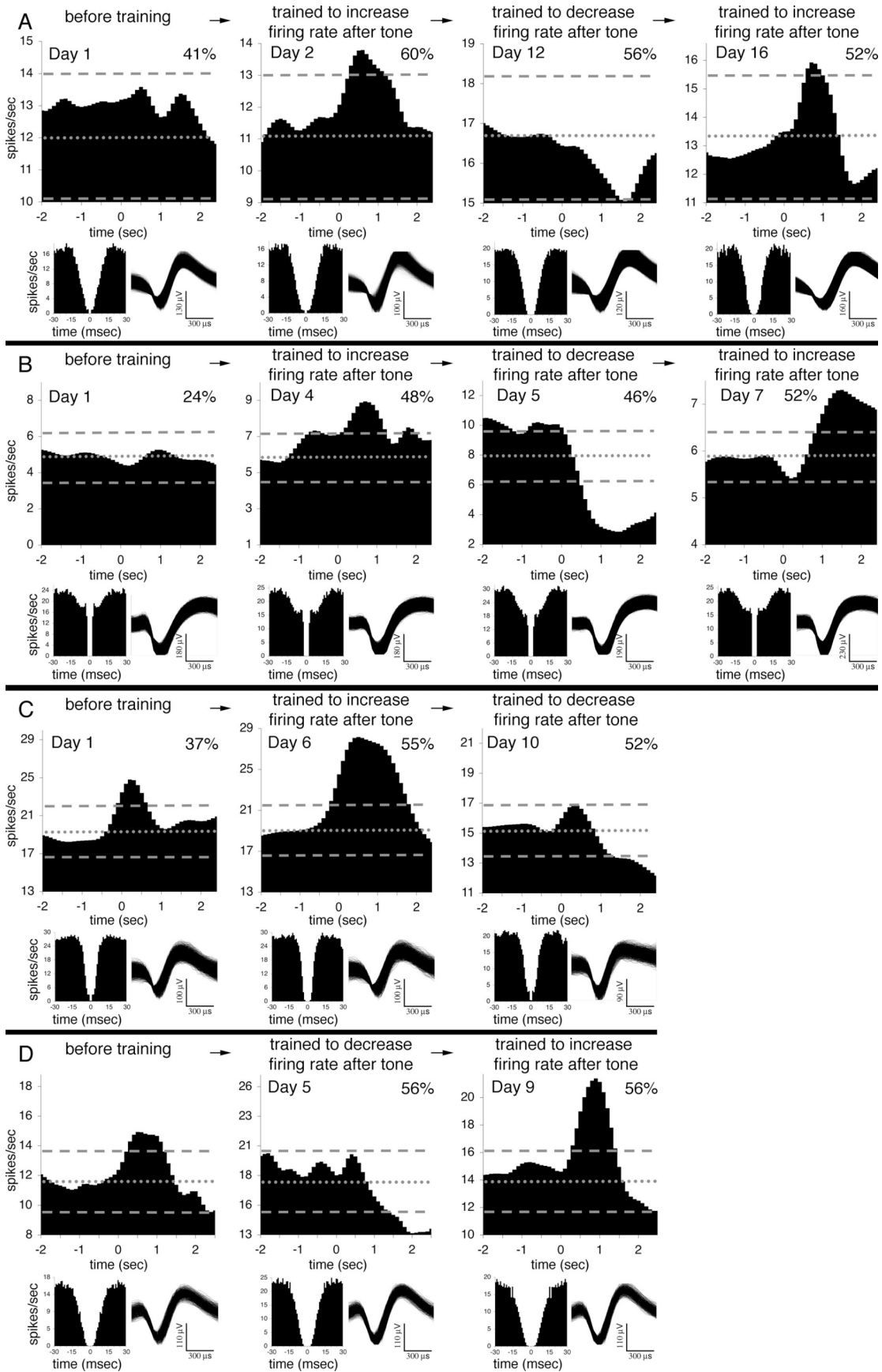
Figure 2.4 Legend: **Single Neuron Plastic Responses**

Four single neurons (**A-D**), from three rats (CMI-16. CMI-25, CMI-23, and CMI-16, respectively) that showed responses to changes in rules of reinforcement. Waveforms and autocorrelograms are shown below the PSTH's. PSTH layout is the same as figure 2. PSTH's are Gaussian smoothed over 10 bin widths of 100 ms/bin. Percentage numbers above PSTH's show behavioral performance for the session. Day refers to the day of training. Analysis of the spike train of the neuron shown in **B** revealed it to have a low mean firing rate coupled with bursting behavior. The cell would sometimes not emit a single spike for two seconds but also exhibit intense bursting activity sometimes approaching instant frequencies of 400 -500 Hz with an absolute refractory period of 2 ms. The neuron in **B** was also trained with auditory feedback delivered to the rat. The neuron shown in **C** had a transient response to the tone in all conditions, concurrent with expectation coding theories of the cingulate cortex (Takenouchi et al., 1999). However, even with the constant initial response to the tone, the neuron was still trainable. The neuron shown in **D** was trained immediately after the neuron in **A** (both **A** and **D** are from CMI-16). Thus, the "before training" session in **D** is from the same session as day 16 for the neuron shown in **A** (which explains why the neuron in **D** before training has a prolonged positive response after tone). Note: During training of the neuron in **A**, equipment issues prevented training of the neuron for four days between training days five and six.

tone in order to receive reinforcement. The different responses were required of a single neuron to ensure that two or three neurons were not modulating differentially in this condition.

We were able to record from six neurons, across four subjects, for 9-16 days for our flexibility test experiment (see methods for isolation criteria). Of these six neurons that were held long enough to change reinforcement rules, four of the neurons, from three rats, showed flexible responses. The mean time to learning the transition was 4.2 ± 2.5 days (10.9 ± 6.5 sessions, mean, standard deviation). Figure 4 shows these four neurons that demonstrated ability to modulate in response to changes in rules of reinforcement. Though the baseline activity did slightly change from day to day, ß was changed, if necessary, from session to session to ensure the operant rate (chance) was held at ~35%. For Fig. A-D, the mean and standard deviation of the baseline firing rates for the single neurons across days was: A: 14.8 ± 4.9 Hz, B: 5.2 ± 1.8 Hz, C: 19.7 ± 4.9 Hz, D: 18.0 ± 2.6 Hz.

We were also interested in the network dynamics of the cingulate cortex in our training task. When only a subpopulation of neurons is used for the control signal in a neuroprosthetic device, what occurs to the other neurons in the brain area during the task?

We investigated this by examining neural modulation as a function both of ensemble activity and distance from the trained single neuron or multi-neuron cluster.

We were able to demonstrate training for 23 out of 34 single neurons and multi-neuron clusters in this study; however, during the course of the training, we also were able to record far more cells than we trained. In total we were able to record from 234 cells (77 single neurons and 157 multi-neuron clusters). See Table 2 for the full description of this data. We found that 71 of 77 single neurons showed some modulation in response to the tone, but the modulation did not necessarily follow that of the trained cell. Approximately half increased firing rate, and half decreased firing rate. Similar results were obtained for the 75 of the 157 multi-neuron clusters that showed responses to the tone. The heterogeneity of firing rate modulation, for both the multi-neuron clusters and single neurons, occurred regardless of whether the selected trained cell was trained to increase or decrease firing rate. Thus, ensemble cingulate cortex neurons did not necessarily follow the firing rate modulation of the trained cingulate neuron, suggesting additional independent control signals may be available for a neuroprosthetic device.

Since the geometry of our silicon probes is fixed due to the fabrication process (Vetter et al., 2004), we were able to examine whether cells in closer physical proximity to the cell being trained showed different responses to cells that were farther away on the electrode array. We analyzed cells at the beginning of training and at the end of training and scored neural activity via firing rate modulation in response to the tone stimulus. We hypothesized that closer cells would show similar firing rate modulation as the selected trained cell. We found that the only difference in populations, using an alpha value of 0.10 (Curran-Everett and Benos, 2004), was between cells with any modulation and cells that had no responses at all (student's t test, *p=0.09*). Responding cells were an average of 364 μm (σ = 215 μm, n=109) away from the trained cell, and non-responding cells were an average of 414 μm (σ = 230 μm, n=53) away from the trained cell. All other classes, such as cells that increased or decreased firing rates after the tone during training and cells that maintained their elevated or depressed firing rates after the tone during training, were not statistically significant with respect to distance to the trained cell

		All Sessions	When Selected Cell Trained to Increase Firing Rate	When Selected Cell Trained to Decrease Firing Rate
A	Total Cells Recorded	234	199	35
	Single Cells	77 (33%)	62 (31%)	15 (43%)
	Multi-Cell Clusters	157 (67%)	137 (69%)	20 (57%)
B	Total Cells Modulating Firing Rate	146	119	27
	Single Cells Modulating Firing Rate	71 (49%)	57 (48%)	14 (52%)
	Multi-Cell Clusters Modulating Firing Rate	75 (51%)	62 (52%)	13 (48%)
C	Single Cells Increasing Firing Rate	40 (56%)	33 (58%)	7 (50%)
	Single Cells Decreasing Firing Rate	31 (44%)	24 (42%)	7 (50%)
	Multi-Cell Clusters Increasing Firing Rate	40 (53%)	32 (52%)	8 (62%)
	Multi-Cell Clusters Decreasing Firing Rate	35 (47%)	30 (48%)	5 (38%)

2.Table.2 Legend: **Ensemble Analysis**

Ensemble analysis tabulation of all cells recorded from the microelectrode arrays when selected cells were trained. In **A**, total cells recorded are subdivided into single cells and multi-cell clusters. **B** shows the subpopulation of cells and multi-cell clusters that showed significant modulation by crossing the 95% confidence intervals of firing rate after tone presentation. **C** shows the same data as **B**, but classes the single cells and multi-cell clusters by method of firing rate modulation.

(student's t test, *p>0.10*). Again, this suggests multiple independent control channels may be available within the cingulate cortex.

IV. Discussion

The aim of this study was to investigate the possibility that the cingulate cortex could be used as an output control signal for a neuroprosthetic device, and our data indeed suggest this. Sixty eight percent of our sampled neurons in the cingulate cortex could be voluntarily modulated by the rats, and single neurons were flexible in changing their response properties due to changes in the rules of reinforcement.

During the course of the training experiments, we did observe stereotyped motor behaviors in the rats, but the movements appeared to be highly variable. For example, rats would turn their heads left or right, duck, or paw at the food aperture upon tone onset during many of the experiments. Whether these stereotyped behaviors were related to the cingulate cortex neurons' firing rate modulation, or whether the motor behaviors were merely superstitious behaviors, is not known. Recent studies have shown that humans can modulate the gross metabolic activity of their cingulate cortices in a real-time functional magnetic resonance imaging (fMRI) scanner where movement is severely constrained (Weiskopf et al., 2003, Weiskopf et al., 2004, Decharms et al., 2005). Such human data provides compelling evidence that the cingulate cortex can be modulated with minimal motor movement of subjects.

Intuitively, some areas of the brain may be more useful than others as control signals for a neuroprosthetic device. The parietal cortex, as it encodes goal-directed location in space, has been demonstrated to be a useful site for neuroprosthetic control signals (Musallam et al., 2004). The premotor cortices and motor cortex, involved in movement planning and voluntary movement, have been the primary target structures for many research groups (Kennedy et al., 2000, Serruya et al., 2002, Carmena et al., 2003, Taylor et al., 2003, Hochberg et al., 2006, Santhanam et al., 2006). Other areas of the prefrontal cortex, however, have been neglected. In our rat model, the cingulate cortex was the most compelling implantation site due to its involvement in encoding reward-based motor planning (Shima and Tanji, 1998, Shidara and Richmond, 2002). Anatomically, the cingulate cortex has synaptic connections with both the motor cortex (Gu et al., 1999) and nucleus accumbens (Berendse et al., 1992), potentially providing the cingulate cortex with highly flexible properties in response to varying demands of a neuroprosthetic device. The cingulate cortex may be able to "switch" between different device modes more readily than

other cortical implantation sites. Experiments in primate models, using real-time decoding of cursor control and other devices, could test this hypothesis.

Since the cingulate cortex is involved in expectation coding (Takenouchi et al., 1999), the possibility exists that the responses observed in figures 2 and 3 were due to Pavlovian learning rather than operant conditioning or, alternatively, that the responses were a manifestation of habits (due to overtraining) rather than goal-directed behavior. However, since we were constantly changing which cells the animals had to modulate in order to receive reward, we effectively locked the task perpetually in the early learning stages, ensuring that the animals never achieved mastery of the task through over-training. For example, previous work in our group (Gage et al., 2005) has achieved performance rates of 90% through extensive training, but the rats in our current study rarely achieved performance rates beyond approximately 60%, even when operant rates were kept at the reasonably high rate of 35%. In addition, our work demonstrates that the cingulate cortex neurons' responses could change response properties due to changes in reinforcement rules (positive ß vs. negative ß) even though the stimuli and reward were exactly the same throughout. It is unlikely that such flexibility is the result of habits or associative learning.

However, though the cingulate cortex may be a useful alternative site for a neuroprosthetic device due to its role in reward-based motor planning (Shima and Tanji, 1998, Shidara and Richmond, 2002), some limitations may exist. The cingulate cortex is also involved in pain perception, error detection, social evaluations, attention, and a variety of other functions (Devinsky et al., 1995, Gehring and Willoughby, 2002, Eisenberger et al., 2003, Williams et al., 2004). Any output signals in the cingulate cortex may be masked by the inherent processing of the cingulate cortex in a real world environment. Though our rats which received feedback were still able to modulate their cingulate activity even in the presence of constant tone presentation, our experiments still occurred in the highly artificial environment of a behavioral box. In addition, due to the cingulate cortex's medial location and proximity to the sagittal sinus, implantation in a human patient is inherently more difficult than a motor cortex implantation.

Our work builds on that of E. Fetz and M. Baker (Fetz and Baker, 1973) in which they trained single units using single microelectrode recording in the primate motor cortex. In their study they found 33 units that could be trained and 18 units that could not. This

results in an approximate 65% training rate for the motor cortex cells in their data set. Our data in the cingulate cortex are in agreement with Fetz's data in that approximately 68% of our cingulate cortex cells examined under similar criteria could operantly conditioned by rats. Perhaps this ~65% training rate represents an approximate "ceiling" of trainable cells in neocortex, regardless of neocortical area.

In addition, Fetz and Baker were sometimes able to track two neurons simultaneously. They found that though they could train two different neurons in opposite response patterns, without such a contingency most neurons followed each other (i.e., if one cell was trained to increase its firing rate, the other cell would usually follow it). We did not see this effect in our data, but our neurons were recorded from a much broader sampling area with our 16-channel microelectrode array. We recorded an average of 9.8 additional cells in the ensemble per trained neuron, and we did not find any consistent relationship between the response of the trained cell and the responses of the neighboring cells. Since the neuron pairs in Fetz and Baker's study were always from the same microelectrode, they were no doubt observing closely coupled circuits over a probable 100-150 microns distance (Humphrey and Schmidt, 1990), whereas we could record larger scale circuits with a maximal ~850 micron distance between the most distant microelectrodes on the same array.

We found that approximately 68% of the neurons or multi-neuron clusters selected for training could be successfully trained, and all of the implanted rats with sufficient unit activity were able to modulate the cingulate cortex to receive reward. Assuming a binomial probability model, this results in a 95% confidence interval of 52-84%. Thus, any neuron or multi-neuron cluster recorded from the cingulate cortex has a 52-84% chance of being trainable, which, given large multi-electrode arrays, may be sufficient for a neuroprosthetic device. With algorithm improvement and different training paradigms, it is possible that more neurons could be recruited, more states could be discriminated, and learning could be faster.

V. Conclusion

We report that the cingulate cortex of rats can come under voluntary control. Thus, if the motor cortex is damaged by a neurodegenerative disease such as primary lateral sclerosis and cannot be used for a neuroprosthetic device, the cingulate cortex can potentially be used in neuroprosthetic devices in human patients.

References:

ABELES, M. (1982) Quantification, smoothing, and confidence limits for single-units' histograms. *J Neurosci Methods*, 5, 317-25.

BERENDSE, H. W., GALIS-DE GRAAF, Y. & GROENEWEGEN, H. J. (1992) Topographical organization and relationship with ventral striatal compartments of prefrontal corticostriatal projections in the rat. *J Comp Neurol*, 316, 314-47.

BUSSEY, T. J., MUIR, J. L., EVERITT, B. J. & ROBBINS, T. W. (1997) Triple dissociation of anterior cingulate, posterior cingulate, and medial frontal cortices on visual discrimination tasks using a touchscreen testing procedure for the rat. *Behav Neurosci*, 111, 920-36.

CARDINAL, R. N., PARKINSON, J. A., MARBINI, H. D., TONER, A. J., BUSSEY, T. J., ROBBINS, T. W. & EVERITT, B. J. (2003) Role of the anterior cingulate cortex in the control over behavior by Pavlovian conditioned stimuli in rats. *Behav Neurosci*, 117, 566-87.

CARMENA, J. M., LEBEDEV, M. A., CRIST, R. E., O'DOHERTY, J. E., SANTUCCI, D. M., DIMITROV, D., PATIL, P. G., HENRIQUEZ, C. S. & NICOLELIS, M. A. (2003) Learning to control a brain-machine interface for reaching and grasping by primates. *PLoS Biol*, 1, E42.

CONNORS, B. W. & GUTNICK, M. J. (1990) Intrinsic firing patterns of diverse neocortical neurons. *Trends Neurosci*, 13, 99-104.

CONNORS, B. W., GUTNICK, M. J. & PRINCE, D. A. (1982) Electrophysiological properties of neocortical neurons in vitro. *J Neurophysiol*, 48, 1302-20.

CURRAN-EVERETT, D. & BENOS, D. J. (2004) Guidelines for reporting statistics in journals published by the American Physiological Society. *Physiol Genomics*, 18, 249-51.

DE WIT, S., KOSAKI, Y., BALLEINE, B. W. & DICKINSON, A. (2006) Dorsomedial prefrontal cortex resolves response conflict in rats. *J Neurosci*, 26, 5224-9.

DECHARMS, R. C., MAEDA, F., GLOVER, G. H., LUDLOW, D., PAULY, J. M., SONEJI, D., GABRIELI, J. D. & MACKEY, S. C. (2005) Control over brain activation and pain learned by using real-time functional MRI. *Proc Natl Acad Sci U S A*, 102, 18626-31.

DEVINSKY, O., MORRELL, M. J. & VOGT, B. A. (1995) Contributions of anterior cingulate cortex to behaviour. *Brain*, 118 (Pt 1), 279-306.

EISEN, A. & WEBER, M. (2001) The motor cortex and amyotrophic lateral sclerosis. *Muscle Nerve*, 24, 564-73.

EISENBERGER, N. I., LIEBERMAN, M. D. & WILLIAMS, K. D. (2003) Does rejection hurt? An FMRI study of social exclusion. *Science*, 302, 290-2.

FETZ, E. E. (1969) Operant conditioning of cortical unit activity. *Science*, 163, 955-8.

FETZ, E. E. & BAKER, M. A. (1973) Operantly conditioned patterns on precentral unit activity and correlated responses in adjacent cells and contralateral muscles. *J Neurophysiol*, 36, 179-204.

GAGE, G. J., LUDWIG, K. A., OTTO, K. J., IONIDES, E. L. & KIPKE, D. R. (2005) Naive coadaptive cortical control. *J Neural Eng*, 2, 52-63.

GEHRING, W. J. & WILLOUGHBY, A. R. (2002) The medial frontal cortex and the rapid processing of monetary gains and losses. *Science*, 295, 2279-82.

GU, X., STAINES, W. A. & FORTIER, P. A. (1999) Quantitative analyses of neurons projecting to primary motor cortex zones controlling limb movements in the rat. *Brain Res,* 835**,** 175-87.

HADLAND, K. A., RUSHWORTH, M. F., GAFFAN, D. & PASSINGHAM, R. E. (2003) The anterior cingulate and reward-guided selection of actions. *J Neurophysiol,* 89**,** 1161-4.

HAN, C. J., O'TUATHAIGH, C. M., VAN TRIGT, L., QUINN, J. J., FANSELOW, M. S., MONGEAU, R., KOCH, C. & ANDERSON, D. J. (2003) Trace but not delay fear conditioning requires attention and the anterior cingulate cortex. *Proc Natl Acad Sci U S A,* 100**,** 13087-92.

HARRIS, K. D., HENZE, D. A., CSICSVARI, J., HIRASE, H. & BUZSAKI, G. (2000) Accuracy of tetrode spike separation as determined by simultaneous intracellular and extracellular measurements. *J Neurophysiol,* 84**,** 401-14.

HOCHBERG, L. R., SERRUYA, M. D., FRIEHS, G. M., MUKAND, J. A., SALEH, M., CAPLAN, A. H., BRANNER, A., CHEN, D., PENN, R. D. & DONOGHUE, J. P. (2006) Neuronal ensemble control of prosthetic devices by a human with tetraplegia. *Nature,* 442**,** 164-71.

HUMPHREY, D. R. & SCHMIDT, E. M. (1990) Extracellular single-unit recording methods. IN BOULTON, A. A., BAKER, G. B. & VANDERWORLD, C. H. (Eds.) *Neurophysiological Techniques: Applications to Neural Systems.* Humana Press.

KENNEDY, P. R., BAKAY, R. A., MOORE, M. M., ADAMS, K. & GOLDWAITHE, J. (2000) Direct control of a computer from the human central nervous system. *IEEE Trans Rehabil Eng,* 8**,** 198-202.

LEBEDEV, M. A., CARMENA, J. M., O'DOHERTY, J. E., ZACKSENHOUSE, M., HENRIQUEZ, C. S., PRINCIPE, J. C. & NICOLELIS, M. A. (2005) Cortical ensemble adaptation to represent velocity of an artificial actuator controlled by a brain-machine interface. *J Neurosci,* 25**,** 4681-93.

MANLY, B. F. J. (1997) *Randomization, bootstrap, and Monte Carlo methods in biology,* New York, Chapman & Hall.

MARZULLO, T. C., MILLER, C. R. & KIPKE, D. R. (2006) Suitability of the cingulate cortex for neural control. *IEEE Trans Neural Syst Rehabil Eng,* 14**,** 401-9.

MORRISON, B. M., HOF, P. R. & MORRISON, J. H. (1998) Determinants of neuronal vulnerability in neurodegenerative diseases. *Ann Neurol,* 44**,** S32-44.

MUIR, J. L., EVERITT, B. J. & ROBBINS, T. W. (1996) The cerebral cortex of the rat and visual attentional function: dissociable effects of mediofrontal, cingulate, anterior dorsolateral, and parietal cortex lesions on a five-choice serial reaction time task. *Cereb Cortex,* 6**,** 470-81.

MUSALLAM, S., CORNEIL, B. D., GREGER, B., SCHERBERGER, H. & ANDERSEN, R. A. (2004) Cognitive control signals for neural prosthetics. *Science,* 305**,** 258-62.

NADASDY, Z., HIRASE, H., CZURKO, A., CSICSVARI, J. & BUZSAKI, G. (1999) Replay and time compression of recurring spike sequences in the hippocampus. *J Neurosci,* 19**,** 9497-507.

PAXINOS, G. & WATSON, C. (1998) *The rat brain in stereotaxic coordinates,* San Diego, Academic Press.

SANTHANAM, G., RYU, S. I., YU, B. M., AFSHAR, A. & SHENOY, K. V. (2006) A high-performance brain-computer interface. *Nature,* 442**,** 195-8.

SCHWARTZ, A. B. (2004) Cortical neural prosthetics. *Annu Rev Neurosci,* 27**,** 487-507.

SERRUYA, M. D., HATSOPOULOS, N. G., PANINSKI, L., FELLOWS, M. R. & DONOGHUE, J. P. (2002) Instant neural control of a movement signal. *Nature,* 416**,** 141-2.

SHIDARA, M. & RICHMOND, B. J. (2002) Anterior cingulate: single neuronal signals related to degree of reward expectancy. *Science,* 296**,** 1709-11.

SHIMA, K. & TANJI, J. (1998) Role for cingulate motor area cells in voluntary movement selection based on reward. *Science,* 282**,** 1335-8.

TAKENOUCHI, K., NISHIJO, H., UWANO, T., TAMURA, R., TAKIGAWA, M. & ONO, T. (1999) Emotional and behavioral correlates of the anterior cingulate cortex during associative learning in rats. *Neuroscience,* 93**,** 1271-87.

TAYLOR, D. M., TILLERY, S. I. & SCHWARTZ, A. B. (2002) Direct cortical control of 3D neuroprosthetic devices. *Science,* 296**,** 1829-32.

TAYLOR, D. M., TILLERY, S. I. & SCHWARTZ, A. B. (2003) Information conveyed through brain-control: cursor versus robot. *IEEE Trans Neural Syst Rehabil Eng,* 11**,** 195-9.

VETTER, R. J., OTTO, K. J., MARZULLO, T. C. & KIPKE, D. R. (2003) Brain-machine interfaces in rat motor cortex: neuronal operant conditioning to perform a sensory detection task. *1st International IEEE EMBS Conference on Neural Engineering.* Capri, Italy.

VETTER, R. J., WILLIAMS, J. C., HETKE, J. F., NUNAMAKER, E. A. & KIPKE, D. R. (2004) Chronic neural recording using silicon-substrate microelectrode arrays implanted in cerebral cortex. *IEEE Transactions on Biomedical Engineering,* 51**,** 1-9.

WALTON, M. E., BANNERMAN, D. M., ALTERESCU, K. & RUSHWORTH, M. F. (2003) Functional specialization within medial frontal cortex of the anterior cingulate for evaluating effort-related decisions. *J Neurosci,* 23**,** 6475-9.

WEISKOPF, N., SCHARNOWSKI, F., VEIT, R., GOEBEL, R., BIRBAUMER, N. & MATHIAK, K. (2004) Self-regulation of local brain activity using real-time functional magnetic resonance imaging (fMRI). *J Physiol Paris,* 98**,** 357-373.

WEISKOPF, N., VEIT, R., ERB, M., MATHIAK, K., GRODD, W., GOEBEL, R. & BIRBAUMER, N. (2003) Physiological self-regulation of regional brain activity using real-time functional magnetic resonance imaging (fMRI): methodology and exemplary data. *Neuroimage,* 19**,** 577-86.

WESSBERG, J., STAMBAUGH, C. R., KRALIK, J. D., BECK, P. D., LAUBACH, M., CHAPIN, J. K., KIM, J., BIGGS, S. J., SRINIVASAN, M. A. & NICOLELIS, M. A. (2000) Real-time prediction of hand trajectory by ensembles of cortical neurons in primates. *Nature,* 408**,** 361-5.

WILLIAMS, Z. M., BUSH, G., RAUCH, S. L., COSGROVE, G. R. & ESKANDAR, E. N. (2004) Human anterior cingulate neurons and the integration of monetary reward with motor responses. *Nat Neurosci*.

Chapter III

Spikes, Local Field Potentials, and Electrocorticogram Correlations in the Motor Cortex
of Rats

Abstract

Neuroprosthetic development for limb or computer cursor control typically falls
into two arenas, invasive extracellular recording and non-invasive electroencephalogram
recording methods. The relationship between action potentials and field potentials is not
well understood, and investigation of the co-dependencies between the two types of
signals may improve design of neuroprosthetic control systems. To this end, we recorded
spikes, local field potentials (LFPs), and electrocorticograms (ECoGs) simultaneously
from the motor cortex of rats during three behavioral states: anesthetized, performing a
motor learning task, and performing a motor unit operant conditioning task. In the motor
learning task, the rats had to simultaneously place both forepaws on levers on the cage
floor while holding their snouts in a nosepoke aperture. After the rats learned the motor
learning task, they were trained on an operant conditioning task whereby they had to
modulate their spiking activity during the delay period in order to receive a food reward.
We hypothesized that 1) during anesthesia, the spikes would phase-lock to the 1-2
ketamine oscillation rhythms, 2) during motor learning epochs, the spikes would phase-
lock to the 20 Hz movement related ß rhythms, and 3) during the neural operant
conditioning task, the spikes would phase-lock to the high frequency (>30 Hz) gamma
rhythms.

During anesthesia, the spikes phase-locked to the 1-2 Hz ketamine rhythm, and
during the motor learning and operant conditioning tasks, the spikes phase-locked to the
theta (8 Hz) rhythm. We did not see any gamma frequency modulation in any behavioral
condition. Thus, combining spikes and field potentials for a neuroprosthetic control
signal may be feasible in the motor cortex if the local field potentials are high-passed

above 10 Hz. In addition, perhaps the <10 Hz rhythms may provide an indicator of cortical modulation for a neuroprosthetic device should the recordings of spiking activity fail.

I. Introduction

The past decade has seen a dramatic growth in the technology of neuroprosthetic devices. By recording and providing computer monitor feedback of the spiking activity of motor cortex neurons to awake subjects, many research groups have demonstrated 2D or 3D cursor control, as well as the manipulation of robotic arms (Kennedy et al., 2000, Carmena et al., 2003, Taylor et al., 2003, Musallam et al., 2004, Hochberg et al., 2006, Velliste et al., 2008). However, there is a concurrent drive to develop lower-cost lower-risk brain-computer interface alternatives, specifically, using the electroencephalogram activity (recorded from the scalp) (Wolpaw and McFarland, 2004, Trejo et al., 2006) or the electrocorticogram activity (recorded from the cortical surface) (Leuthardt et al., 2004, Wilson et al., 2006, Schalk et al., 2008). Combining the resolution of motor cortex spiking activity with long-term stability of the population field potential provide the best solution of long-term viability with high information transmission for a neuroprosthetic device controller.

However, local field potential modulation for neuroprosthetics remains unexplored, with only two brief reports demonstrating use of LFP amplitude modulation (Kennedy et al., 2004a, Kennedy et al., 2004b). In addition, the relationship between action potentials and field potentials in awake, behaving subjects is currently an active subject of speculation, research, and debate in neurophysiology.

The majority of neuroprosthetics target the motor cortex (for review, see (Schwartz, 2004, Fetz, 2007); thus, we focused our attention on oscillations of the motor cortex during motor learning tasks. In monkeys, a "preparatory potential" of the 25-35 Hz beta rhythm occurs when monkeys are actively exploring or planning to move (Murthy and Fetz, 1996a, Murthy and Fetz, 1996b), and the single units isolated during these experiments indicated the spikes were phase-locking to the 25-35 Hz rhythm (See Figure 13). Other groups have found additional ~20 Hz potential modulation during the preparatory phase of movements in monkeys (Donoghue et al., 1998, Baker et al., 1999) and a quadriplegic human (Hochberg et al., 2006). In spite of this, it was recently found

that <13 Hz frequency bands and 60-200 Hz frequency bands code for movement direction more accurately than 20-50 Hz in a center-out reaching task (Mehring et al., 2003, Mehring et al., 2004, Rickert et al., 2005). Moran and his colleagues additionally found high frequencies (50 – 200 Hz) in both ECoGs and LFPs encode movement direction in eight and four directions, respectively (Leuthardt et al., 2004, Heldman et al., 2006).

As the monkey neocortex and rat hippocampus literature has indeed shown that spikes tend to fire in phase with certain frequency ranges of the field potential during specific behavioral epochs (Murthy and Fetz, 1996a, Fries et al., 2001, Womelsdorf et al., 2006, Kjelstrup et al., 2008), we hypothesized that the spikes of the motor cortex neurons would also phase lock to specific frequencies of the field potentials during different behavioral epochs, and our study aimed to determine this.

We sampled spikes, LFPs, and ECoGs simultaneously in a chronic preparation during multiple behavioral states: ketamine-induced anesthesia, a motor learning task, and a neural operant conditioning task. In the motor learning task, rats were trained to simultaneously place both forepaws on levers on the cage floor while performing a simple nosepoke task and holding the position for 1-5 seconds. After the rats learned this task, the rats were then trained in a neural operant conditioning mode whereby they had to modulate the spiking activity of cells in the motor cortex during the delay period in order to receive a food reward. We hypothesized that 1) during anesthesia, the spikes would phase-lock to the 1-2 ketamine oscillation rhythms (Fontanini et al., 2003), 2) during motor learning epochs, the spikes would phase-lock to the 20 Hz movement related ß rhythms (Murthy and Fetz, 1996b), and 3) during the neural operant conditioning task, the spikes would phase-lock to the high frequency (>30 Hz) gamma rhythms (Gray and Singer, 1989, Fries et al., 2001).

Using the spike-triggered averages of single neurons with regard to the simultaneously recorded LFPs and ECoGs, in the anesthetized state the spikes aligned precisely in phase with the slow 1-2 Hz rhythm, whereas in the motor learning and neural operant conditioning states the spikes synchronized to the theta rhythms (8 Hz). Surprisingly, we did not observe any evidence of phase locking to gamma rhythms during periods of firing rate modulation. Thus, the low frequencies of the LFP and ECoG do not
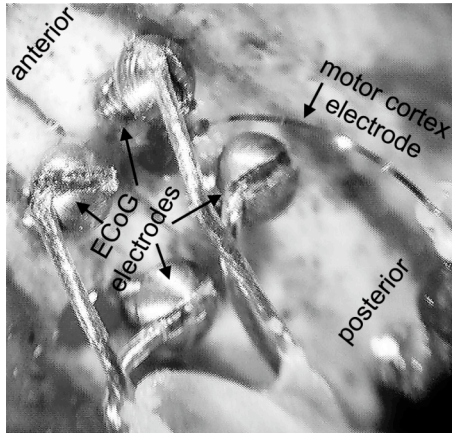
Fig. 3.1 Electrode Placement. Above image shows arrangement of ECoG electrodes and motor cortex depth electrode in a rat during surgical implantation.

provide additional information than spikes alone. However, if the spiking activity fails, the lower frequencies of the field potential can potentially be used as an alternative cortical control signal.

II. Methods:

A. Surgical Preparation

All animal procedures were approved by the University of Michigan University Committee on Use and Care of Animals and were in accordance with the National Institutes of Health guidelines. Three hundred gram, three months old Long Evans rats were chronically implanted with silicon substrate multi-site microelectrode arrays into the motor cortex. Surgery was done as previously described (Vetter et al., 2004, Marzullo et al., 2006). Anesthesia was maintained through intraperitoneal injections of a mixture of 50 mg/ml ketamine, five mg/ml xylazine, and one mg/ml acepromazine at an injection volume of 0.125 ml/100 g body weight. Every subsequent hour of surgery, 0.1 ml ketamine (50 mg/ml) was delivered to the animal to maintain anesthesia. Each animal was secured to a standard stereotaxic frame, and three stainless steel bone screws were inserted into the skull. A stainless steel ground wire attached to the electrode connector was connected to one bone screw over the parietal cortex to provide a ground point and temporary mechanical support until the connector was permanently cemented to the skull using dental acrylic. A craniotomy (approximately three mm by two mm) was made over the target cortical area, and the dura mater was cut away to reveal the cortical surface. The electrode array was inserted by hand using #5 fine Teflon-coated forceps into the
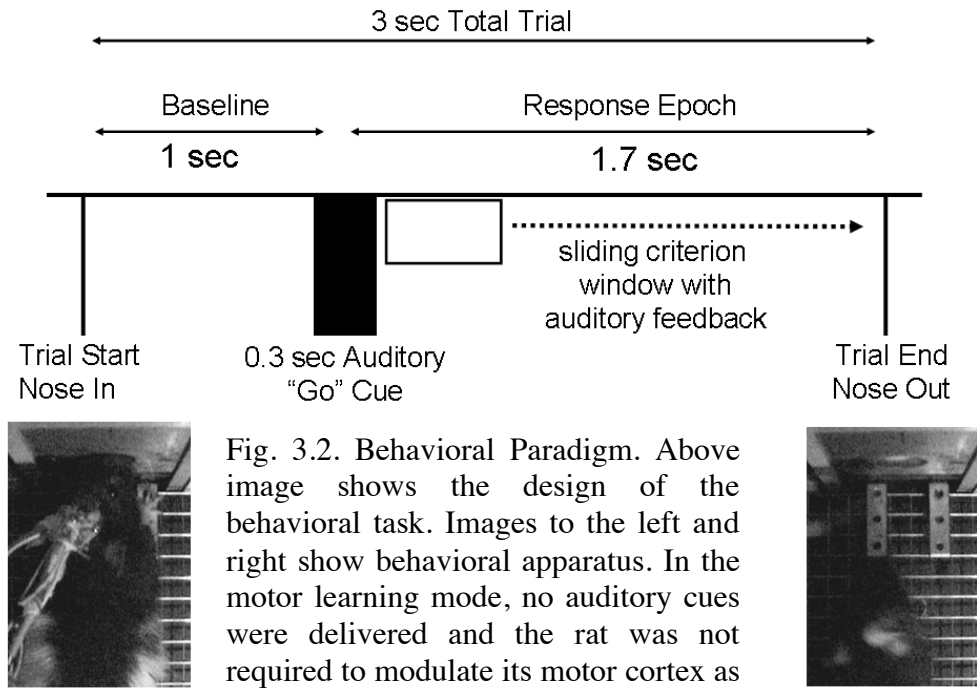
Fig. 3.2. Behavioral Paradigm. Above image shows the design of the behavioral task. Images to the left and right show behavioral apparatus. In the motor learning mode, no auditory cues were delivered and the rat was not required to modulate its motor cortex as in the neuroprosthetic task.

target cortical area. The surface of the brain was sealed with the biocompatible hydrogel ALGEL (Neural Intervention Technologies, Ann Arbor, MI), the electrode assembly was wrapped with GelFoam (Pfizer, Inc., New York), and the entire assembly was sealed with dental acrylic. The skin around the acrylic was tightened with sutures, anti-bacterial cream was applied, and the animal was then given two days to recover from the surgery.

Each electrode consisted of a single silicon shank with sixteen 1250 μm^2 platinum/iridium electrode sites separated by 100 μm (catalog c1x16-6mm100-1250, NeuroNexus Technologies, Ann Arbor, MI). We chose our implantation coordinates to span the forelimb/neck area of the right rat motor cortex (Sanes et al., 1990): 1-3 mm anterior to bregma, 2-3 mm lateral from bregma, and 1.5 mm deep from the surface of the brain (Paxinos and Watson, 1998). Each electrode was inserted in an attempt to ensure that the dorsal electrode site was at the top of the brain.

Electrocorticograms (ECoGs) were recorded via screws inserted into the skull with wire leads coming off the screws (catalog number E363/20/1.6, PlasticsOne, Roanoke, VA) (see Fig. 1 for electrode schemata). The ECoG electrodes were implanted such that the base of the screw was in contact with the dura mater of the brain. The electrode wire sleeves were then mounted in a pedestal on the animal's head for chronic

recording (MS363 pedestal, PlasticsOne, Roanoke, VA). Two ECoG screws were placed approximately two mm anterior and two mm posterior to the microelectrode craniotomy. A ground ECoG was placed over the cerebellum of the rat.

B. Electrophysiology and Behavior System

Units were sorted via a Multichannel Neuron Acquisition System (Plexon, Inc., Dallas, TX) and spike times were relayed with nominal delays via TCP/IP to a dual 1.25 GHz Dell Dimension Computer (Dell, Inc., Austin, TX) that both analyzed the spike activity using in-house designed software (Mathworks, Inc., Natick, MA) and controlled the behavioral box (Coulborne Instruments, Inc., Allentown, PA). During each experimental session neural electrophysiological data from the 16 electrode channels sampled at 40 kHz were simultaneously amplified and bandpass filtered (450 – 5000 Hz). Manual spike sorting was conducted prior to each experimental session. LFPs were amplified 500 Hz and filtered from 3-90 Hz. The spikes and LFPs shared a common ground over the cerebellum. The ECoGs were recorded with a SR560 low noise preamplifer (Stanford Research Systems, Sunnyvale, CA), at 5000x gain, filtered at 0.3-300 Hz with a 6 dB rolloff, in differential mode between the anterior and posterior ECoG screws about the motor cortex with respect to a cerebellar ground ECoG screw.

The auditory stimuli were delivered via a speaker (Yamaha NS-10M Studio, Yamaha Corporation, Buena Park, CA) located 35 cm directly above the test box. The system delivered a near-flat frequency response between 500 Hz and 32 kHz. The system was calibrated to a position at the food delivery tray, although calibration measurements indicated that the test box approximated a free field.

C. Behavioral Training and Neuroprosthetic Algorithm

Upon surgical recovery (typically one week), the rats were trained to insert their noses in an aperture in the behavioral cage in order to receive a food pellet. See Fig. 1 for a depiction of the behavioral task. After learning this task (typically five days), the foot pedals were introduced. These foot pedals consisted of 3 in by 1 in platforms attached to clicker switches. After about a week of training, the rats were able to place both forepaws on the platforms while simultaneously placing their nose in the aperture, and gradual shaping procedures enabled the rats to be able to maintain this position for 3 seconds. Though the rats were able to keep both paws on the platform and their noses in the

aperture to attain the reward, video observation of the rats revealed an "anxious" behavior whereby the rats would often manically contract and twist their shoulder and neck muscles while in the nosepoke task.

After a week of training in this mode, the rats were trained on the neural operant conditioning task whereby the rats had to modulate the ensemble neural activity of the motor cortex to receive a food reward. Formal mathematical details of this algorithm (Marzullo et al., 2007) consist of the following:

We used an in-house developed z-scored based weighted *ad hoc* linear algorithm. Trials consisted of a 1 sec baseline, a 0.3 sec 1 kHz tone stimulus period, and a 1.7 sec response window. The mean baseline firing rate and standard deviation were calculated by sliding a 450 ms window in 90 ms second steps over the baseline period. The response firing rate was calculated similarly by sliding 450 ms in 90 ms steps. In general, if the rat's motor cortex firing rates response level was greater than a given threshold on a given trial ($R_t > T_t$), the animal was rewarded. The response level R_t was calculated on every trial as:

$$R_t = \sum_{c=1}^{n} \left| \frac{r_{c,t}}{b_{c,t}} \right| (W_{c,t})$$

(1)

Where $r_{c,t}$ is the number of spikes in the sliding 500 ms response window; $b_{c,t}$ is the mean baseline number of spikes, and $W_{c,t}$ is the individual channel weight. The subscripts c and t refer to a given channel on a given trial. n is the number of channels. The threshold T_t was calculated on every trial as:

$$T_t = \sum_{c=1}^{n} \left(1 + \frac{\kappa \sigma_{c,t}}{b_{c,t}} \right) W_{c,t}$$

(2)

Where κ is an arbitrary coefficient, usually set to 2.5, used to set the difficulty of the task, and $\sigma_{t,c}$ is the baseline firing rate standard deviation.

Initially, the weights were all set to one but were then updated after each successful trial as:
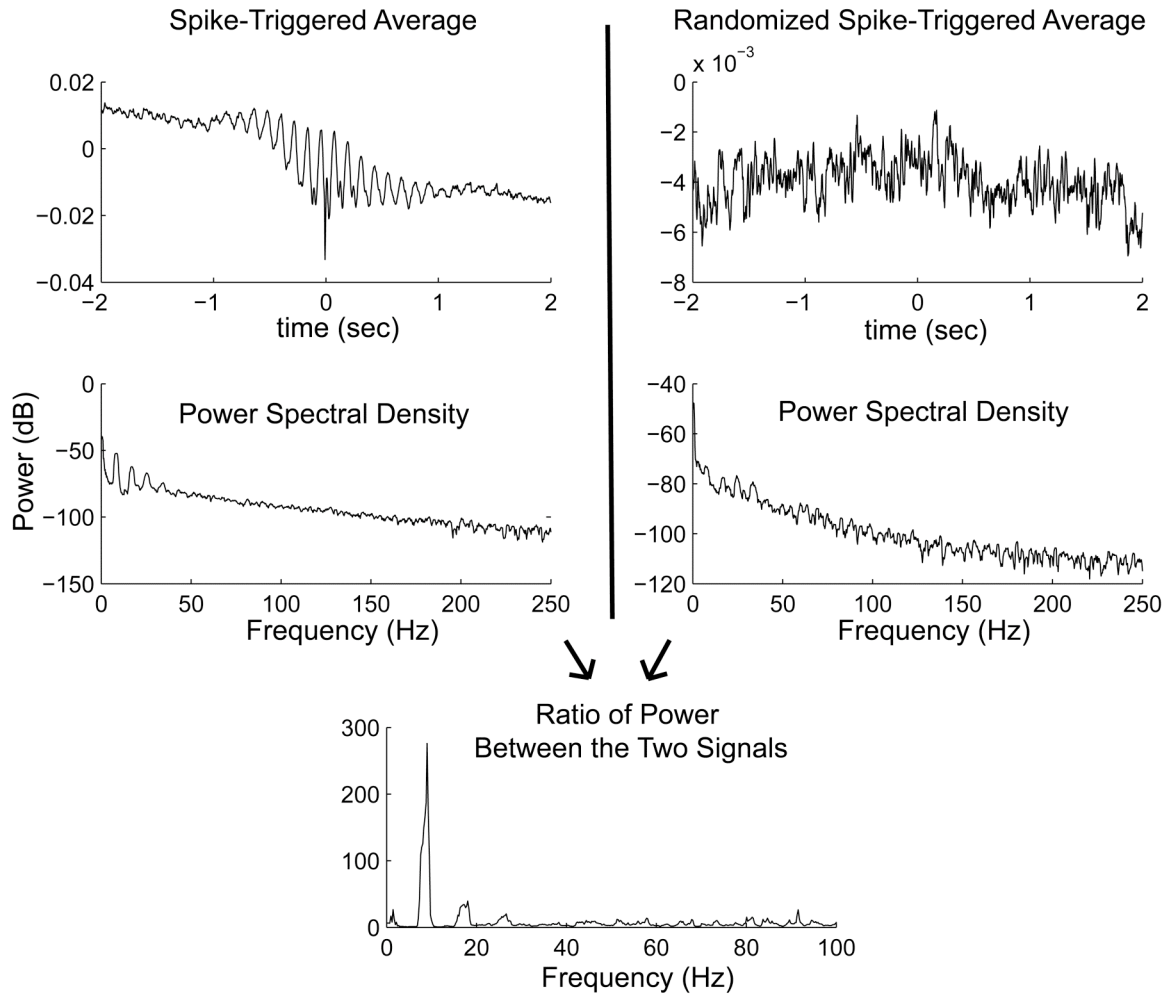
Fig. 3.3. Normalization of spike-triggered averages. Left Top shows spike-triggered average of a spike/LFP pair and its accompanying power spectral density. Right Top shows a randomized spike-triggered average and its accompanying power spectral density. Bottom graph shows the ratio of the power between the two spectra. This "power ratio" vs. frequency was used as our chief metric for all subsequent analysis.

$$(3) \qquad W_{c,t} = \frac{1}{m} \sum_{?=t-m+1}^{t} w_{c,?}$$

Where m is a history buffer of previous trials, and $W_{c,t}$ was the ten trial average weight for each channel. In our experiments, m was set to ten, meaning the weights were calculated as a running average of the previous ten successful trials. $w_{c,t}$ (individual channel, individual trial weight) was calculated as:

$$w_{c,t} = \frac{Z_{c,t}}{\sum_{c=1}^{n} Z_{c,t}}$$

(4)

Where $Z_{c,t}$ is:

$$Z_{c,t} = \left| \frac{r_{c,t} - b_{c,t}}{\sigma_{c,t}} \right|$$

(5)

Our group has empirically found that operant rates of 35-40% are optimal for quick learning in cortical control applications. Thus, we changed the κ value from eq. 2, if necessary session-to-session, to keep chance ~40%.

In addition, auditory feedback, in the form of pure tones delivered every 90 ms, was continuously given to the rat during the response period to give the rat some indication of the state of the neural ensemble. As the rat's R_t approached T_t, the frequency of the auditory tone would increase from 0-1000 Hz. If the rat achieved the firing rates necessary for reward T_t prior to the end of the three second window, the auditory tone would continue as 1000 Hz pips until the end of the nose-in period.

D. Data Analysis

All neurons were subject to automated (using Matlab) autocorrelogram analysis, whereby the absolute refractory period was examined to determine whether the unit was a single neuron or multi-neuron cluster. Neurons with an absolute refractory period of 2 ms were considered to be single units (Henze et al., 2000).

The single units were then analyzed using spike-triggered averages (STAs) to the adjacent (100 μm distance) electrode's LFP as well as the ECoG. The power spectral density of the STA was then used to determine the frequency of phase-locking as a function of behavioral state. In order to normalize for the effects of electrode impedance and animal variation, the STA was calculated again for the same spike train, but the spike train was randomized such that the timing of all the spikes was shuffled. The power spectral density of the normal STA was then divided by the randomized STA to determine the magnitude of the phase-locking frequencies. See figure 3 for a graphical explanation of this technique.
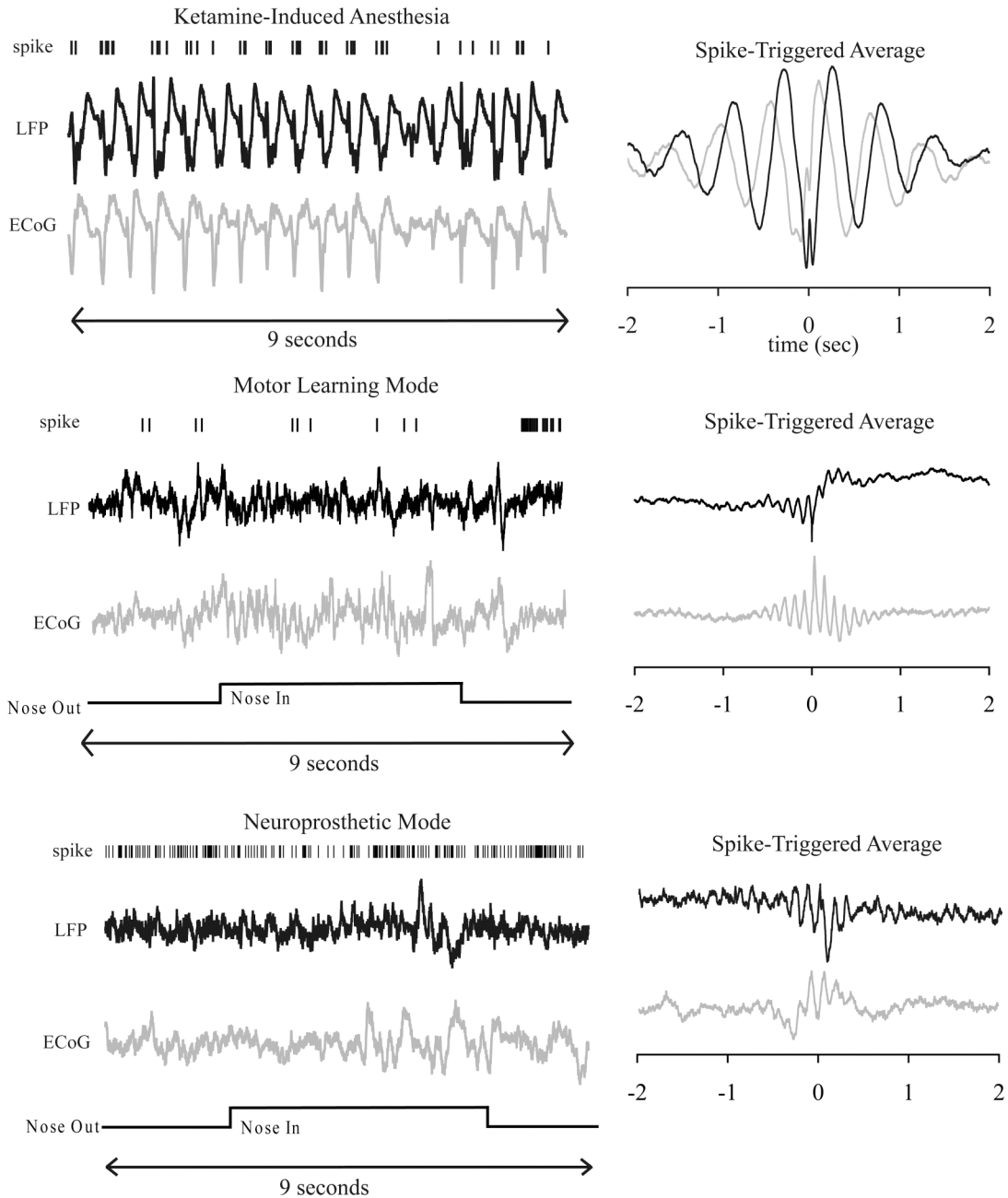
Fig. 3.4. Neural Traces of the Three States. Figures above show rasters of the spikes and traces of the LFPs and ECoGs. The spikes are single units, and the LFP from the same channel, and accompanying ECoG, are displayed below the rasters (LFP in black, and the ECoG in grey). Nine second snapshots are shown. The spike-triggered averages for the accompanying LFPs and ECoGs are shown on the right.

In addition, the spike-triggered averages were also subjected to an interval filter whereby only periods of high spiking modulation (two standard deviations above the neural firing rate means, assuming a Poisson distribution of the spike firing) were
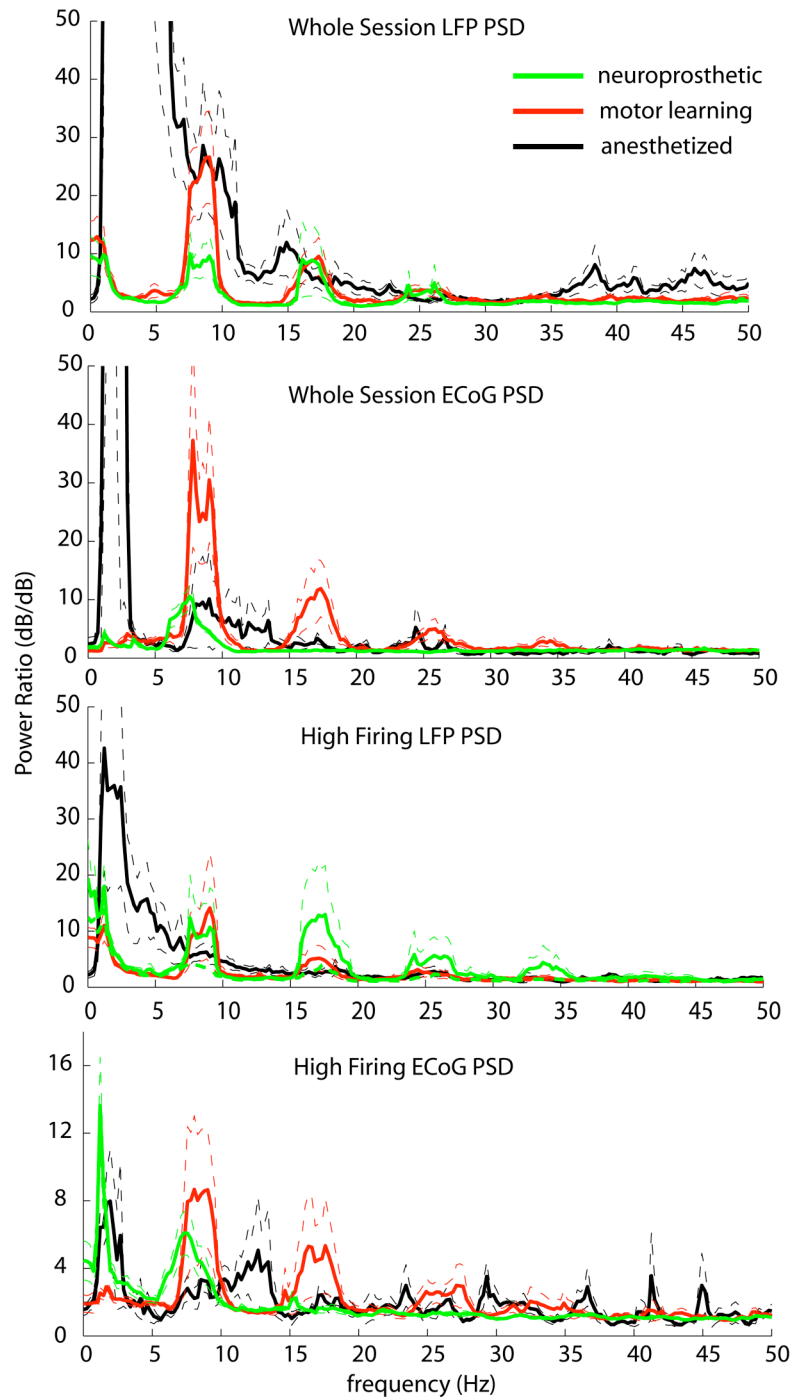
Fig. 3.5 Power Spectral Densities across all Neurons. Green line indicates neuroprosthetic mode, red line indicates motor learning mode, and black line represents anesthetized mode. Whole Session indicates the spike triggered averages were calculated over the whole behavioral session, and High Firing indicates the spike triggered averages were calculated over epochs where the firing rate exceeded two standard deviations of the neural firing rates mean. Dashed lines indicate standard error of the mean of the power ratio for a given frequency. Notice harmonics of theta (8 Hz) are prominent. Only frequencies up to 50 Hz are plotted; higher frequencies had

Fig. 3.6 Comparison of Power Spectral Densities between Motor Learning and Neuroprosthetic Modes for the LFP and ECoG for the three seconds prior to food delivery.

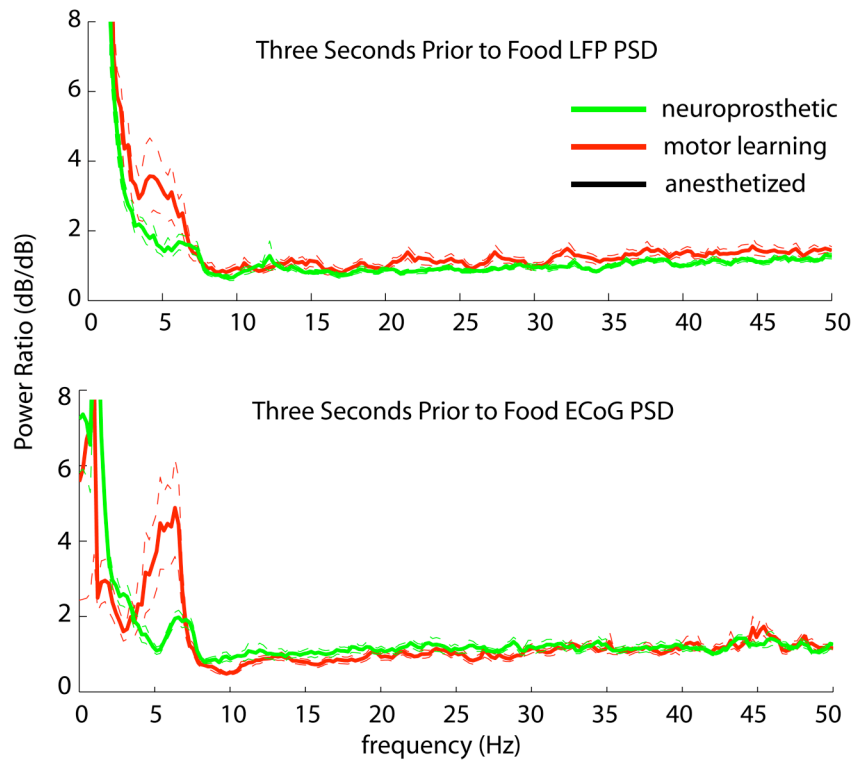analyzed to determine frequency of phase locking during neural spiking modulation. Finally, the periods during nose insertion (three seconds before food delivery) in both the motor learning and neural operant conditioning modes were also subjected to the STA analysis.

III. Results:

The data set consists of an analysis of 6 animals, and we were able to record a total of 1934 units (under the assumption of treating every training day as unique). Upon analysis of the autocorrelograms of the units to reveal absolute refractory periods of 2 ms (Connors et al., 1982, Connors and Gutnick, 1990, Henze et al., 2000), we isolated 310 single neurons. Of these, 199 of them had noise-free ECoGs, 212 had noise-free LFPs, and 120 had simultaneous noise-free LFPs and ECoGs. Thus, we recorded 15 anesthetized, 80 motor learning, and 117 neural operant conditioning STA-LFP pairs, and 4, 67, and 128, respectively, STA-ECoG pairs. We here present the analysis of these STA pairs.

During ketamine anesthesia (immediately after the implantation surgery), the spikes, LFPs, and ECoGs were all highly synchronized to the 1-2 Hz ketamine rhythm (Fontanini et al., 2003). See figure 4 for a raster plot of anesthetized single unit activity, combined with its respective LFP and ECoG traces and STAs. See figure 5 for the population analysis of single unit phase-locking during anesthesia.

During the motor learning and neural operant conditioning tasks, the spikes were weakly entrained to the theta rhythm (~8 Hz) in both the ECoG and LFP. However, we hypothesized that if we sorted the spikes to only calculate the STAs during periods of high firing, perhaps the phase-locking would shift from the low frequencies (specifically, theta) to the high >10 Hz brain rhythms. See figure 5 for a population level analysis of the single neurons during the whole session and the periods of the high spiking. Though the power of the phase-locking in the theta bands and its respective harmonics was reduced (though still present) in the neural operant conditioning period, we did not observe any phase-locking in the gamma frequencies in either the motor learning or neural operant conditioning tasks during periods of high firing.

However, since the rats were also trained to insert their nose in an aperture for a certain delay period in order to receive a food reward, we analyzed the three second period prior to food reward in 1) the motor learning task where the rat simply had to hold still and 2) the neuroprosthetic task where the rat had to modulate its firing rate activity while holding still in order to receive the food reward. In these epochs of STA analysis, there was still weak phase locking to the theta rhythm, but again, there was no entrainment to any high frequency >10 Hz ranges. See figure 6 for the population level analysis during the epochs prior to food delivery.

IV. Discussion:

Why did we not observe any phase locking to >10 Hz oscillations (beyond harmonics of the 8 Hz theta rhythms)? Though theta rhythms have been relatively unexplored in the motor cortex, it has been previously reported that theta rhythms are modulated in the motor cortex of dogs (Black and Young, 1972). Other groups have observed high frequency oscillations as a function of movement direction in monkeys (Heldman et al., 2006). Perhaps because we did not have a movement direction task, we did not observe the gamma oscillations. Figure 7 shows a snapshot spectrogram of our
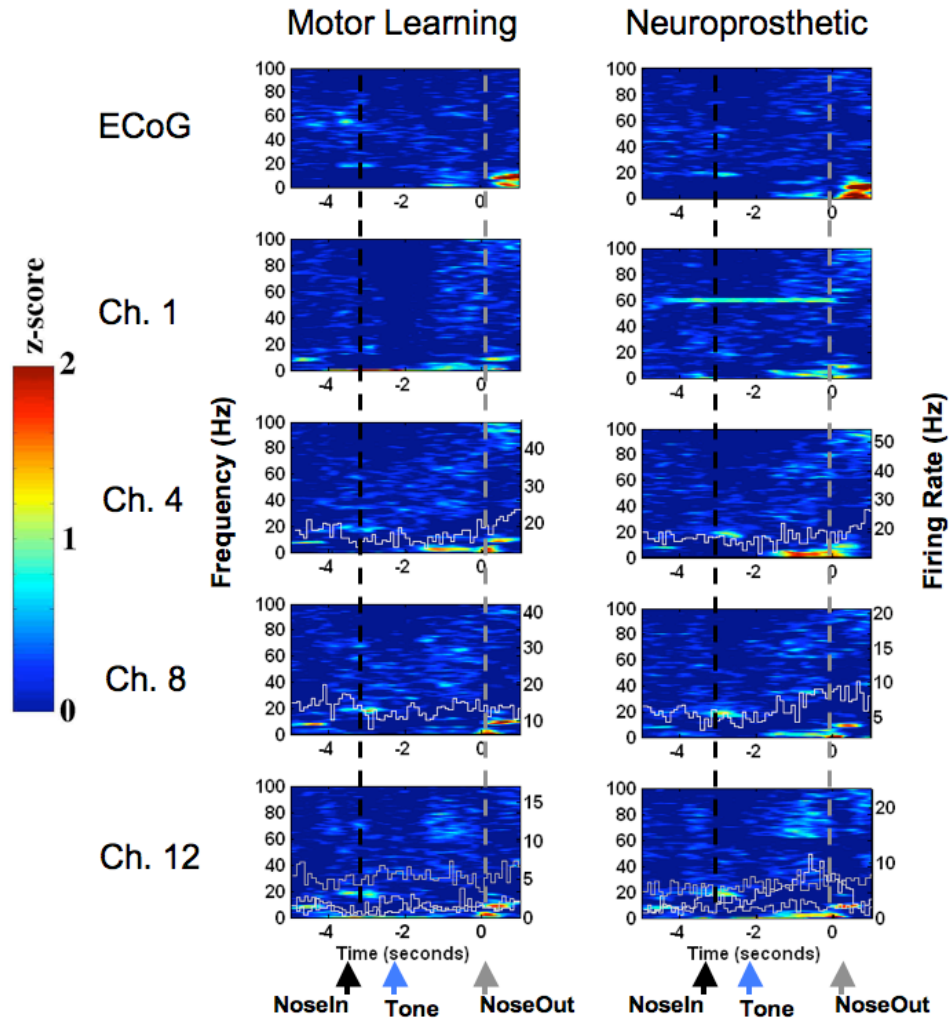
Fig. 3.7: Spectrograms of Motor Learning and Neuroprosthetic Mode LFPs and ECoGs during Two Exemplary Sessions. Notice an obvious lack of significant frequency modulation in the LFP and ECoG channels above >20 Hz frequencies. Grey line overlays on spectrograms indicate spike firing rate modulation on the same channel. Firing rates of spikes are shown on the right y-axis.

behavioral task; there are no clear gamma oscillations.

Our results in our rat model indicate that spiking modulation in the motor cortex in rats is largely correlated with the theta rhythm. In designing a neuroprosthetic control system, the frequency ranges of the gamma rhythms could still be added as an additional control signal for a neuroprosthetic device, but it is doubtful the controller would actually use/modulate the gamma frequencies. Of course, this will have to be verified by further experimentation. To design a neuroprosthetic control system in a rat combining both LFPs and spikes, an algorithm could bandpass the LFPs to only include the >10 Hz

frequencies, and use the bandpassed amplitude of the LFPs as an additional information channel. The "weights" $W_{c,t}$ of equation 3 in the methods above could then be examined to determine whether the animals are indeed using the LFPs as a modulating signal in preference to, or in equality with, the spiking activity.

As local field potentials can be recorded relatively easily when recording extracellular multi and single-unit activity, it has been proposed in the neural engineering community that local field potentials and spikes could be combined to create a high fidelity neuroprosthetic device controller. Here we report that the two signals are not exclusively independent. Thus, if field potentials, as well as ECoGs, were to be used concurrently with spikes for a neuroprosthetic device controller, the lower frequencies (<10 Hz) would provide redundant information. This may provide a benefit should the spiking activity fail; the low frequency field potentials could then be used for the control signal.

<div align="center">Acknowledgements:</div>

References:

BAKER, S. N., KILNER, J. M., PINCHES, E. M. & LEMON, R. N. (1999) The role of synchrony and oscillations in the motor output. *Exp Brain Res,* 128**,** 109-17.

BLACK, A. H. & YOUNG, G. A. (1972) Electrical activity of the hippocampus and cortex in dogs operantly trained to move and to hold still. *J Comp Physiol Psychol,* 79**,** 128-41.

CARMENA, J. M., LEBEDEV, M. A., CRIST, R. E., O'DOHERTY, J. E., SANTUCCI, D. M., DIMITROV, D., PATIL, P. G., HENRIQUEZ, C. S. & NICOLELIS, M. A. (2003) Learning to control a brain-machine interface for reaching and grasping by primates. *PLoS Biol,* 1**,** E42.

CONNORS, B. W. & GUTNICK, M. J. (1990) Intrinsic firing patterns of diverse neocortical neurons. *Trends Neurosci,* 13**,** 99-104.

CONNORS, B. W., GUTNICK, M. J. & PRINCE, D. A. (1982) Electrophysiological properties of neocortical neurons in vitro. *J Neurophysiol,* 48**,** 1302-20.

DONOGHUE, J. P., SANES, J. N., HATSOPOULOS, N. G. & GAAL, G. (1998) Neural discharge and local field potential oscillations in primate motor cortex during voluntary movements. *J Neurophysiol,* 79**,** 159-73.

FETZ, E. E. (2007) Volitional control of neural activity: implications for brain-computer interfaces. *J Physiol,* 579**,** 571-9.

FONTANINI, A., SPANO, P. & BOWER, J. M. (2003) Ketamine-xylazine-induced slow (< 1.5 Hz) oscillations in the rat piriform (olfactory) cortex are functionally correlated with respiration. *J Neurosci,* 23**,** 7993-8001.

FRIES, P., REYNOLDS, J. H., RORIE, A. E. & DESIMONE, R. (2001) Modulation of oscillatory neuronal synchronization by selective visual attention. *Science,* 291**,** 1560-3.

GRAY, C. M. & SINGER, W. (1989) Stimulus-specific neuronal oscillations in orientation columns of cat visual cortex. *Proc Natl Acad Sci U S A,* 86**,** 1698-702.

HELDMAN, D. A., WANG, W., CHAN, S. S. & MORAN, D. W. (2006) Local field potential spectral tuning in motor cortex during reaching. *IEEE Trans Neural Syst Rehabil Eng,* 14**,** 180-3.

HENZE, D. A., BORHEGYI, Z., CSICSVARI, J., MAMIYA, A., HARRIS, K. D. & BUZSAKI, G. (2000) Intracellular features predicted by extracellular recordings in the hippocampus in vivo. *J Neurophysiol,* 84**,** 390-400.

HOCHBERG, L. R., SERRUYA, M. D., FRIEHS, G. M., MUKAND, J. A., SALEH, M., CAPLAN, A. H., BRANNER, A., CHEN, D., PENN, R. D. & DONOGHUE, J. P. (2006) Neuronal ensemble control of prosthetic devices by a human with tetraplegia. *Nature,* 442**,** 164-71.

KENNEDY, P., ANDREASEN, D., EHIRIM, P., KING, B., KIRBY, T., MAO, H. & MOORE, M. (2004a) Using human extra-cortical local field potentials to control a switch. *J Neural Eng,* 1**,** 72-7.

KENNEDY, P. R., BAKAY, R. A., MOORE, M. M., ADAMS, K. & GOLDWAITHE, J. (2000) Direct control of a computer from the human central nervous system. *IEEE Trans Rehabil Eng,* 8**,** 198-202.

KENNEDY, P. R., KIRBY, M. T., MOORE, M. M., KING, B. & MALLORY, A. (2004b) Computer control using human intracortical local field potentials. *IEEE Trans Neural Syst Rehabil Eng,* 12**,** 339-44.

KJELSTRUP, K. B., SOLSTAD, T., BRUN, V. H., HAFTING, T., LEUTGEB, S., WITTER, M. P., MOSER, E. I. & MOSER, M. B. (2008) Finite scale of spatial representation in the hippocampus. *Science,* 321**,** 140-3.

LEUTHARDT, E. C., SCHALK, G., WOLPAW, J. R., OJEMANN, J. G. & MORAN, D. W. (2004) A brain-computer interface using electrocorticographic signals in humans. *J Neural Eng,* 1**,** 63-71.

MARZULLO, T. C., GAGE, G. J., LEHMKUHLE, M. J. & KIPKE, D. R. (2007) A direct visual and motor neural interface demonstration in a rat. *3rd International IEEE/EMBS Conference on Neural Engineering.* Kohala Coast, HI.

MARZULLO, T. C., MILLER, C. R. & KIPKE, D. R. (2006) Suitability of the cingulate cortex for neural control. *IEEE Trans Neural Syst Rehabil Eng,* 14**,** 401-9.

MEHRING, C., NAWROT, M. P., DE OLIVEIRA, S. C., VAADIA, E., SCHULZE-BONHAGE, A., AERTSEN, A. & BALL, T. (2004) Comparing information about arm movement direction in single channels of local and epicortical field potentials from monkey and human motor cortex. *J Physiol Paris,* 98**,** 498-506.

MEHRING, C., RICKERT, J., VAADIA, E., CARDOSA DE OLIVEIRA, S., AERTSEN, A. & ROTTER, S. (2003) Inference of hand movements from local field potentials in monkey motor cortex. *Nat Neurosci,* 6**,** 1253-4.

MURTHY, V. N. & FETZ, E. E. (1996a) Oscillatory activity in sensorimotor cortex of awake monkeys: synchronization of local field potentials and relation to behavior. *J Neurophysiol,* 76**,** 3949-67.

MURTHY, V. N. & FETZ, E. E. (1996b) Synchronization of neurons during local field potential oscillations in sensorimotor cortex of awake monkeys. *J Neurophysiol,* 76**,** 3968-82.

MUSALLAM, S., CORNEIL, B. D., GREGER, B., SCHERBERGER, H. & ANDERSEN, R. A. (2004) Cognitive control signals for neural prosthetics. *Science,* 305**,** 258-62.

PAXINOS, G. & WATSON, C. (1998) *The rat brain in stereotaxic coordinates,* San Diego, Academic Press.

RICKERT, J., OLIVEIRA, S. C., VAADIA, E., AERTSEN, A., ROTTER, S. & MEHRING, C. (2005) Encoding of movement direction in different frequency ranges of motor cortical local field potentials. *J Neurosci,* 25**,** 8815-24.

SANES, J. N., SUNER, S. & DONOGHUE, J. P. (1990) Dynamic organization of primary motor cortex output to target muscles in adult rats. I. Long-term patterns of reorganization following motor or mixed peripheral nerve lesions. *Exp Brain Res,* 79**,** 479-91.

SCHALK, G., MILLER, K. J., ANDERSON, N. R., WILSON, J. A., SMYTH, M. D., OJEMANN, J. G., MORAN, D. W., WOLPAW, J. R. & LEUTHARDT, E. C. (2008) Two-dimensional movement control using electrocorticographic signals in humans. *J Neural Eng,* 5**,** 75-84.

SCHWARTZ, A. B. (2004) Cortical neural prosthetics. *Annu Rev Neurosci,* 27**,** 487-507.

TAYLOR, D. M., TILLERY, S. I. & SCHWARTZ, A. B. (2003) Information conveyed through brain-control: cursor versus robot. *IEEE Trans Neural Syst Rehabil Eng,* 11**,** 195-9.

TREJO, L. J., ROSIPAL, R. & MATTHEWS, B. (2006) Brain-computer interfaces for 1-D and 2-D cursor control: designs using volitional control of the EEG spectrum or

steady-state visual evoked potentials. *IEEE Trans Neural Syst Rehabil Eng*, 14**,** 225-9.

VELLISTE, M., PEREL, S., SPALDING, M. C., WHITFORD, A. S. & SCHWARTZ, A. B. (2008) Cortical control of a prosthetic arm for self-feeding. *Nature*, 453**,** 1098-101.

VETTER, R. J., WILLIAMS, J. C., HETKE, J. F., NUNAMAKER, E. A. & KIPKE, D. R. (2004) Chronic neural recording using silicon-substrate microelectrode arrays implanted in cerebral cortex. *IEEE Transactions on Biomedical Engineering*, 51**,** 1-9.

WILSON, J. A., FELTON, E. A., GARELL, P. C., SCHALK, G. & WILLIAMS, J. C. (2006) ECoG factors underlying multimodal control of a brain-computer interface. *IEEE Trans Neural Syst Rehabil Eng*, 14**,** 246-50.

WOLPAW, J. R. & MCFARLAND, D. J. (2004) Control of a two-dimensional movement signal by a noninvasive brain-computer interface in humans. *Proc Natl Acad Sci U S A*, 101**,** 17849-54.

WOMELSDORF, T., FRIES, P., MITRA, P. P. & DESIMONE, R. (2006) Gamma-band synchronization in visual cortex predicts speed of change detection. *Nature*, 439**,** 733-6.

Chapter IV

A Sensorimotor Closed-loop Neural Interface Case Study in Rats

Abstract:

Developments of the past decades have shown it is possible to extract and decode control signals directly from the brain for use in neuromotor prosthetics. Currently, there is a push towards developing closed-loop interface systems combining recording output signals and, via microstimulation techniques, generating input feedback signals. Here we describe our iterative results in a rat model of a sensory/motor neurophysiological feedback control system.

Five rats were chronically implanted with microelectrode arrays in both the motor and visual cortices. The rats were subsequently trained over weeks to modulate their motor cortex ensemble in response to intra-cortical microstimulation (ICMS) of the visual cortex in order to receive a food reward. Rats were also given continuous feedback via visual cortex ICMS during the response periods of the behavioral trials that was representative of the motor cortex ensemble dynamics. The animals were able to use the feedback as a signal, and analysis revealed the rats were using the feedback as indicators of behavioral trials. We also show exemplary data with motor movement minimization as well as using electrical brain stimulation as reward.

Combining ICMS of sensory cortex with ensemble decoding of motor cortex holds promise for future neuroprosthetic applications, and our preparation offers a useful test model for improving the technology of closed-loop neural devices.

I. Introduction

Technological developments over the past decade have caused a dramatic growth in the capabilities of brain-controlled applications in rats (Chapin et al., 1999, Gage et al., 2005), monkeys (Wessberg et al., 2000, Serruya et al., 2002, Taylor et al., 2002, Carmena et al., 2003, Musallam et al., 2004), and humans (Kennedy and Bakay, 1998, Kennedy et

al., 2000, Hochberg et al., 2006). However, all the studies above focused on exploiting/creating output signals of the brain, with either visual or auditory feedback given to the experimental subjects indicating the state of the respective neural ensembles. The scientific community speculates that the next technological growth area will be delivering feedback of neural output states directly back to sensory areas of the central nervous system (Abbott, 2006, Fagg et al., 2007), as doing so could potentially improve operator performance and efficacy of neuroprosthetics. For example, in a recent report (Velliste et al., 2008) in which a monkey controlled a robot arm to feed itself using its motor cortex activity, the monkey had to visually watch the arm's movement to control it. While visual feedback is sufficient for the highly controlled lab environment, this severely limits the use of a neuroprosthetic device if the user has to carefully watch the device/limb everytime he uses it (for example, typing on a computer, playing a musical instrument, and walking/running are motor behaviors that humans do without looking directly at their limbs). Thus, there is increasing itself in delivering feedback to the brain of the "state" of a neuroprosthetic device,

Concurrent with the development of neuroprosthetic output devices, some groups have explored sensory replacement/augmentation and fundamental neural encoding through delivering sensory information to the neocortex in the form of electrical stimulation (Dobelle et al., 1979, Romo et al., 1998, Bradley et al., 2005, Fitzsimmons et al., 2007, London et al., 2008). However, the simultaneous use of neural recording/decoding techniques with sensory cortex intracortical microstimulation (ICMS) in real-time for neuroprosthetic models remains unexplored.

Our group has previously investigated both ensemble decoding for neuroprosthetics (Gage et al., 2005, Marzullo et al., 2006) and sensory cortex ICMS (Rousche et al., 2003, Otto et al., 2005) in separate experiments, and here we combine these two techniques for a closed-loop preparation with the long-term goal of improving both neuroprosthetic applications. We explored 1) the feasibility of sensory cortex ICMS as a "go" stimulus in a cortical control task, and 2) the use of sensory cortex ICMS feedback simultaneously with motor ensemble decoding.

In this report we describe, case by case, our iteratively developed preparation. Five rats were trained to modulate their motor cortices in response to ICMS of the visual

cortex. Three of these animals were also given feedback, via visual cortex ICMS, during the response periods that was representative of the dynamics of the motor cortex ensembles. The rats were able to use the ICMS as an information source and were able to appropriately modulate the motor cortex. We also report pilot results utilizing electrical stimulation of the reward pathway and minimization of motor movement. Finally, we discuss the limitations of our model, technological issues, and future applications.

II. Methods

A. Electrode Arrays, Surgical Procedure, and Neural Recordings

All animal procedures were approved by the University of Michigan University Committee on the Use and Care of Animals and were in accordance with the National Institutes of Health guidelines. Five male Long-Evans Rats (400-500 grams) naïve to the behavioral task were implanted with two 16 or 32-channel chronic silicon-substrate microelectrodes (Vetter et al., 2004), each consisting of a single silicon shank with 1250 μm^2 platinum/iridium electrode sites separated by 100 μm (catalog #3mmChron100-1250, Center for Neural Communication Technology, University of Michigan, Ann Arbor or catalog #6mmChron100-1250, NeuroNexus Technologies, Inc., Ann Arbor, MI). The visual cortex electrodes were activated prior to the surgery using cyclic voltammetry through the electrode sites to create an iridium oxide layer to both increase charge capacity and reduce the impedance (Weiland and Anderson, 2000). In addition some rats were implanted with medial forebrain bundle electrodes (MFB) at 4.6 mm posterior to bregma, 0.9 mm lateral from bregma, and 8.4 mm deep from the surface of the skull, using bipolar concentric electrodes (catalog #MS308, PlasticsOne Inc., Roanoke, VA).

Surgery was performed as previously described (Vetter et al., 2004, Marzullo et al., 2006). Briefly, the rats were anesthetized with a ketamine/xylazine cocktail, and heart rate and blood oxygen were monitored with a pulsoximeter. The skull was exposed and 3 mm diameter craniotomies were made over the target cortical areas. The silicon electrodes were inserted in the motor cortex (target 2.5-3.0 mm anterior to bregma, 2.5 mm lateral from bregma) (Sanes et al., 1990) and visual cortex (0 mm posterior to lambda, 3-4 mm lateral from bregma) (Shuler and Bear, 2006). The electrodes were hand-inserted using #5 Teflon coated forceps, and the electrode ribbon cables were wrapped with gelfoam before enclosing the whole electrode assembly in acrylic. Total

surgery time was typically seven hours, and rats were given a week to recover before training began.

During each experimental session neural electrophysiological data from the electrode channels sampled at 40 kHz were simultaneously amplified and bandpass filtered (450 – 5000 Hz) on a Multichannel Neuronal Acquisition Processor (MNAP; Plexon Inc, Dallas, TX). Local field potentials were amplified at 500x and filtered from 1-500 Hz.

B. Visual Cortex Characterization

Immediately after surgery, while the animal was still anesthetized, it was placed in a dark behavioral box, and visual and motor cortex neural responses were recorded as the house lights flashed on and off every 20 seconds. The spiking and field potential responses about light onset and offset were then analyzed with peri-event time histograms (PETHs) to determine the extent of visual evoked responses. The visual cortex channel with the most robust response, as determined by a maximal increase in spiking unit firing rate or maximal field potential amplitude at light onset, was used as the stimulation channel in subsequent behavioral experiments after surgical recovery.

C. Training Paradigm:

After surgical recovery, all rats were maintained at 85% of their free-feeding weight. For each behavioral session, the rats were plugged into the headstage and commutator cables and placed into the dark behavioral box. Rats were typically trained 4-6 days a week, at 2-5 sessions per day. Units were sorted by hand prior to each training session using Plexon Sortclient software (Plexon Inc, Dallas, TX). All spike times from the sorted units were then relayed with nominal delays via TCP/IP to a dual 1.25 GHz Dell Dimension Computer (Dell, Inc., Austin, TX) that analyzed the spike activity using in-house designed software (Mathworks, Inc., Natick, MA) and controlled both the behavioral box (Coulborne Instruments, Inc., Allentown, PA) and the stimulation hardware (A-M Systems 2200 Analog Stimulus Isolator, Sequim, WA, for single channel stimulation or Tucker Davis Technologies Multichannel Stimulator RX7 with MS16 Stimulator Base Station, TDT Systems, Alachua, FL, for multichannel stimulation).

Initially, we used an *ad hoc* linear algorithm to train the rats (Rats M5, M6). Briefly, this algorithm transformed the firing rates of all the sorted units into z-scores
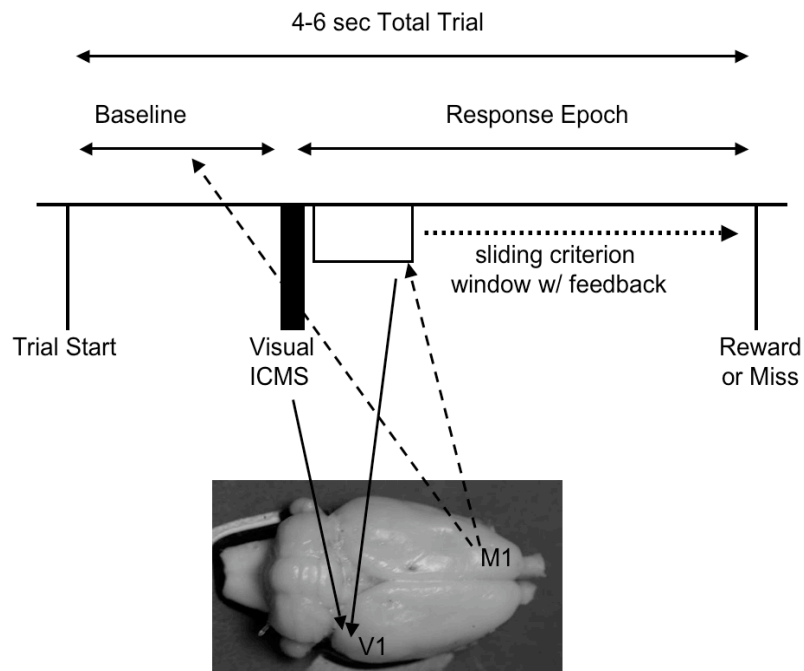
Fig. 4.1: General Behavioral Scheme. Rats M5 and M6 were trained without feedback (with the exception of the motor minimization training with rat M5), whereas M10, M11, and M12 were trained with feedback.

based on the neural firing rate means, and the rats were rewarded for increasing the neural firing rates an experimenter-determined z-score away from the firing rate means after presentation of the visual cortex ICMS "go" cue. See Fig. **1** for a schematic of the behavioral task. Formal mathematical details of this algorithm are previously published by our group (Marzullo et al., 2007).

However, the *ad hoc* linear algorithm does not allow the animal to initiate a trial (trials occur at random 8-12 second inter-trial intervals), so subsequent rats (M10-M12) were trained using a co-adaptive Kalman filter based on previous work by our group (Gage et al., 2005). Briefly, the co-adaptive Kalman filter finds correlated signals in the neural patterns that modulate from baseline firing rates with respect to the visual cortex ICMS "go" cue. To begin a trial, the rat had to maintain its motor cortex ensemble baseline firing rates, calculated in running two minute averages, for 450 ms (giving the rat some indirect power to "decide" when a trial begins). The visual cortex ICMS "go" cue then occurred, and the rat had to modulate its motor cortex for 450 ms within the 4-5 s response window in order to receive the food reward. We did not consider decreases in firing rates to be a neural response for reasons described below.

In all training paradigms, Monte Carlo simulations, in which the visual cortex stimulation times were shuffled while keeping the spike trains intact, were done offline to determine whether the animals were performing above chance (Gage et al., 2005, Marzullo et al., 2006). On a given session, if a rat performed at a percent correct rate that was greater than the 95% distribution of the Monte Carlo simulations (*p<0.05*), the session was considered a demonstration of learning. The mean of the Monte Carlo simulations for each session was also used as our metric of chance performance (operant rate) for a given session.

Our stimulation parameters used in the visual cortex ICMS "go" stimulus consisted of cathodic first, 200 μsec/phase biphasic pulses, delivered at 150 Hz, for 0.25 seconds, at an amplitude of 50-98 μA peak-to-peak for rats M5 and M6, and 20 μA for rats M10-M12. These parameters were chosen as such stimulation has been shown to be both perceivable, safe, and exhibits reversible faradaic reactions at the electrode interface (Rousche et al., 2003, Merrill et al., 2005). Periodically (every month), impedances at one kHz where taken for both the motor and visual electrodes with an Autolab system (Eco Chemie, Utrecht, Netherlands) to determine if any electrode sites had failed (typically revealed by an impedance >2-3 MΩ). If bad sites were found, the channels were dropped from the visual cortex ICMS paradigms during subsequent training.

D. Feedback

The three rats run on the Kalman filter training algorithm were also given feedback during the response window in the form of visual cortex ICMS representative of the motor cortex ensemble activity. However, as clearly seen in Figs. **3-8** (see neural responses at time = 0, or visual cortex ICMS "go" cue delivery), delivering current into the visual cortex causes a stimulation artifact in the motor cortex recordings. The amplifier saturation artifact prevents the recording of spikes during the ICMS, in effect reducing the observed firing rates of the motor cortex ensemble. To mitigate ICMS artifacts corrupting the motor cortex recordings, we used an interleaved feedback system. All of our training software used 90 ms clock cycles, whereby the number of spike occurrences since the last query to the neurophysiology system, and all calls to hardware, were made every 90 ms. Only during the first 10 ms of each 90 ms cycle was ICMS feedback delivered to the visual cortex. This effectively resulted in a drop of ~11% in

recordable spikes in the motor cortex recordings, but nonetheless was designed such that this "spike-drop rate" would still be minimal enough to observe the rat's motor cortex modulations during the response period. However, since the Kalman filter would interpret a consistent ~11% drop in firing rates across the ensemble during the response period as the rat decreasing firing rates in order to be rewarded, we modified the algorithm to only allow increases in firing rate to be considered actual neural responses to the visual cortex ICMS "go" stimulus.

We used three feedback codes over the course of our experiments as our hardware and software became more sophisticated: first an amplitude-based code, then a rate-based code, and finally a spatial-based code. In the amplitude-based code, the same parameters as the initial visual stimulus were used (a 150 Hz pulse train), but only two pulses were delivered every 90 ms, and the amplitude of these two pulses was varied from 0 μA to the amplitude of the initial stimulus (50-98 μA) in a linear transformation of distance between the baseline firing rates and reward threshold firing rates. Simply put, if the initial visual stimulus was 50 μA, and the animal's motor cortex ensemble firing rates were at baseline, the amplitude of the two feedback pulses was 0 μA. If the animal's response firing rates were midway between the baseline and threshold for reward, the amplitude of the two pulses was 25 μA. If the animal's response firing rates were at the threshold for reward, the amplitude of the two pulses was 50 μA. Thus, in this feedback model, the volume of the tissue activated, and hence putatively the magnitude and salience of the perceived stimulus, would be the feedback signal (Penfield and Perot, 1963, Brindley and Lewin, 1968, Merrill et al., 2005).

In the rate-based code, the amplitude of the feedback was invariant (identical to the amplitude of the initial visual cortex ICMS "go" stimulus), but the pulse rate was modulated. During the first 10 ms of every 90 ms of the response window, 0-10 pulses were delivered with inter-biphasic pulse intervals of 600 μsec. Thus, if the animal's firing rates were at baseline, zero pulses were delivered, and if the animal's response firing rates were in the response band necessary to be rewarded, 10 pulses were delivered. In this model, putatively the volume of activation is kept the same, but the firing rates of the activated neurons in the same volume are modulated by the feedback ICMS.
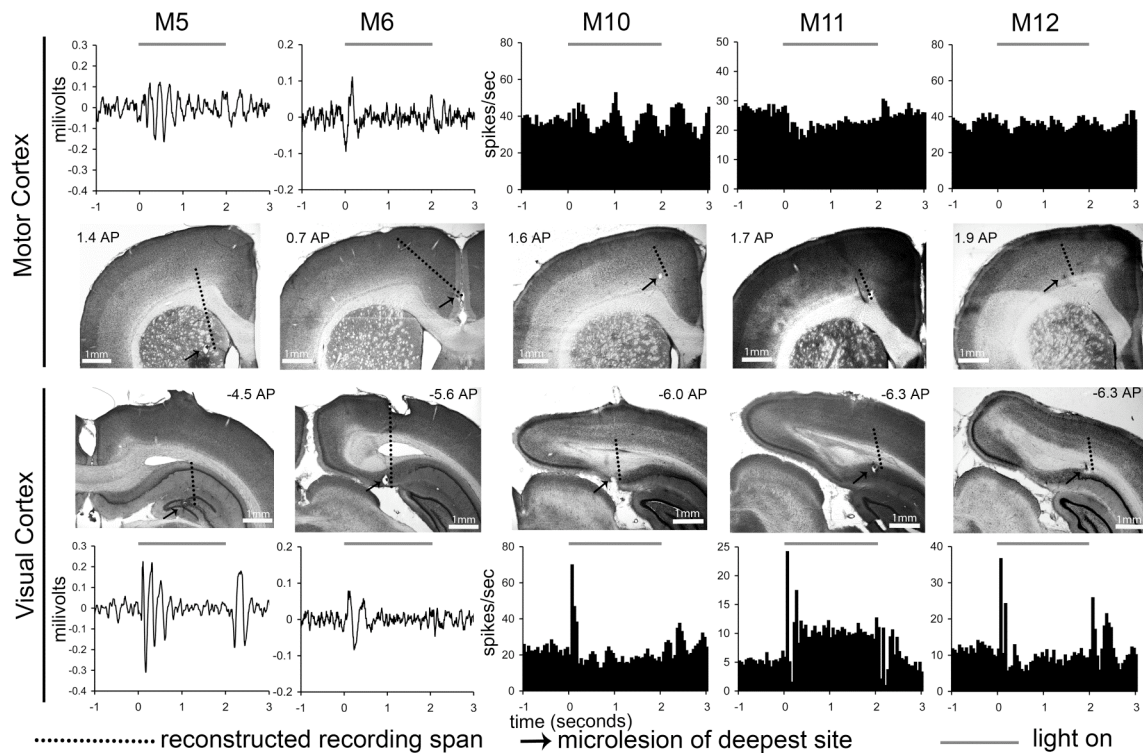
Fig 4.2: Histology and Evoked Responses to Light Flash. M5 and M6 depict LFP evoked responses to light flash, whereas M10-M12 depict spiking responses to light flash. Evoked responses in both motor cortex and visual cortex were recorded simultaneously post-surgery. Grey line above each evoked response shows time light was presented to the ketamine-anesthetized rats. The length of the dotted line on the histology images, showing the reconstruction of the recording tract, was calculated with a combination of measuring the angles of the electrodes *post mortem* along with the location of the microlesions. The AP numbers above each brain image are the distance, in mm, from bregma. Positive values represent anterior to bregma. These AP values were reconstructed by comparing the images to standards in a popular rat brain atlas (Paxinos and Watson, 1998). These slices only show the location of the most ventral electrode site; electrodes were implanted in a posterior angle for motor cortex and an anterior angle for visual cortex.

In the spatial-based code, the top electrode in the electrode array was stimulated as the initial visual cortex ICMS "go" stimulus, initiating a trial. This feedback paradigm consisted of stimulating the electrode sites in a dorsal direction as the animal's response firing rates got closer and closer to the threshold for reward. That is, if the animal's response firing rates were at baseline, the bottom-most site was stimulated. If the animal's response firing rates were in the response band necessary to be rewarded, the top-most site was stimulated. In the spatial feedback scheme, five biphasic pulse pairs were

delivered to the appropriate electrode site with an inter-biphasic pulse interval of 600 μsec. Only one electrode site was stimulated at any given moment in this paradigm.

During all feedback sessions, 15-20% of the trials were "catch trials" where either 1) feedback was randomized, or 2) no feedback was delivered. Percentage correct, and latency to reward, between the "normal trials" and "catch trials" were then used as our metrics in determining whether the rats were using the feedback signal.

E. Data Analysis

Peri-event time histograms (PETHs) of spikes about the visual cortex ICMS "go" cue were examined to see whether the spiking activity of the neurons increased in response to the stimulus. To determine if a recorded unit showed an excitatory response, 95% confidence intervals were calculated for the peri-event histograms using the NeuroExplorer software package (NeuroExplorer, Littleton, MA). The computations for these intervals assumed spike trains are the result of independent Poisson-point processes as described in the literature (Abeles, 1982). For the sessions with feedback, a chi-square test with a Yates correction was used to determine whether the "catch trials" percentage correct and the "normal trials" percentage correct were significantly different from each other (Pagano and Gauvreau, 2000).

F. Histology

Upon completion of training, the top, middle, and bottom sites of the multielectrode arrays were microlesioned by passing 35 µA of constant DC current for two seconds while the animal was anesthetized. Three hours after the microlesioning procedure, the rats were euthanized by intraperitoneal overdose of sodium pentobarbital. Following transcardial perfusion with 4% formaldehyde, the brain was removed, sectioned into coronal 100 µm slices, and stained with conventional cresyl violet Nissl stains. The sections were then analyzed using a Leica MZFLIII light microscope (Leica Microsystems, Inc., Germany) to determine probe placement. Upon extraction of the skull, we were able to keep the probes intact in situ, and thus we were able to post mortem measure implantation angles with respect to the skull in order to reconstruct the recording spans shown in Fig. 2.
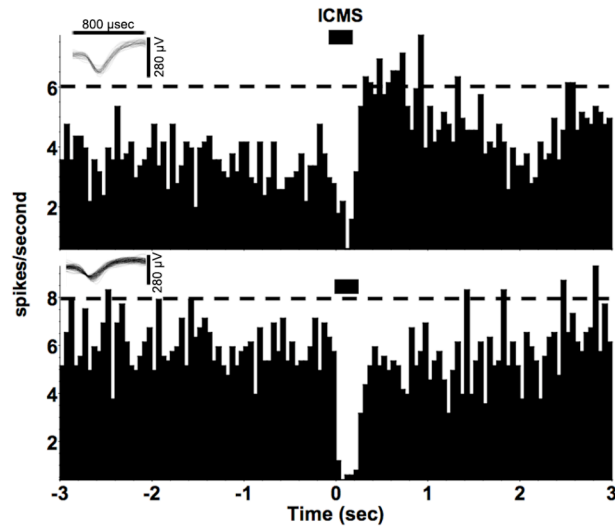
III. Results

Fig. 4.3: Initial Feasibility of Visual Cortex ICMS with Motor Cortex Control. PETHs above show two motor cortex units, from rat M5, modulating (top), and not (bottom), in response to the visual cortex ICMS "go" cue. Dashed lines indicate upper 95% confidence level of the mean of the neurons' firing rates. Insets show waveform samples of the respective neurons. Time zero indicates the delivery of the 0.25 second ICMS pulse train delivered to the visual cortex, signaling the beginning of a trial. Notice the ICMS artifact causing a transient decrease in observable firing rates. Feedback during the response period was not given in this case.

The objective of this study was to determine if microstimulation of the visual cortex could be combined successfully with real-time ensemble decoding of the motor cortex with the ultimate goal of fine-tuning the variety of technical issues involved with a closed-loop neuroprosthetic device. We below discuss our iterative progress on the five rats successfully implanted in this study (rats M5, M6, M10, M11, M12).

A. Visual-Evoked Responses

Fig. **2** shows the histology for both the motor and visual cortex implantation sites for the five rats used in this study, as well as the evoked responses to light flash in both the visual and motor cortices. Immediately after surgery, both M5 and M6's discernable unit activity in both motor and visual cortex did not reveal any evoked response to light flash. However, in both rats the local field potentials (LFPs) revealed an evoked response. M5's visual cortex evoked LFP response had a 2-fold greater amplitude than the motor cortex response, while M6's visual cortex evoked response had a similar amplitude to the motor cortex evoked response. M10-M12 had discernable units immediately after surgery in both the motor and visual cortex; for these rats the visual cortex spiking evoked

responses to light flash were much greater than the motor cortex spiking evoked responses. Spiking unit responses in visual cortex were typically very rapid with a 3-5 fold increase in firing rate with light onset and offset.

B. Feasibility of Visual Cortex ICMS Stimuli with Motor Cortex Ensemble Training

Fig. **3** shows PETHs from rat M5 during successful modulation of motor cortex neurons in response to visual cortex ICMS. The rat was trained using the *ad hoc* linear algorithm without feedback; for clarity only two neurons of the six neurons used are shown. The top PETH shows the neuron that was driving successful performance of the task by increasing firing rate after visual cortex ICMS, and the bottom PETH shows an unresponsive neuron, which was characteristic of the other four cells in the ensemble. In the early stages of the training, the rat was observed to simply scurry around the food tray and eat the food pellets when it would randomly get the task right. However, on learning sessions where the rat performed above chance, we observed the rat would immediately turn its head left after the visual cortex ICMS "go" cue. This motor behavior was likely the behavioral correlate of the modulation of the motor cortex. Rat M5 was able to learn the task within seven days of training, after which was it was trained with the "movement minimization" method discussed below in *Section D*.

Rat M6 was trained with the *ad hoc* linear algorithm as well, but beyond the exemplary medial forebrain bundle stimulation data discussed below in *Section E*, the rat never was able to successfully perform the task after four weeks of training. One possible cause may be the weakness of the *ad hoc* algorithm; all subsequent rats were trained with the Kalman Filter algorithm. Another possible cause may be that the visual cortex ICMS was not sufficiently salient a signal for this particular rat (notice in Fig. **2** that the visual cortex evoked response to light flash in this rat was identical to the motor cortex evoked response). However, the results with rat M5 showed that the visual cortex ICMS "go" stimulus could be perceived, and in our subsequent rats we moved to examining the use of ICMS feedback.

C. Feasibility of Visual Cortex ICMS Feedback with Motor Cortex Ensemble Training

Figs. **4-6** depict the behavioral learning curves and spiking responses for the three rats (M10-M12) trained with visual cortex ICMS feedback during the response period.
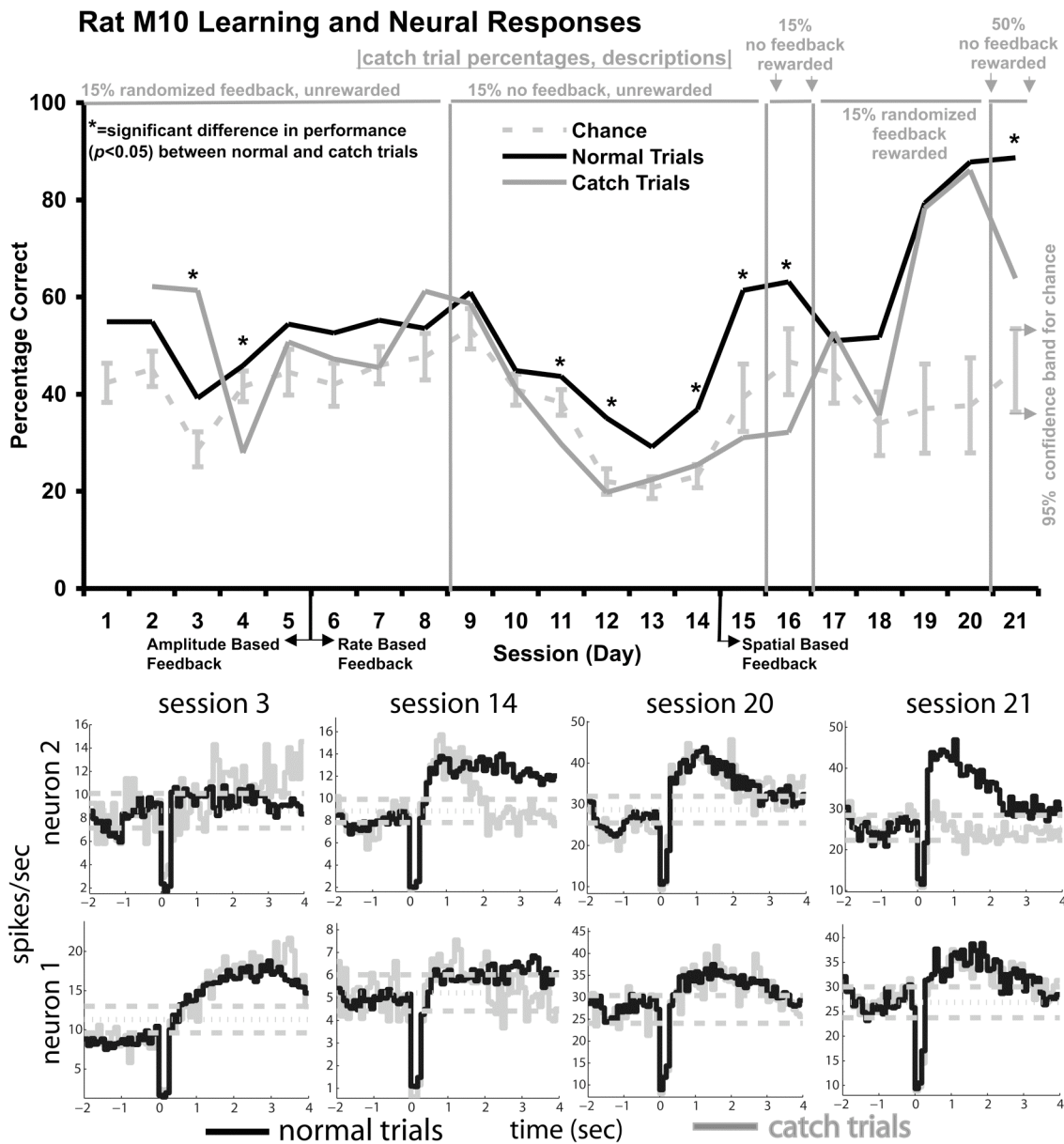
Figure 4.4: Rat M10 Learning Curve and Motor Cortex Spiking Responses. Top: Graph shows performance for M10. Chance calculation includes 95% confidence bands. Text at the top of graph indicates the percentage of total trials consisting of catch trials, the type of catch trials, and whether these catch trials were rewarded. Bottom: PETHs of responses to visual cortex ICMS "go" cue (time=0) for both normal trials and catch trials from selected sessions. For clarity, only two neural units, typically the most modulated of the ensemble, are shown per session. Dotted line on neural responses indicates neuron's mean firing rate, and dashed lines indicated 99% confidence bands for the mean firing rate, for the entire session. Each session refers to a different day of training, except for sessions 20 and 21, which are from the same day and show the same two units.

Figure 4.5: Rat M11 Learning Curve and Motor Cortex Spiking Responses. The format is identical to figure 4. In sessions 19-21, no visual cortex ICMS "go" cue was delivered. As such, time = 0 on the session 21 PETHs indicates the beginning of the feedback delivery.
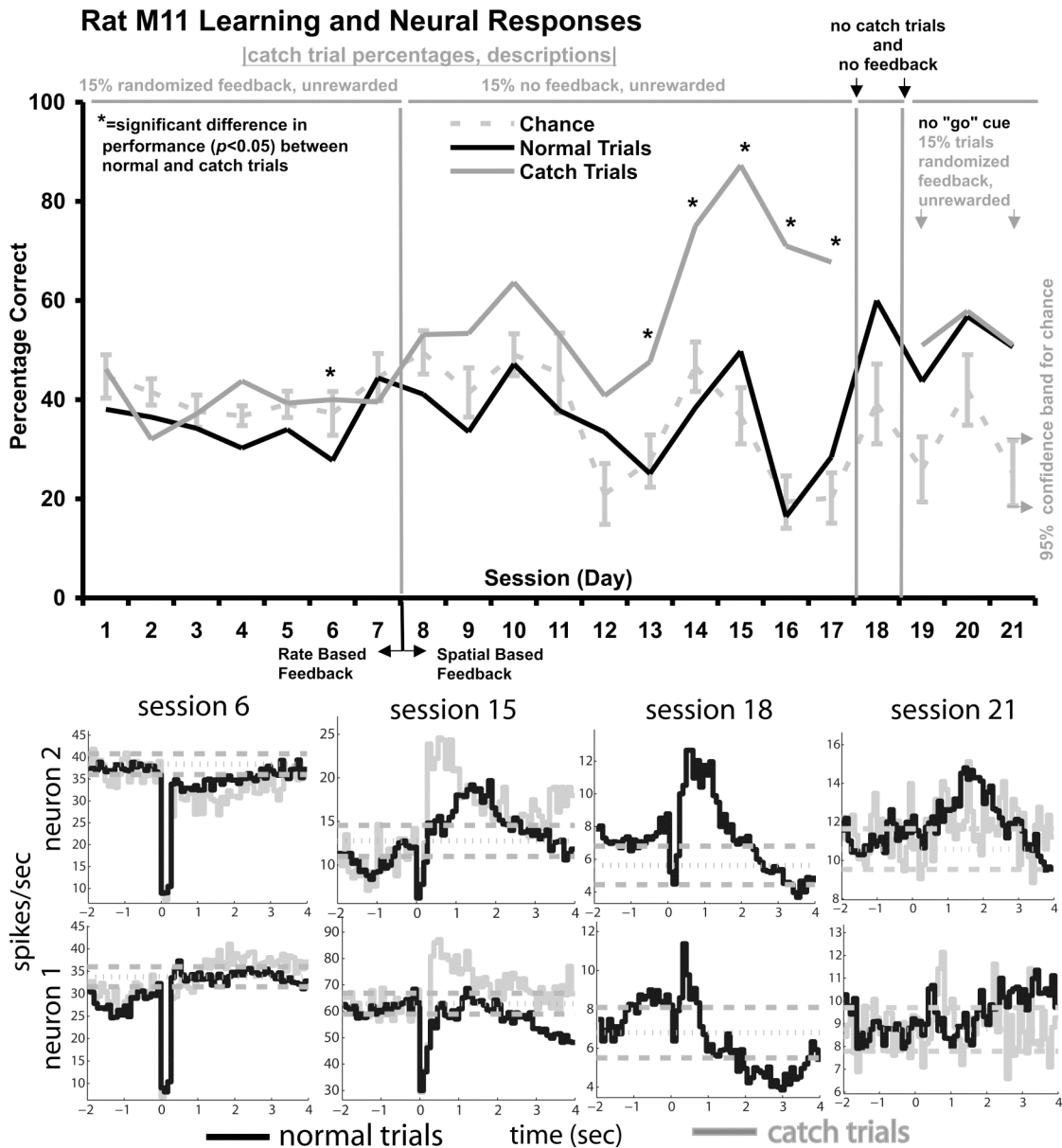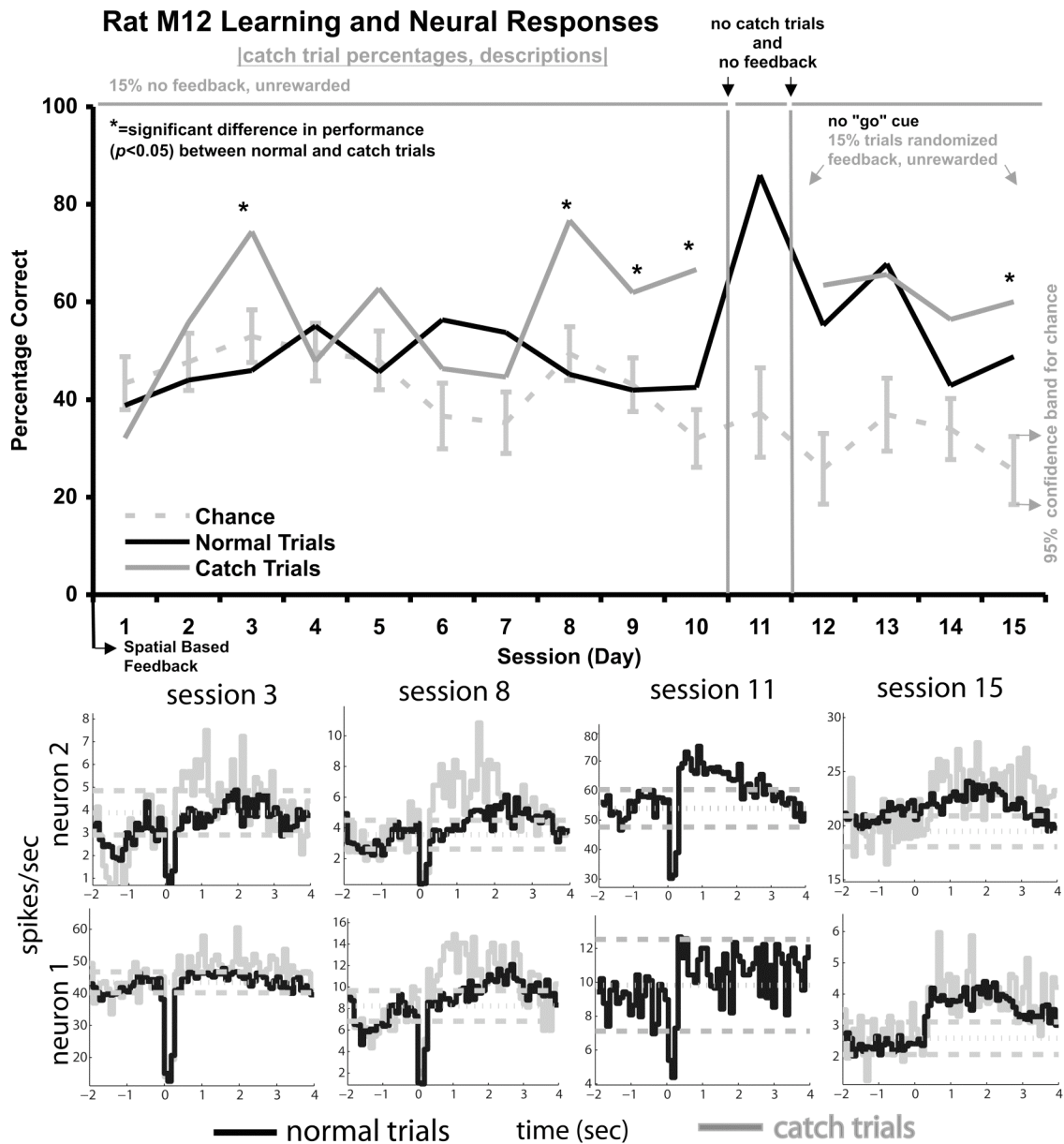
Figure 4.6: Rat M12 Learning Curve and Motor Cortex Spiking Responses. The format is identical to figure 4. In sessions 12-15, no visual cortex ICMS "go" cue was delivered. As such, time = 0 on the session 15 PETHs indicates the beginning of the feedback delivery.

Sessions where behavioral performance for the normal trials was significantly different from the catch trials, at an alpha value of 0.05 using a chi-square test with a Yates correction (Pagano and Gauvreau, 2000), are indicated by asterisks. PETHs show spiking responses to the visual cortex ICMS "go" cue from two selected neurons of the ensemble used in the respective sessions. Results from these three animals are presented in sequence below.

Rat M10 (Fig. **4**) was initially trained on the amplitude-based feedback (sessions 1-5), then on the rate-based feedback (sessions 6-14), and finally on the spatial-based feedback (sessions 15-21). Note that rat M10 was able to achieve performance above chance with all three feedback schemes, though performance was best with the spatial-based feedback. Whether this was due to the spatial-based feedback being more salient or the rat simply performing better with time cannot be determined with this dataset. It may seem surprising that rat M10 was able to perform the task above chance on the first day. However, for one week prior to session one, the rat was run with developmental versions of the Kalman filter algorithm and thus the rat might have already been familiar with the general nature of the task.

For rat M10, the normal trials and the catch trials began to be consistently different in performance rates in sessions 11-15. In these sessions, catch trials occurred 15% of the time and had no feedback during the response window. M10 performed significantly better ($p<0.05$) on the normal trials than the catch trials, indicating that the rat was using the feedback as a source of information (see Fig. **4**, session 14 neural response).

We examined the salience of the feedback by testing the hypothesis that behavioral performance on normal trials should be better than the catch trials regardless of reward. This was answered in two ways. First, the non-feedback catch trials were rewarded if the animal successfully modulated its motor cortex (session 16). Second, in sessions 17-20 the catch trials consisted of randomized feedback such that the feedback was not related to the motor cortex ensemble firing rates. In session 16 the performance of the normal trials was significantly higher than the catch trials even though the catch trials were rewarded, arguing that the rat was using the feedback as a source of information and not simply responding to the visual cortex ICMS "go" cue. However, in

sessions 17-20, where the catch trials consisted of randomized feedback, there was no significant difference in performance between the normal trials and the catch trials, even though the animal could still perform the task above chance (see neural responses in Fig. **4**, session 20; the normal trials and catch trials are effectively identical). These results argue that the rat was using the feedback as a measure of whether a trial was still occurring but not attending to the subtle features of the feedback signal. Indeed, on the last session (21) of rat M10 (Fig. **4**), 50% of the trials had no feedback. Though the rat performed above chance in both the feedback and non-feedback trials, the animal performed significantly better during feedback trials than the non-feedback trials, and the neural responses during the feedback trials was greater than the non-feedback trials for some neurons (see Fig **4**, session 21, neuron 1).

Rat M11 (Fig. **5**) was initially trained on the rate-based feedback (sessions 1-7) before being trained on the spatial-based feedback (sessions 8-21). The rat only performed above chance during the spatial-based feedback sessions, but again, whether this was due to the higher salience of the spatial-based feedback, or simply delayed learning of the general nature of the task, remains to be explored. During sessions 8-17, in which the catch trials contained no feedback, this animal actually performed better on the catch trials than the normal trials (see Fig **5**, session 15. Notice the neural responses on the catch trials are greater than the normal trials). We hypothesized that the rat was merely paying attention to the initial visual cortex ICMS "go" stimulus, and the feedback merely made the task harder because of the ~11% reduction of detectable spikes during the response window. We tested this hypothesis by training the animal for one session where the feedback was removed, and only the initial visual cortex ICMS "go" cue was delivered to the animal. The rat was then immediately able to perform the task above chance (see Fig **5**, session 18). We then trained the animal for three additional sessions in which the initial visual cortex ICMS "go" cue was removed, spatial-based feedback was re-introduced, and the catch trials consisted of randomized feedback. In this manipulation, the rat was able to perform the task successfully above chance, but with no significant difference in performance between the randomized feedback catch trials and the normal feedback trials. Thus the animal was able to do the task even with the feedback causing the reduction in detectable spikes, suggesting that it was able to perceive the spatial-based

feedback as indicative of an ongoing trial (see Fig. **5**, session 21). However, the behavioral performance similarity between the normal and catch trials suggests the rat was not using the information in the subtle features of the spatial-based feedback. Whether this was due to a lack of perception or a lack of learning is unknown.

Rat M12 (Fig. **6**) was trained only on the spatial-based feedback scheme, but other than that difference, the performance, training manipulations, and interpretations of the behavioral results are the same as M11, with one exception. Like M11, during the last sessions of training (Fig. **6**, sessions 12-15), no visual cortex ICMS "go" cue was delivered, and the feedback was the only indicator to the rat that a trial was occurring. Also like M11, the rat was able to perform the task above chance for both the normal trials and randomized feedback catch trials. In the first three of the four days of this manipulation, there was no significant difference in performance between the two types of trials. However, on the last session, the randomized feedback catch trials were significantly higher in performance than the non-randomized feedback normal trials (Fig. **6**, session 15). One potential explanation is that randomized spatial feedback may be more salient in that it is more likely to activate a broader area of the visual cortex. For example, in the normal feedback trials, the rat has to be close to the threshold for reward for the most dorsal electrode sites to be stimulated. In the randomized feedback, any site on the visual cortex electrode array is as likely to be stimulated as any other, regardless of how close the animal is to achieving reward.

We also analyzed reaction times in rats M10-M12, but significant differences in reaction time to reward (student's t-test) between catch trials and normal trials were sporadic across the training data, and no consistent patterns were observed. Since catch trials only occupied 15-20% of all the trials, we often needed differences in mean reaction time on the order of 600 ms to have the power to detect a significant difference. As such, the low number of catch trials often prevented us from detecting a difference in reaction time between the catch and normal trials, regardless if such differences indeed existed.

D. Minimization of Movement During Closed-Loop Control

A potential concern with this work is that the trained animals were not behaviorally clamped; that is, the rats were free to use any strategy they wished in order to modulate their motor cortices to receive the food reward. To address this, rat M5 was
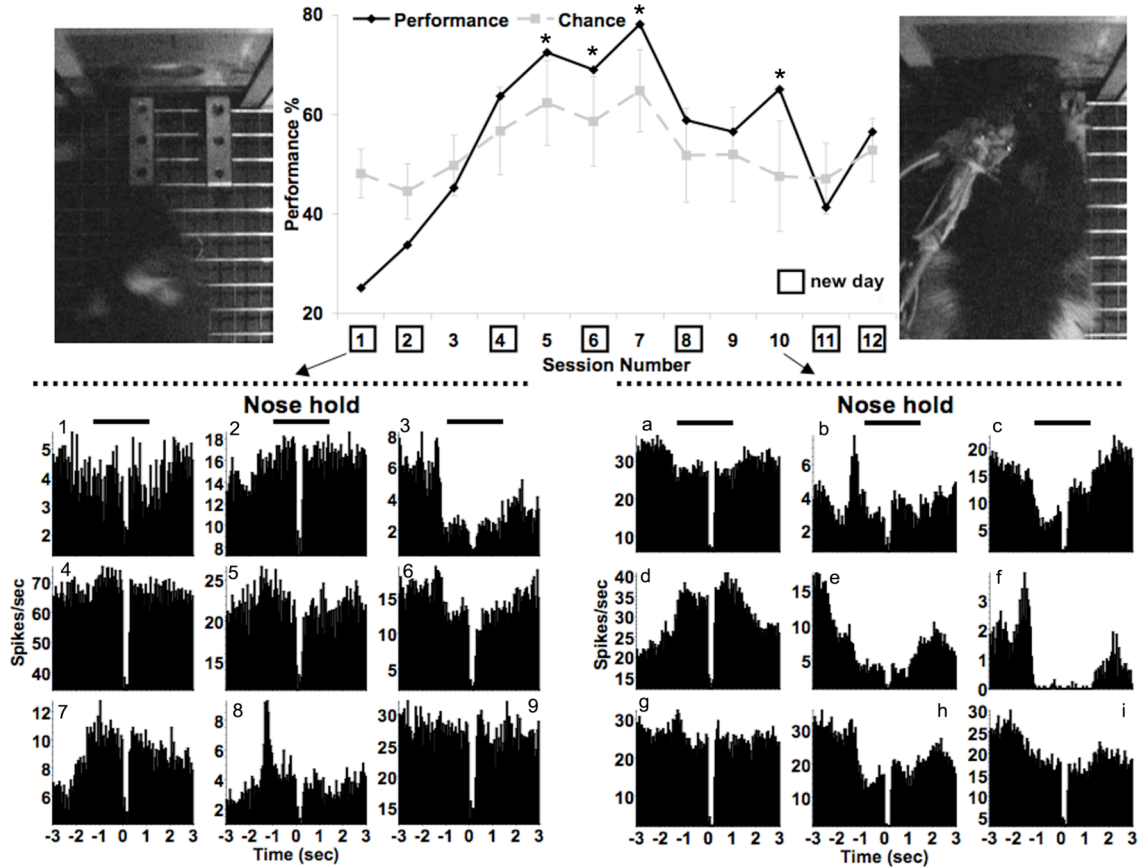
Figure 4.7: Rat M5 Nosepoke Motor Minimization Cortical Control Task. **Top**: Graph shows performance of rat M5 performing motor ensemble modulation in response to visual cortex ICMS while simultaneously holding its snout in an aperture during the "movement minimization" task. Chance calculations on animal performance include the 95% confidence bands. Photos on sides of top graph depict behavioral apparatus. **Bottom**: Ensemble PETHs at beginning and end of training. Neurons are numbered on the left, and alphabetized on the right, to indicate that the neurons are not necessarily the same. Notice, on session 10 PETHs, units b, c, and h increased firing rates immediately after visual cortex ICMS "go" cue (time=0).

pre-trained for a week to keep its snout in an aperture in the behavioral box for three seconds in order to receive a food pellet. Following this pre-training, the rat was trained on the cortical control task. Once the rat put its nose in the aperture, 1.1 seconds of baseline motor cortex ensemble firing rate data were collected, followed by the visual cortex ICMS "go" cue after which the rat, with its snout still in the aperture, had to modulate its motor cortex ensemble activity in order to receive a food reward (using the *ad hoc* linear algorithm). The rat was also given feedback during the response window using the amplitude-based code described above. Fig. **7** (top) shows the learning curve

for the rat. On the first two days the rat performed significantly below chance, likely because the feedback, mentioned above, drops the recordable spike firing rates by ~11%. Out of 12 sessions (seven days) of training, the rat was able to perform significantly above chance during four sessions (three days, sessions 5, 6, 7, and 10). The PETHs for the neural responses at the beginning of training and near the end of training are shown in Fig. **7** (bottom left and right, respectively). It is especially evident in the PETHs for both instances that around -2 seconds and +2 seconds relative to visual cortex ICMS "go" cue delivery, robust modulation occurs on almost all the units. Video monitoring indicated that this robust modulation was likely due to the rat inserting and exiting its nose in the nosepoke aperture, as the motor cortex implant was in the neck/shoulder region of motor cortex (Sanes et al., 1990).

However, during the actual behavioral trial, when the rat's nose was in the aperture and the rat was performing above chance, a modulation signal can be seen on units b, c, and h (Fig. **7**, bottom right) where the neurons increased firing rates after the visual cortex ICMS "go" cue. Thus, even in this movement minimization model, where the behavior was clamped, we were still able to train the rat to modulate its motor cortex. Such exemplary data suggests that our preparation is viable even in a more realistic neuroprosthetic model where movement is constrained.

E: Medial Forebrain Bundle Stimulation (MFB) Reward during Closed-Loop Control

The experiments described in this manuscript were developed to explore the technology of closed-loop neuroprosthetic devices combining motor ensemble decoding with sensory cortex ICMS. However, in one accessory experiment, deep brain stimulation (DBS) of the MFB, part of the classic reward pathway, was used to replace food reward. In this unique preparation, the entire behavioral task, with the stimulus, behavioral action, and consequence, was "virtual," done solely through multiple brain-machine interfaces.

The efficacy of the MFB stimulation was determined, prior to the closed-loop sessions, by running a brief task in which the rat had to put its nose in an aperture in the behavioral cage in order to receive 30 pulses of biphasic MFB stimulation at 60 Hz (Olds and Milner, 1954). Ideal current was determined by increasing current amplitude, starting at 40 μA and proceeding in 20 μA steps, until the rat began inserting its nose approximately once every 10-15 seconds. Once the rat was effectively "self-stimulating,"
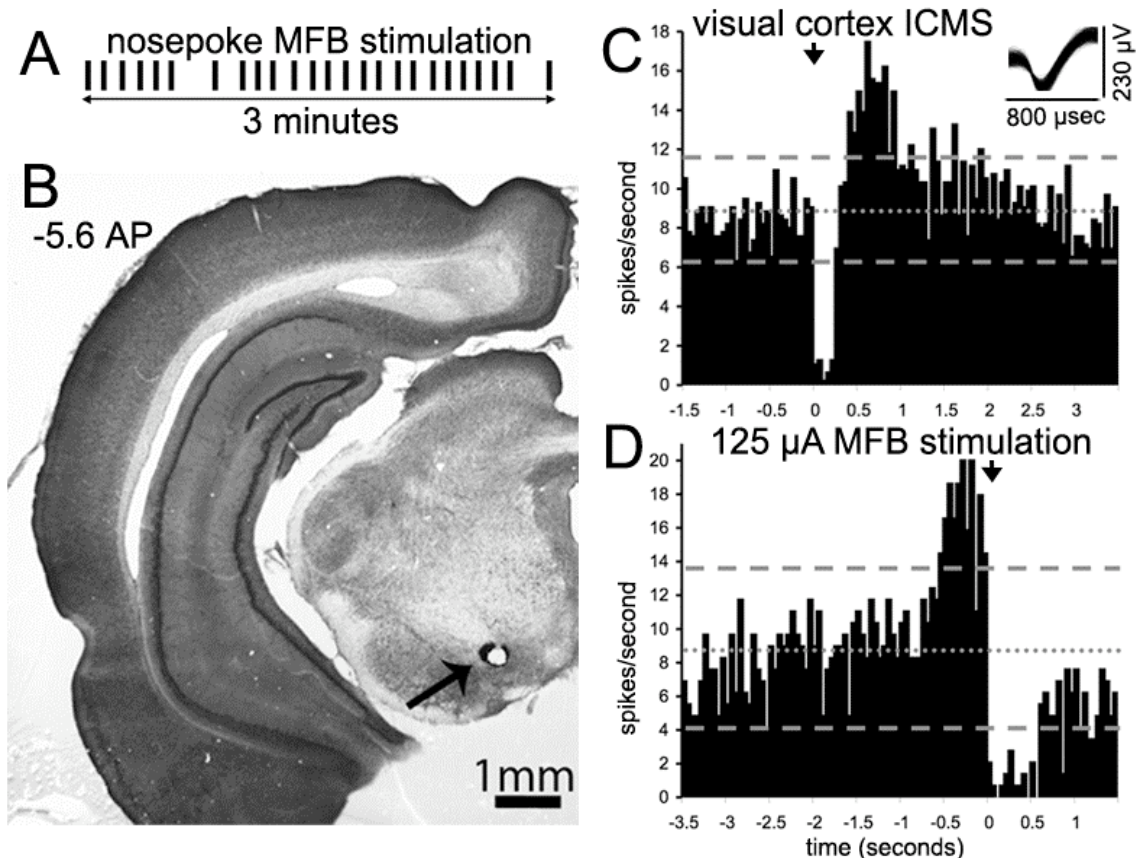
Fig 4.8: Rat M6 MFB Closed-Loop Self-Stimulation. **A.** Immediately prior to the closed-loop session, the efficacy of the MFB self-stimulation was assessed by a nosepoke paradigm where the rat's MFB was stimulated every instance it put its nose in an aperture. Schematic shows how many times the rat self-stimulated over three minutes. **B.** Histology of MFB implant (see Fig. **2** for the histology of the visual and motor cortex). Arrow shows electrode tip location. **C**. PETH of motor cortex unit aligned to visual cortex ICMS "go" cue. Dotted line indicates neuron's mean firing rate, and dashed lines indicate 95% confidence bands for mean firing rate. Inset shows waveform samples for this unit. **D**. PETH of same motor cortex unit aligned to MFB stimulation.

the rat was then run on the neuromodulation task using the *ad hoc* linear algorithm.

Given the complexity of the surgery with multiple brain regions implanted with recording and stimulating electrodes, along with accurately targeting the MFB, only one of the implanted rats (M6) self-stimulated reliably. The rat was run on 26 sessions of 100-200 trials each, and in an exemplary session the rat performed above chance (*p=0.03*). Fig. **8A** depicts the rat successfully self-stimulating with the initial nosepoke test, done immediately prior to the closed-loop task. Fig. **8B** shows the histological location of the medial forebrain bundle implant. Fig. **8C** shows the PETH of a neuron the rat was modulating during the task to obtain the MFB reward. Notice the neuron increased its

firing rate from 9 Hz to 16 Hz after the visual cortex ICMS "go" cue. Fig. **8D** shows the PETH of the same neuron aligned to the MFB stimulation event. As the internal capsule lies near the MFB, perhaps the increase in firing rate seen in Fig. **8C** is due to antidromic stimulation of the upper motor neurons. However, the rat had to modulate its motor cortex *before* it received MFB stimulation, thus any antidromic stimulation could only occur *after* the reward stimulus. Indeed, Fig. **8D** demonstrates the motor neuron modulation occurring only *before* the MFB stimulation reward.

We attempted this technique in three rats (M6, M10, and M12), and only in the data described above did we get successful performance, and even then, in only one session. The low overall performance, though disappointing, is probably due to the "highly unnatural" form of the task. The rat had to perceive a putative phosphene-like percept due to the visual cortex ICMS and then modulate its motor cortex neural firing rates in order to receive a DBS reward. In addition, we noted that the DBS reward was much more of an ephemeral motivator than the food reward. The rats rewarded with food pellets would continually work over hours in order to obtain the reward, whereas the rats rewarded with DBS would quickly lose motivation if they had not received a DBS reward in the previous two minutes, and the rats would then simply fall asleep in the cage. In addition, as the MFB stimulating electrode is made of stainless steel, it has a lower charge carrying capacity (50 μC/cm^2) than other materials such as the iridium oxide electrodes we implanted in the visual cortex (2200 μC/cm^2). It is possible we were eventually damaging the MFB by causing irreversible faradaic reactions (Merrill et al., 2005). Nonetheless, further technological and behavioral development may improve this technique, and we show the exemplary data here as it may be of broad interest to other investigators attempting to develop similar preparations.

IV. Discussion

As the technology of neuroprosthetics moves forward, the use of neocortex ICMS as a feedback signal for control of a neuromotor device is speculated to increase (Fagg et al., 2007). Here we present proof-of-concept results of a rat model closed-loop neuroprosthetic system by combining recording from motor cortex with electrical stimulation of sensory cortex. Previous work has demonstrated the use of simultaneous recording and stimulation techniques for neuroprosthetics, though almost entirely for

functional electrical stimulation (FES) applications, whereby neural activity from dorsal roots of the spinal cord or peripheral nerves are then used as a signal to stimulate limb musculature (Popovic et al., 1993, Strange and Hoffer, 1999, Weber et al., 2007). One recent exception is a study that combined stimulation and recording in the motor cortex to investigate plasticity of muscle representation (Jackson et al., 2006). However, delivering ICMS feedback to sensory cortex as a direct consequence of motor cortex activity in a cortical control task remains unexplored, and as a proof-of-concept we have developed a suitable preparation with which to improve and examine closed-loop control technology for neuroprosthetics.

Despite the success of this model, we feel that increased technological development needs to occur before significant improvements can be made. First and foremost, the brain does not encode sensory features by firing action potentials for 10 ms out of every 90 ms, as was the protocol with our interleaved feedback scheme. The only way to avoid an interleaved feedback scheme is to find a way to excite brain tissue at fine temporal resolution without the stimulation artifact interfering with the signals on the recording electrodes. One solution may be via hardware development, such as faster switching amplifiers and improved artifact cancellation. Another solution may be through improved electrode technology, such as reducing the impedance of the electrodes via bioactive polymers conjugated to the electrode site, which would cause a reduction in the compliance voltage needed to stimulate at physiological current levels (Ludwig et al., 2006). Yet, a promising technique would be to avoid ICMS altogether and excite brain tissue with optical methods (Boyden et al., 2005, Farah et al., 2007).

As is the case with any microstimulation experiment, the question of perception is always of paramount importance. Our visual cortex characterization consisted of measuring the neural responses to bright-field illumination immediately after surgery. Animals M5 and M6 only had evoked local field potential responses to the illumination, whereas M10, M11, and M12 had robust evoked spiking responses to the illumination. M5's visual cortex implant straddled the hippocampus for the majority of its length. It is highly unlikely that this animal perceived phosphenes, though M5 was still able to successfully perform the task. This begs the questions of what exactly the animal had perceived. M10-M12's visual cortex implants were almost all deep enough in the visual

cortex that half of the electrodes were in the axonal fiber tracts. Since all these rats could respond to the microstimulation appropriately, there is no doubt they perceived the stimuli. In the absence of more rigorous behavioral experiments (Bradley et al., 2005, Otto et al., 2005), the question of what these animals perceived is merely a subject of conjecture and not necessarily of importance for the success of this model. The variability in the visual cortex implantation sites in our study actually offers compelling evidence that using ICMS feedback is generalizable to many other areas of the brain.

Since rats use their whiskers profusely for tactile sensation, perhaps utilizing the barrel cortex instead of the visual cortex would convey more salient perceptions of the feedback signal. While previous work by our group has used ICMS in the auditory cortex (Rousche et al., 2003, Otto et al., 2005), we choose to implant the visual cortex because the surgical access of visual cortex in the rat is less difficult than the auditory cortex, especially in the context of multiple implants in a single animal.

The use of the feedback in rats M10-M12 varied across the subjects. M10 appeared to be using the feedback, as it didn't perform above chance on the non-feedback catch trials from sessions 10-16 (Fig. **4**). However, in sessions in which the catch trials consisted of randomized feedback, M10 achieved the same performance level between the catch trials and the normal trials. Thus, M10 was merely using the feedback as an indicator of whether the trial was still occurring. Rather surprisingly, M11 and M12 performed better on the trials where feedback was not delivered. The visual cortex ICMS feedback, even in our interleaved stimulation paradigm, would drop the recording of spikes by our acquisition hardware by ~11%. Since decreasing motor cortex firing rates were not considered a behavioral response by our algorithms precisely for this reason, the task was more difficult with the feedback, as the animals had to work harder to increase their firing rates to an appropriate level to be rewarded. When we removed the visual cortex ICMS "go" cue, forcing the animals to attend to the feedback, animals M11 and M12 were able to do the task significantly above chance (M11: sessions 19-21, M12: sessions 12-15). We believe the animals were thus perceiving the visual cortex ICMS and appropriately modulating their motor cortex ensemble, though in reality the task would probably be easier with traditional tone-based or light-based feedback.

Ideally, delivering ICMS without causing artifact in the motor cortex recordings would ensure a greater transmission of the ensemble dynamics. Development of stimulation and recording technology that ameliorates the artifact remains a priority of neural engineering. Finally, though the animals were able to consistently perform above chance, alternative algorithms, such as Bayesian state estimators (Lehmkuhle et al., 2006, Achtman et al., 2007) or support vector machines (Olson et al., 2005), may improve performance and learning in our closed-loop preparation.

Acknowledgements:

References:

ABBOTT, A. (2006) Neuroprosthetics: in search of the sixth sense. *Nature,* 442**,** 125-7.

ABELES, M. (1982) Quantification, smoothing, and confidence limits for single-units' histograms. *J Neurosci Methods,* 5**,** 317-25.

ACHTMAN, N., AFSHAR, A., SANTHANAM, G., YU, B. M., RYU, S. I. & SHENOY, K. V. (2007) Free-paced high-performance brain-computer interfaces. *J Neural Eng,* 4**,** 336-47.

BOYDEN, E. S., ZHANG, F., BAMBERG, E., NAGEL, G. & DEISSEROTH, K. (2005) Millisecond-timescale, genetically targeted optical control of neural activity. *Nat Neurosci,* 8**,** 1263-8.

BRADLEY, D. C., TROYK, P. R., BERG, J. A., BAK, M., COGAN, S., ERICKSON, R., KUFTA, C., MASCARO, M., MCCREERY, D., SCHMIDT, E. M., TOWLE, V. L. & XU, H. (2005) Visuotopic mapping through a multichannel stimulating implant in primate V1. *J Neurophysiol,* 93**,** 1659-70.

BRINDLEY, G. S. & LEWIN, W. S. (1968) The sensations produced by electrical stimulation of the visual cortex. *J Physiol,* 196**,** 479-93.

CARMENA, J. M., LEBEDEV, M. A., CRIST, R. E., O'DOHERTY, J. E., SANTUCCI, D. M., DIMITROV, D., PATIL, P. G., HENRIQUEZ, C. S. & NICOLELIS, M. A. (2003) Learning to control a brain-machine interface for reaching and grasping by primates. *PLoS Biol,* 1**,** E42.

CHAPIN, J. K., MOXON, K. A., MARKOWITZ, R. S. & NICOLELIS, M. A. (1999) Real-time control of a robot arm using simultaneously recorded neurons in the motor cortex. *Nat Neurosci,* 2**,** 664-70.

DOBELLE, W. H., QUEST, D. O., ANTUNES, J. L., ROBERTS, T. S. & GIRVIN, J. P. (1979) Artificial vision for the blind by electrical stimulation of the visual cortex. *Neurosurgery,* 5**,** 521-7.

FAGG, A. H., HATSOPOULOS, N. G., DE LAFUENTE, V., MOXON, K. A., NEMATI, S., REBESCO, J. M., ROMO, R., SOLLA, S. A., REIMER, J., TKACH, D., POHLMEYER, E. A. & MILLER, L. E. (2007) Biomimetic brain machine interfaces for the control of movement. *J Neurosci,* 27**,** 11842-6.

FARAH, N., REUTSKY, I. & SHOHAM, S. (2007) Patterned optical activation of retinal ganglion cells. *Conf Proc IEEE Eng Med Biol Soc,* 1**,** 6368-70.

FITZSIMMONS, N. A., DRAKE, W., HANSON, T. L., LEBEDEV, M. A. & NICOLELIS, M. A. (2007) Primate reaching cued by multichannel spatiotemporal cortical microstimulation. *J Neurosci,* 27**,** 5593-602.

GAGE, G. J., LUDWIG, K. A., OTTO, K. J., IONIDES, E. L. & KIPKE, D. R. (2005) Naive coadaptive cortical control. *J Neural Eng,* 2**,** 52-63.

HOCHBERG, L. R., SERRUYA, M. D., FRIEHS, G. M., MUKAND, J. A., SALEH, M., CAPLAN, A. H., BRANNER, A., CHEN, D., PENN, R. D. & DONOGHUE, J. P. (2006) Neuronal ensemble control of prosthetic devices by a human with tetraplegia. *Nature,* 442**,** 164-71.

JACKSON, A., MAVOORI, J. & FETZ, E. E. (2006) Long-term motor cortex plasticity induced by an electronic neural implant. *Nature,* 444**,** 56-60.

KENNEDY, P. R. & BAKAY, R. A. (1998) Restoration of neural output from a paralyzed patient by a direct brain connection. *Neuroreport,* 9**,** 1707-11.

KENNEDY, P. R., BAKAY, R. A., MOORE, M. M., ADAMS, K. & GOLDWAITHE, J. (2000) Direct control of a computer from the human central nervous system. *IEEE Trans Rehabil Eng,* 8**,** 198-202.

LEHMKUHLE, M. J., NORMANN, R. A. & MAYNARD, E. M. (2006) Trial-by-trial discrimination of three enantiomer pairs by neural ensembles in mammalian olfactory bulb. *J Neurophysiol,* 95**,** 1369-79.

LONDON, B. M., JORDAN, L. R., JACKSON, C. R. & MILLER, L. E. (2008) Electrical stimulation of the proprioceptive cortex (area 3a) used to instruct a behaving monkey. *IEEE Trans Neural Syst Rehabil Eng,* 16**,** 32-6.

LUDWIG, K. A., URAM, J. D., YANG, J., MARTIN, D. C. & KIPKE, D. R. (2006) Chronic neural recordings using silicon microelectrode arrays electrochemically deposited with a poly(3,4-ethylenedioxythiophene) (PEDOT) film. *J Neural Eng,* 3**,** 59-70.

MARZULLO, T. C., GAGE, G. J., LEHMKUHLE, M. J. & KIPKE, D. R. (2007) A direct visual and motor neural interface demonstration in a rat. *3rd International IEEE/EMBS Conference on Neural Engineering.* Kohala Coast, HI.

MARZULLO, T. C., MILLER, C. R. & KIPKE, D. R. (2006) Suitability of the cingulate cortex for neural control. *IEEE Trans Neural Syst Rehabil Eng,* 14**,** 401-9.

MERRILL, D. R., BIKSON, M. & JEFFERYS, J. G. (2005) Electrical stimulation of excitable tissue: design of efficacious and safe protocols. *J Neurosci Methods,* 141**,** 171-98.

MUSALLAM, S., CORNEIL, B. D., GREGER, B., SCHERBERGER, H. & ANDERSEN, R. A. (2004) Cognitive control signals for neural prosthetics. *Science,* 305**,** 258-62.

OLDS, J. & MILNER, P. (1954) Positive reinforcement produced by electrical stimulation of septal area and other regions of rat brain. *J Comp Physiol Psychol,* 47**,** 419-27.

OLSON, B. P., SI, J., HU, J. & HE, J. (2005) Closed-loop cortical control of direction using support vector machines. *IEEE Trans Neural Syst Rehabil Eng,* 13**,** 72-80.

OTTO, K. J., ROUSCHE, P. J. & KIPKE, D. R. (2005) Cortical microstimulation in auditory cortex of rat elicits best-frequency dependent behaviors. *J Neural Eng,* 2**,** 42-51.

PAGANO, M. & GAUVREAU, K. (2000) *Principles of Biostatistics,* Pacific Grove, CA., Duxbury.

PAXINOS, G. & WATSON, C. (1998) *The rat brain in stereotaxic coordinates,* San Diego, Academic Press.

PENFIELD, W. & PEROT, P. (1963) The Brain's Record of Auditory and Visual Experience. A Final Summary and Discussion. *Brain,* 86**,** 595-696.

POPOVIC, D. B., STEIN, R. B., JOVANOVIC, K. L., DAI, R., KOSTOV, A. & ARMSTRONG, W. W. (1993) Sensory nerve recording for closed-loop control to restore motor functions. *IEEE Trans Biomed Eng,* 40**,** 1024-31.

ROMO, R., HERNANDEZ, A., ZAINOS, A. & SALINAS, E. (1998) Somatosensory discrimination based on cortical microstimulation. *Nature,* 392**,** 387-90.

ROUSCHE, P. J., OTTO, K. J., REILLY, M. P. & KIPKE, D. R. (2003) Single electrode micro-stimulation of rat auditory cortex: an evaluation of behavioral performance. *Hear Res,* 179**,** 62-71.

SANES, J. N., SUNER, S. & DONOGHUE, J. P. (1990) Dynamic organization of primary motor cortex output to target muscles in adult rats. I. Long-term patterns of reorganization following motor or mixed peripheral nerve lesions. *Exp Brain Res,* 79**,** 479-91.

SERRUYA, M. D., HATSOPOULOS, N. G., PANINSKI, L., FELLOWS, M. R. & DONOGHUE, J. P. (2002) Instant neural control of a movement signal. *Nature,* 416**,** 141-2.

SHULER, M. G. & BEAR, M. F. (2006) Reward timing in the primary visual cortex. *Science,* 311**,** 1606-9.

STRANGE, K. D. & HOFFER, J. A. (1999) Restoration of use of paralyzed limb muscles using sensory nerve signals for state control of FES-assisted walking. *IEEE Trans Rehabil Eng,* 7**,** 289-300.

TAYLOR, D. M., TILLERY, S. I. & SCHWARTZ, A. B. (2002) Direct cortical control of 3D neuroprosthetic devices. *Science,* 296**,** 1829-32.

VELLISTE, M., PEREL, S., SPALDING, M. C., WHITFORD, A. S. & SCHWARTZ, A. B. (2008) Cortical control of a prosthetic arm for self-feeding. *Nature,* 453**,** 1098-101.

VETTER, R. J., WILLIAMS, J. C., HETKE, J. F., NUNAMAKER, E. A. & KIPKE, D. R. (2004) Chronic neural recording using silicon-substrate microelectrode arrays implanted in cerebral cortex. *IEEE Trans Biomed Eng,* 51**,** 896-904.

WEBER, D. J., STEIN, R. B., EVERAERT, D. G. & PROCHAZKA, A. (2007) Limb-state feedback from ensembles of simultaneously recorded dorsal root ganglion neurons. *J Neural Eng,* 4**,** S168-80.

WEILAND, J. D. & ANDERSON, D. J. (2000) Chronic neural stimulation with thin-film, iridium oxide electrodes. *IEEE Trans Biomed Eng,* 47**,** 911-8.

WESSBERG, J., STAMBAUGH, C. R., KRALIK, J. D., BECK, P. D., LAUBACH, M., CHAPIN, J. K., KIM, J., BIGGS, S. J., SRINIVASAN, M. A. & NICOLELIS, M. A. (2000) Real-time prediction of hand trajectory by ensembles of cortical neurons in primates. *Nature,* 408**,** 361-5.

Chapter V

Conclusion

The microelectrode continues to be the primary tool for neuroprosthetics of limb and cursor control; however, there remains the critically important problem of long-term recording of unit activity. In order for cortical neuroprosthetics to become part of the milieu of modern medical technology like pacemakers, deep brain stimulators (DBS), and cochlear implants, cortical microelectrodes need to reliably record unit activity over a period of years. While some examples exist in the literature of long-term recording up to a year (Vetter et al., 2004, Suner et al., 2005), reliability remains the *essential problem* in neural engineering. The theory of why electrodes fail to reliably record stable neural signals over time is unknown and a largely speculative area of debate.

Our group, and others, are beginning to systematically examine the problem through a combination of measuring electrode impedance over time, electrode/tissue interface modeling, unit reliability recordings combined with chemical sensing, and careful histological examinations (Szarowski et al., 2003, Subbaroyan et al., 2005, Ludwig et al., 2006, Johnson et al., 2007, Seymour and Kipke, 2007). One reason why electrodes fail may be microvasculature damage upon insertion of the probe. A way to avoid this damage would be to map the microvasculature prior to the insertion. Continued improvements in optical imaging of cerebral vasculature *in vivo* may allow this to occur (Schaffer et al., 2006).

For brain stimulation applications, the technology is more mature (given the development of pacemakers, cochlear implants, and DBS for Parkinson's disease over the past decades), as stimulating electrodes are not limited by the technical requirement of recording small voltage signals over time. Stimulating electrodes are only limited by biocompatibility issues, maintaining reversible faradaic reactions at the tissue interface, and mitigating the tissue response and scarring to the surrounding area of tissue. However, stimulation technology for sensory replacement/feedback in neocortex still has

fundamental engineering limitations. Some work in primates has attempted to design a visual cortex prosthesis with intracortical microelectrode arrays (Bradley et al., 2005), but the authors note that to have a visual neocortex array that would faithfully replicate vision would require implanting a high density array over the entire posterior pole of the brain. Such technology has not yet been invented.

Though the ultimate goal of the neuroprosthetic community is to restore fine limb control to humans with complete sensory feedback, sub-optimal restoration of motor commands and senses is still an improvement for some people. For example, even though cochlear implants do not have the dynamic tonal range of normal hearing, they still improve quality of life for the deaf (Moller, 2006). And though control systems of functional electrical stimulation (FES) of limb musculature are not nearly as graceful as natural brain control, again, the crude technology is still an improvement (Popovic et al., 2007). Thus, even though there are fundamental problems to high-density recording/stimulation of brain tissue and musculature, continued development in these technologies may further ameliorate nervous system pathologies.

This dissertation covered three promising new areas for neuroprosthetics: alternative cortical areas (chapter 2), alternative cortical signals (chapter 3), and sensory cortex ICMS feedback (chapter 4). Progress was made in all three of these arenas, but limitations exist.

The cingulate cortex experiments only trained the animals on a one state (one degree of freedom) task, and the animals were free-moving (that is, the behavior was not clamped). Whether the cingulate cortex can be used for a multiple degree of freedom control system for a human paralyzed patient is unknown. It is also debatable whether the cingulate cortex function in rats is generalizable to the function of the cingulate cortex in humans. To escape this generalization problem, neurosurgeons would have to implant humans in the cingulate cortex for a cortical control task. However, to date most humans implanted with a neuroprosthetic device have been quadriplegic due to spinal cord injury (Hochberg et al., 2006); thus their motor cortex is not degenerated due to an upper motor neuron disease. In these patients there is no compelling reason to implant the cingulate cortex, especially given the cingulate cortex's proximity to the saggital sinus.
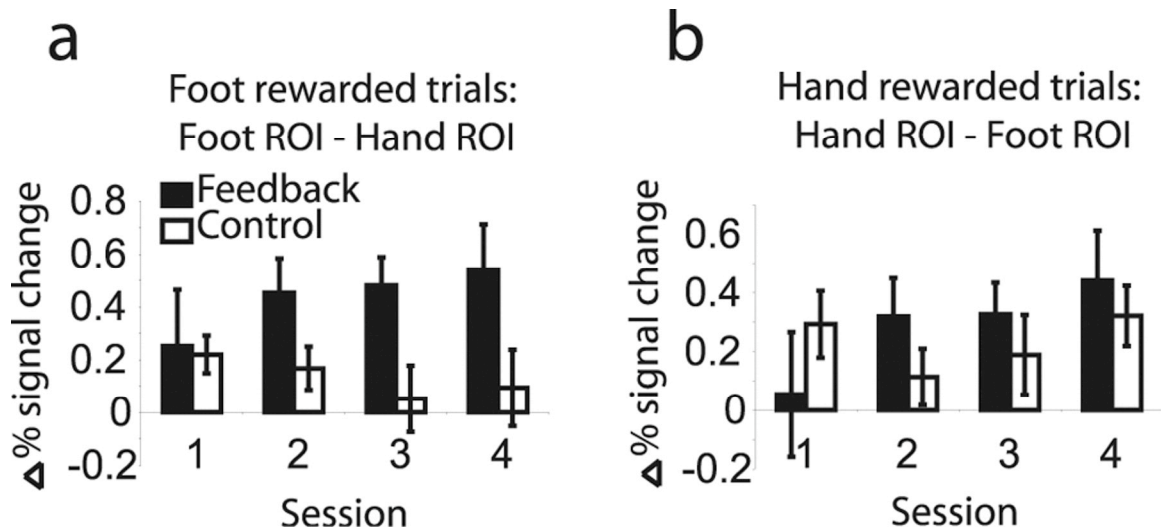
Figure 5.1: Self Modulation of the fMRI BOLD signal in human subjects. Subjects were instructed to imagine movements of either the foot or the hand, and feedback was given in the form of a monetary reward if the subject successfully increased the BOLD signal. Left: Subjects had to modulate the foot area of motor cortex. Notice increasing signal change over time. Right: Subjects had the modulate the hand area. Again, notice increasing signal change over time (Bray et. al, 2007)

In the beginning of this decade, the question of whether non-purely motor areas could be used for a neuroprosthetic control signal was still very much an active topic of research. Since then, the work in this dissertation, along with work by other groups, has indeed shown that much of the parietal (Musallam et al., 2004, Lebedev et al., 2005), temporal (Leuthardt et al., 2004, Felton et al., 2007), and prefrontal lobes (Santhanam et al., 2006) of the neocortex can be used as alternative implantation sites. Indeed, recent advances in fMRI using biofeedback of the BOLD signal has begun to *systematically map* which areas of the brain can be self-modulated by human subjects (Weiskopf et al., 2003, Decharms et al., 2005, Bray et al., 2007, Yoo et al., 2007) (see Figure 1).

Local field potential control has remained unexplored in the neuroprosthetic community, though groups continue to show, as indeed this dissertation did, that the LFP is co-modulated along with spikes during a given behavioral task (Mehring et al., 2003, Rickert et al., 2005, Heldman et al., 2006). Perhaps investigators have tried to train subjects to modulate local field potentials but have failed to achieve compelling results similar to spike-driven cursor or limb control. Such a result would be curious, as the

spikes in the motor cortex appear to be tightly coupled to the oscillatory periods of local field potential modulation.

In the experiments in this dissertation investigating the relationships of spikes to LFPs and ECoGs, correlations existed between all three signals, but as a function of *specific frequency oscillations*. Specifically, during anesthesia, the spikes entrained to the 1-2 Hz ketamine-induced oscillation, and during the motor learning and neuroprosthetic modes, the spikes entrained to the 8 Hz theta rhythm. During periods of high spiking, the spikes continue to entrain to theta, though at a lower power. Thus, a potential human neuroprosthetic device may gain an additional control signal by adding local field potentials and ECoGs high passed above 10 Hz. However, should the spiking activity fail, the local field potential frequency components below 10 Hz could also be used. However, this still needs to be experimentally verified by inputting field potentials and spikes into a real-time controller and measuring user-performance compared to traditional spiking based cortical control algorithms. Such experiments can be easily implemented in animal models.

Finally, delivering feedback to the brain for control of a neuroprosthetic device is an obvious iterative technological development. Though yet still undemonstrated, the community hypothesizes that giving feedback about the output states of a neural controller directly back to the central nervous system (either through sensory neocortex or the dorsal roots of the spinal cord) would optimize operator performance of a neuroprosthetic device (Abbott, 2006, Fagg et al., 2007). To investigate this, in this dissertation's final data chapter, the visual cortex and motor cortex of rats was implanted, and the animals were trained to modulate the ensemble activity of the motor cortex in response to visual cortex ICMS. Though the preparation was moderately successful (the animals could indeed interpret visual cortex ICMS as a signal during a neuromodulation task), technical limitations existed as to the feasibility of simultaneous microstimulation with motor cortex recording.

The microstimulation codes used in the experiments did not mimic or emulate the visual cortex's naturalistic encoding of visual stimuli. The experiments also did not determine what the animals were perceiving in response to visual cortex ICMS. In addition, continuous feedback was not used whereby information about the "state" of the

motor ensemble was constantly being delivered to the rat. Because the ICMS artifact swamped the recording amplifiers, an interleaved feedback scheme was implemented where ICMS was delivered only during the first 10 ms of every 90 ms. Until a further understanding of the electrical properties of the artifact occurs, and ways to ameliorate it are further developed (Boyden et al., 2005), the combination of naturalistic sensory cortex ICMS with motor cortex ensemble decoding is impossible.

Regardless, the animals (four of five) were still able to do the task, showing that interleaved feedback schemes are feasible when combined with motor cortex ensemble decoding. The experiments then reached a stopping point, as the stimulation artifact prevented any improvements in the ICMS encoding. At this point, further experiments *should not* examine 1) determining what the animals are perceiving, 2) improving the ensemble decoding algorithms, or 3) examining the efficacy of various sensory areas of the brain. Two more basic improvements need to be made: 1) investigating methods of reducing the stimulation artifact, and 2) enabling the recording of back voltage during stimulation to make sure that excessive charge is not being delivered through the stimulating electrodes, possibly causing irreversible faradaic reactions and damaging the brain tissue (Merrill et al., 2005).

*****

This thesis covered three avenues in the parameter space of neuroprosthetic design, and promising directions were presented for future technological refinement. However, basic development in fundamental electrode technology needs to occur before fully operational and long-term viable neuroprosthetics can be clinically implemented beyond the demonstration stage.

As a final dalliance, in my experimental endeavors I often recollected the following passage from the final chapter of Henry David Thoreau's "Walden."

"There was an artist in the city of Kouroo who was disposed to strive after perfection. One day it came into his mind to make a staff. Having considered that in an imperfect work time is an ingredient, but into a perfect work time does not enter, he said to himself, "It shall be perfect in all respects, though I should do nothing else in my life." He proceeded instantly to the forest for wood, being resolved that it should not be made of unsuitable material; and as he searched for and rejected stick after stick, his friends gradually deserted him, for they grew old in their works and died, but he grew not older by a moment. His

singleness of purpose and resolution, and his elevated piety, endowed him, without his knowledge, with perennial youth. As he made no compromise with Time, Time kept out of his way, and only sighed at a distance because he could not overcome him. Before he had found a stock in all respects suitable the city of Kouroo was a hoary ruin, and he sat on one of its mounds to peel the stick. Before he had given it the proper shape the dynasty of the Candahars was at an end, and with the point of the stick he wrote the name of the last of that race in the sand, and then resumed his work. By the time he had smoothed and polished the staff Kalpa was no longer the pole-star; and ere he had put on the ferule and the head adorned with precious stones, Brahma had awoke and slumbered many times. But why do I stay to mention these things? When the finishing stroke was put to his work, it suddenly expanded before the eyes of the astonished artist into the fairest of all the creations of Brahma. He had made a new system in making a staff, a world with full and fair proportions; in which, though the old cities and dynasties had passed away, fairer and more glorious ones had taken their places. And now he saw by the heap of shavings still fresh at his feet, that, for him and his work, the former lapse of time had been an illusion, and that no more time had elapsed than is required for a single scintillation from the brain of Brahma to fall on and inflame the tinder of a mortal brain. The material was pure, and his art was pure; how could the result be other than wonderful? "

References:

ABBOTT, A. (2006) Neuroprosthetics: in search of the sixth sense. *Nature,* 442**,** 125-7.

BOYDEN, E. S., ZHANG, F., BAMBERG, E., NAGEL, G. & DEISSEROTH, K. (2005) Millisecond-timescale, genetically targeted optical control of neural activity. *Nat Neurosci,* 8**,** 1263-8.

BRADLEY, D. C., TROYK, P. R., BERG, J. A., BAK, M., COGAN, S., ERICKSON, R., KUFTA, C., MASCARO, M., MCCREERY, D., SCHMIDT, E. M., TOWLE, V. L. & XU, H. (2005) Visuotopic mapping through a multichannel stimulating implant in primate V1. *J Neurophysiol,* 93**,** 1659-70.

BRAY, S., SHIMOJO, S. & O'DOHERTY, J. P. (2007) Direct instrumental conditioning of neural activity using functional magnetic resonance imaging-derived reward feedback. *J Neurosci,* 27**,** 7498-507.

DECHARMS, R. C., MAEDA, F., GLOVER, G. H., LUDLOW, D., PAULY, J. M., SONEJI, D., GABRIELI, J. D. & MACKEY, S. C. (2005) Control over brain activation and pain learned by using real-time functional MRI. *Proc Natl Acad Sci U S A,* 102**,** 18626-31.

FAGG, A. H., HATSOPOULOS, N. G., DE LAFUENTE, V., MOXON, K. A., NEMATI, S., REBESCO, J. M., ROMO, R., SOLLA, S. A., REIMER, J., TKACH, D., POHLMEYER, E. A. & MILLER, L. E. (2007) Biomimetic brain machine interfaces for the control of movement. *J Neurosci,* 27**,** 11842-6.

FELTON, E. A., WILSON, J. A., WILLIAMS, J. C. & GARELL, P. C. (2007) Electrocorticographically controlled brain-computer interfaces using motor and sensory imagery in patients with temporary subdural electrode implants. Report of four cases. *J Neurosurg,* 106**,** 495-500.

HELDMAN, D. A., WANG, W., CHAN, S. S. & MORAN, D. W. (2006) Local field potential spectral tuning in motor cortex during reaching. *IEEE Trans Neural Syst Rehabil Eng,* 14**,** 180-3.

HOCHBERG, L. R., SERRUYA, M. D., FRIEHS, G. M., MUKAND, J. A., SALEH, M., CAPLAN, A. H., BRANNER, A., CHEN, D., PENN, R. D. & DONOGHUE, J. P. (2006) Neuronal ensemble control of prosthetic devices by a human with tetraplegia. *Nature,* 442**,** 164-71.

JOHNSON, M. D., KAO, O. E. & KIPKE, D. R. (2007) Spatiotemporal pH dynamics following insertion of neural microelectrode arrays. *J Neurosci Methods,* 160**,** 276-87.

LEBEDEV, M. A., CARMENA, J. M., O'DOHERTY, J. E., ZACKSENHOUSE, M., HENRIQUEZ, C. S., PRINCIPE, J. C. & NICOLELIS, M. A. (2005) Cortical ensemble adaptation to represent velocity of an artificial actuator controlled by a brain-machine interface. *J Neurosci,* 25**,** 4681-93.

LEUTHARDT, E. C., SCHALK, G., WOLPAW, J. R., OJEMANN, J. G. & MORAN, D. W. (2004) A brain-computer interface using electrocorticographic signals in humans. *J Neural Eng,* 1**,** 63-71.

LUDWIG, K. A., URAM, J. D., YANG, J., MARTIN, D. C. & KIPKE, D. R. (2006) Chronic neural recordings using silicon microelectrode arrays electrochemically deposited with a poly(3,4-ethylenedioxythiophene) (PEDOT) film. *J Neural Eng,* 3**,** 59-70.

MEHRING, C., RICKERT, J., VAADIA, E., CARDOSA DE OLIVEIRA, S., AERTSEN, A. & ROTTER, S. (2003) Inference of hand movements from local field potentials in monkey motor cortex. *Nat Neurosci,* 6**,** 1253-4.

MERRILL, D. R., BIKSON, M. & JEFFERYS, J. G. (2005) Electrical stimulation of excitable tissue: design of efficacious and safe protocols. *J Neurosci Methods,* 141**,** 171-98.

MOLLER, A. R. (2006) History of cochlear implants and auditory brainstem implants. *Adv Otorhinolaryngol,* 64**,** 1-10.

MUSALLAM, S., CORNEIL, B. D., GREGER, B., SCHERBERGER, H. & ANDERSEN, R. A. (2004) Cognitive control signals for neural prosthetics. *Science,* 305**,** 258-62.

POPOVIC, D., BAKER, L. L. & LOEB, G. E. (2007) Recruitment and comfort of BION implanted electrical stimulation: implications for FES applications. *IEEE Trans Neural Syst Rehabil Eng,* 15**,** 577-86.

RICKERT, J., OLIVEIRA, S. C., VAADIA, E., AERTSEN, A., ROTTER, S. & MEHRING, C. (2005) Encoding of movement direction in different frequency ranges of motor cortical local field potentials. *J Neurosci,* 25**,** 8815-24.

SANTHANAM, G., RYU, S. I., YU, B. M., AFSHAR, A. & SHENOY, K. V. (2006) A high-performance brain-computer interface. *Nature,* 442**,** 195-8.

SCHAFFER, C. B., FRIEDMAN, B., NISHIMURA, N., SCHROEDER, L. F., TSAI, P. S., EBNER, F. F., LYDEN, P. D. & KLEINFELD, D. (2006) Two-photon imaging of cortical surface microvessels reveals a robust redistribution in blood flow after vascular occlusion. *PLoS Biol,* 4**,** e22.

SEYMOUR, J. P. & KIPKE, D. R. (2007) Neural probe design for reduced tissue encapsulation in CNS. *Biomaterials,* 28**,** 3594-607.

SUBBAROYAN, J., MARTIN, D. C. & KIPKE, D. R. (2005) A finite-element model of the mechanical effects of implantable microelectrodes in the cerebral cortex. *J Neural Eng,* 2**,** 103-13.

SUNER, S., FELLOWS, M. R., VARGAS-IRWIN, C., NAKATA, G. K. & DONOGHUE, J. P. (2005) Reliability of signals from a chronically implanted, silicon-based electrode array in non-human primate primary motor cortex. *IEEE Trans Neural Syst Rehabil Eng,* 13**,** 524-41.

SZAROWSKI, D. H., ANDERSEN, M. D., RETTERER, S., SPENCE, A. J., ISAACSON, M., CRAIGHEAD, H. G., TURNER, J. N. & SHAIN, W. (2003) Brain responses to micro-machined silicon devices. *Brain Res,* 983**,** 23-35.

VETTER, R. J., WILLIAMS, J. C., HETKE, J. F., NUNAMAKER, E. A. & KIPKE, D. R. (2004) Chronic neural recording using silicon-substrate microelectrode arrays implanted in cerebral cortex. *IEEE Transactions on Biomedical Engineering,* 51**,** 1-9.

WEISKOPF, N., VEIT, R., ERB, M., MATHIAK, K., GRODD, W., GOEBEL, R. & BIRBAUMER, N. (2003) Physiological self-regulation of regional brain activity using real-time functional magnetic resonance imaging (fMRI): methodology and exemplary data. *Neuroimage,* 19**,** 577-86.

YOO, S. S., LEE, J. H., O'LEARY, H., LEE, V., CHOO, S. E. & JOLESZ, F. A. (2007) Functional magnetic resonance imaging-mediated learning of increased activity in auditory areas. *Neuroreport,* 18**,** 1915-20.